Role of the Kinesin-like Protein KipB in *Aspergillus nidulans*

Dissertation

zur

Erlangung des Doktorgrades

der Naturwissenschaften

(Dr. rer. nat.)

dem Fachbereich Biologie

der Philipps-Universität, Marburg/Lahn

vorgelegt von

Patricia Elena Rischitor

aus

Iasi / Rumänien

Marburg, Februar 2004

Vom Fachbereich Biologie der Philipps-Universität Marburg als Dissertation angenommen am:

Erstgutachter: HD Dr. R. Fischer
Zweitgutachter: Prof. Dr. M. Bölker

Tag der mündlichen Prüfung:

Die Untersuchungen zur vorliegenden Arbeit wurden von August 2000 bis Februar 2004 im Laboratorium für Mikrobiologie des Fachbereichs Biologie der Philipps-Universität Marburg und am Max-Planck Institut für terrestrische Mikrobiologie in Marburg unter der Leitung von Herrn von HD Dr. R. Fischer durchgeführt.

Ich versichere, dass ich meine Dissertation mit dem Titel “Role of the Kinesin-like Protein KipB in *Aspergillus nidulans*“ selbstständig, ohne unerlaubte Hilfe angefertigt und mich dabei keiner anderen als der von mir ausdrücklich bezeichneten Quellen und Hilfen bedient habe.

Die Dissertation wurde in der jetzigen oder einer ähnlichen Form noch bei keiner anderen Hochschule eingereicht und hat noch keinen sonstigen Prüfungszwecken gedient.

Marburg, 16. Februar 2004 Patricia Elena Rischitor

Im Zusammenhang mit der Thematik der vorliegenden Dissertation wurden bzw. werden folgende Publikationen erstellt:

Rischitor E. P., Konzack S. and Fischer R. (2004). The Kip3-like kinesin KipB moves along microtubules and determines spindle position during synchronized mitoses in hyphae of *Aspergillus nidulans. Eukaryotic Cell*. *In press*

Konzack S., Rischitor E. P. and Fischer R. (2004). The kinesin motor KipA is required for microtubule anchorage and maintenance of directionality of polar growth in *Aspergillus nidulans. Submitted*

Toews W. M., Warmbold J., Konzack S., Rischitor E. P., Veith D., Vienken K., Vinuesa C., Wei H. and Fischer R. (2004). Establishment of mRFP1 as fluorescent marker in *Aspergillus nidulans* and construction of expression vectors for high-throughput protein tagging using recombination *in vitro* (GATEWAY). *Current Genetics. In press*

”The most beautiful thing we can experience is the mysterious. It is the source of all true art and science. He to whom this emotion is a stranger, who can no longer pause to wonder and stand rapt in awe, is as good as dead: his eyes are closed.”

Albert Einstein, in 'What I Believe' 1930

Content

I. Summary 4

Zusammenfassung 6

Rezumat 8

II. Introduction 10

1. **Cytoskeleton** 12
   Microtubules 12
2. **Motor protein superfamilies** 14
3. **Kinesins** 15
   3.1. General structural features of kinesin motors 16
   3.2. Kinesin directionality and motility 17
   3.3. Kinesin motors as molecular machines 18
   3.4. Cellular function of kinesins 19
   3.5. Kip3 family of kinesins 20
   3.6. Kinesins in filamentous fungi 24
   3.7. Kinesin-like proteins of *Aspergillus nidulans* 26

III. Materials and Methods 28

1. **Equipment and chemicals** 28
2. **Organisms used in this study and microbiological methods** 29
   2.1. Organisms 29
   2.2. Cultivation and growing of microorganisms 31
   2.3. Growth conditions and storage of transformed *E. coli* and *A. nidulans* strains 32
   2.4. Determination of spore viability 32
   2.5. Induction of the *alcA* promoter 33
3. **Genetic methods in *A. nidulans*** 34
   3.1. Crossing of *A. nidulans* 34
   3.2. Construction of *A. nidulans* diploid strains 34
4. **Molecular biological methods** 35
   4.1. Plasmids and cosmids 35
   4.2. DNA manipulations 37
   4.2.1. Plasmid DNA preparation from *E. coli* cells 37
   4.2.2. Genomic DNA preparation from *A. nidulans* 37
   4.2.3. Digestion of DNA by restriction endonucleases 38
   4.2.4. Dephosphorylation of digested DNA 38
   4.2.5. DNA precipitation 38
   4.2.6. DNA ligation 39
   4.2.7. DNA agarose gel electrophoresis 39
   4.2.8. PCR 39
   4.2.9. Spore PCR 41
   4.2.10. DNA isolation from agarose gel 42
   4.2.11. DNA sequencing 42
   4.2.12. Transformation of *E. coli* 42

4.2.13. Transformation of *A. nidulans* 42
4.2.14. DNA-DNA hybridization (Southern blot analysis) 43
4.2.15. Colony hybridization 44
4.3. RNA manipulations 44
4.3.1. Isolation of total RNA from *A. nidulans* 44
4.3.2. DNA-RNA hybridization (Northern blot analysis) 45
4.4. Description of DNA constructs (plasmids) 46
4.4.1. Cloning of the *kipB* gene 46
4.4.2. Cloning of the *kipB* disruption construct (pPR13) 46
4.4.3. GFP labeling of KipB (pPR11; pPR38) 46
4.4.4. mRFP1-labeling of KipB (pPND1) 47
4.4.5. HA-labeling of KipB (pPR12) 47
5. **Biochemical methods** 47
5.1. Isolation of protein from *A. nidulans* 47
5.2. Determination of protein concentration (Bradford Assay) 48
5.3. SDS-Polyacrylamide gel electrophoresis (SDS-PAGE) 48
5.4. Western blotting 49
6. **Fluorescence microscopy, live-cell image acquisition and analysis** 50

IV. Results 51

1. **Cloning of the *kipB* gene** 51
2. **Analysis of the protein sequence** 54
3. **Molecular analysis of *kipB* functions** 58
3.1. *kipB* disruption 58
3.2. Disruption of *kipB* affects microtubule stability 62
3.3. KipB is involved in the positioning and morphology of mitotic spindles 64
3.4. *kipB* disruption causes a delay in mitotic progression 67
3.5. Genetic interaction of Δ*kipB* with *bimC4* 69
3.6. Gene dosage of *kipB* determines the frequency of chromosome loss in a diploid strain 70
3.7. Genetic interaction of Δ*kipB* with other motor protein mutants 72
3.8. KipB localizes to mitotic, astral and cytoplasmic microtubules 75

V. Discussion 82

1. **KipB is a member of the Kip3 kinesin family** 83
2. **Microtubule organization in the Δ*kipB* mutant** 85
3. **KipB is involved in spindle architecture, positioning and mitosis** 88
4. **Interactions of *kipB* with other genes** 96
5. **How to get to the end?** 97
6. **Conclusions and future directions** 100

VI. Literature 102

Abbreviations

Amp	Ampicillin
APS	Ammonium persulfate
BSA	Albumine bovine Fraction V
CM	Complete medium
DAPI	4',6-Diamidino-2-phenylindole
DEPC	Diethylpyrocarbonat
EDTA	Ethylenediamine tetraacetic acid
GFP	Green Fluorescent Protein
HA	Hemagglutinin epitope
IPTG	Isopropyl-β-D-thiogalactopyranoside
LB	Luria-Bertani-Medium
MM	Minimal medium
OM	Osmotic medium
PEG	Polyethylene glycol
RNase	Ribonuclease
RT	Room temperature
RT-PCR	Reverse-transcriptase-polymerase chain reaction
SAP	Shrimp alkaline phosphatase
SDS	Sodium dodecyl sulfate
TAE	Tris-Acetate-EDTA
TBS-T	Tris-buffered saline-Tween 20
TE	Tris-EDTA
TEMED	N, N, N', N'-Tetramethylene diamine
X-Gal	5-Brom-4-chlor-3-indoxyl-β-D-Galactoside

I. Summary

Molecular motors are protein machines, which power almost all forms of movement in the living world. Among the best known are the motors that hydrolyze ATP and use the derived energy to generate force. They are involved in a variety of diverse cellular functions as vesicle and organelle transport, cytoskeleton dynamics, morphogenesis, polarized growth, cell movements, spindle formation, chromosome movement, nuclear fusion, and signal transduction. Three superfamilies of molecular motors, kinesins, dyneins, and myosins, have so far been well characterized. These motors use microtubules (in the case of kinesines and dyneins) or actin filaments (in the case of myosins) as tracks to transport cargo materials within a cell.

Analysis of fungal genomes revealed at least 10 distinct kinesins in filamentous fungi, some of which are not found in yeasts. We used the motor domain of conventional kinesin (KinA) from *Aspergillus nidulans* to perfom BLAST searches at the public *A. nidulans* genome database, at the Whitehead Center for Genome Research (Cambridge USA), and identified eleven putative kinesin motors. They grouped into nine of the eleven families, two kinesins being found in the Unc104 familiy and interestingly, one did not fall into any of the known families.

The present work analyses the function of a kinesin-like protein in *A. nidulans*, KipB, which is a member of the Kip3 kinesin family. This family includes one representative in *Saccharomyces cerevisiae* (Kip3, the family founding member), two in *Schizosaccharomyces pombe*, Klp5 and Klp6 and one in *Drosophila*, Klp67A, the single one reported so far for higher eukaryotes in this family. Kip3 kinesins are implicated in microtubule disassembly and are required for chromosome segregation in mitosis and meiosis.

To assess the function of KipB kinesin in *A. nidulans*, a *kipB* disruption strain was constructed. Analysis of the Δ*kipB* mutant revealed new features concerning the cellular functions of Kip3 proteins, but also some conserved ones. *kipB* is not essential for vegetative growth, and meiosis and ascospore formation were not affected in the Δ*kipB* mutant.

The KipB protein was shown to be involved in the turnover of interphase cytoplasmic, mitotic and astral microtubules. Δ*kipB* mutants are less sensitive to the

microtubule-destabilizing drug benomyl, and the microtubule cytoskeleton of interphase cells in Δ*kipB* mutants appears altered. Interestingly, spindle morphology and positioning were severely affected. Spindles were highly mobile, could overpass each other, moved over long distances through the cytoplasm, and displayed in 64% of the cases an extremely bent shape, latter feature being the first time reported for Kip3 kinesins. Mitotic progression was delayed in the Δ*kipB* mutant and a higher number of cytoplasmic microtubules remained intact during mitosis. Δ*kipB* heterozygous strains showed an increased instability of diploid nuclei, which proved once more KipB involvement in mitosis, along with Δ*kipB* clear genetic interaction with a mutation in another mitotic kinesin in *A. nidulans*, *bimC4*.

An N-terminal GFP-KipB construct localized to cytoplasmic microtubules in interphase cells and to spindle and astral microtubules during mitosis, in a discontinuous pattern. Speckles of GFP-KipB appeared to be aligned in the cell. Time-lapse video microscopy indicated that the spots were moving independently towards the microtubule plus ends. This advanced the hypothesis that KipB could display processivity and intrinsic motility along microtubules, or that other kinesins involved in organelle motility are able to target the KipB protein to the microtubule plus ends. In the case of C-terminally truncated GFP-KipB protein versions, a stronger GFP signal was obtained and colocalization with α-tubulin-GFP revealed that they uniformly stain cytoplasmic, mitotic and astral microtubules. This suggests that the C-terminus is important for the correct localization and the movement of KipB protein along microtubules.

Zusammenfassung

Molekulare Motoren sind Maschinen, die fast alle Bewegungsvorgänge in lebenden Organismen antreiben. Die am besten untersuchten Motoren hydrolysieren ATP und nutzen die Energie, um Kraft zu erzeugen. Sie sind an einer Vielzahl von zellulären Funktionen beteiligt, wie z.B. dem Vesikel- und Organelltransport, der Steuerung der Cytoskelettdynamik, der Morphogenese, dem polaren Wachstum, Zellbewegungen, der Spindelbildung, der Chromsomenbewegung, der Zellkernfusion und der Singaltransduktion. Drei Superfamilien von molekularen Motoren, Kinesin, Dynein und Myosin, sind sehr gut untersucht. Diese Motoren benutzen Mikrotubuli (im Falle von Kinesin und Dynein) oder Aktinfilamente (im Falle von Myosin) als Schienen, um Cargoes in der Zelle zu transportieren.

Die Analyse von pilzlichen Genomen ergab das Vorhandensein von mindestens 10 verschiedenen Kinesinen in filamentösen Pilzen, von denen einige nicht in der Bäckerhefe vorkommen. Eine BLAST-Suche der genomischen *A. nidulans* Datenbank am Whitehead Center for Genome Research (Cambridge, USA) mittels der Motordomäne von konventionellem Kinesin (KinA) aus *A. nidulans* ergab elf mögliche Kinesinmotoren, die in neun der elf Familien eingruppiert werden konnten. Interessanterweise wurden zwei Vertreter der Unc104-Familie gefunden und ein *A. nidulans*-Kinesin konnte in keine der beschriebenen Familien eingeordnet werden.

In der vorliegenden Arbeit wurde das kinesin-ähnliche Protein, KipB, in *Aspergillus nidulans* untersucht. KipB gehört zur Familie der Kip3 Kinesine. Diese Familie besitzt einen Vertreter in *Saccharomyces cerevisiae* (Kip3, das namensgebende Kinesin), zwei in *Schizosaccharomyces pombe*, Klp5 und Klp6 und einen in *Drosophila*, Klp67A, das einzige bekannte Kinesin dieser Familie in höheren Eukaryoten. Kip3-Kinesine sind an der Mikrotubulidepolymerisierung beteiligt, und werden für die Chromsomentrennung während der Mitose und Meiose benötigt.

Das *kipB*-Gen wurde im Genom von *A. nidulans* deletiert und der Phänotyp untersucht. Das Gen war nicht essentiell für das vegetative Wachstum oder die asexuelle oder sexuelle Differenzierung. In der Mutante war allerdings die Dynamik aller Mikrotubuli in der Zelle, wie z.B. der interphase, cytoplasmatischen, der mitotischen und der astralen Mikrobutuli gestört. *ΔkipB*-Mutanten waren weniger

empfindlich gegenüber dem mikrotubuli-destabilisierenden Agens Benomyl und das Mikrotubulicytoskelett der Zellen erschien verändert. Interessanterweise war die Spindelpositionierung und die Spindelmorphologie stark beeinträchtigt. Die Spindeln waren sehr mobil und bewegten sich über lange Strecken im Cytoplasma, wobei sie sich teilweise aneinander vorbei bewegten. In 64 % der Fälle erschien die Spindel stark gebogen. Der Verlauf der Mitose war verlangsamt und cytoplasmatische Mikrotubuli waren auch während der Mitose zu sehen, obwohl diese in Wildtypzellen depolymerisiert werden. *ΔkipB*-Mutantenstämme zeigten eine erhöhte Instabilität der diploiden Zellkerne, was wiederum eine Rolle von KipB in der Mitose belegt. Ausserdem wurde eine genetische Interaktion mit einer Mutation in einem weiteren Kinesingen, *bimC4*, gefunden.

Das KipB-Protein wurde durch eine N-terminale GFP-Fusion subzellulär in einer punktförmigen Verteilung entlang von cytoplasmatischen Mikrotubuli in Interphasezellen und an Spindel- und astralen Mikrotubli während der Mitose, lokalisiert. Die GFP-KipB Punkte bewegten sich unabhängig voneinander entlang der Mikrotubuli. Diese Bewegung könnte durch eine eigene Motoraktivität oder durch andere Motoren hervorgerufen werden. Wenn das Protein zu den Mikrotubuli-Plusenden gelangt, depolymerisiert es die Filamente. C-terminal verkürzte Versionen von KipB, die mit GFP fusioniert wurden, lokalisierten gleichmäßig entlang der Mikrotubuli.

Rezumat

Motoarele moleculare sunt maşini proteice care guvernează aproape toate formele de mişcare din lumea vie. Printre cele mai cunoscute dintre ele se numără şi motoarele care hidrolizează ATP şi folosesc energia obținută astfel pentru a genera forță. Aceste motoare sunt implicate in multiple funcții celulare, cum ar fi transportul veziculelor şi al organitelor, dinamica citoscheletului celular, morfogeneza, fuziunea nucleelor in celulă, precum şi transmiterea semnalelor celulare. In momentul de față, trei superfamilii de motoare moleculare au fost caracterizate: kinezinele, dineinele si miozinele. Kinezinele si dineinele folosesc microtubulii, iar miozinele filamentele de actină pentru a asigura transportul biomoleculelor in interiorul celulei.

Analiza genomurilor din fungi a dezvăluit prezența a cel puțin 10 kinezine in fungii filamentoşi, dintre care câteva nu se regăsesc in drojdii. Noi am folosit domeniul motor al kinezinei convenționale (*kinA*) din *Aspergillus nidulans* pentru a efectua cautări de tip BLAST in baza publică de date a genomului din *A. nidulans* la Whitehead Center for Genome Research, în Cambridge USA şi am putut identifica 11 potențiale kinezine motoare. Ele se grupează in 9 din cele 11 familii, două fiind găsite in familia de kinezine Unc-104 si în mod interesant, una dintre ele nu s-a grupat in nici una dintre familiile cunoscute.

În prezenta lucrare se analizează funcția unei proteine de tip kinezină (în *A. nidulans*) numită *kipB*, aceasta facând parte din familia de kinezine Kip3. Această familie cuprinde un reprezentant in *Saccharomyces cerevisiae* (Kip3, kinezina care a fondat familia), doi in *Schizosaccharomyces pombe*, Klp5 and Klp6 si unul in *Drosophila*, Klp67A, de altfel singura kinezină din această familie raportată până in prezent in eucariote. Kinezinele din familia Kip3 sunt implicate in dezasamblarea microtubulilor şi sunt necesare pentru segregarea cromozomilor in mitoză şi meioză.

Pentru a stabili funcția kinezinei KipB in *A. nidulans* s-a creat o tulpină mutantă în *kipB* (Δ*kipB*), în care gena *kipB* a fost distrusă prin înlocuirea unei porțiuni a regiunii de transcripție (ORF) cu gena *argB* pentru un marker nutritiv in *A. nidulans*. Analiza mutantului Δ*kipB* a dezvăluit elemente noi în ceea ce priveşte funcția proteinelor de tip Kip3-kinezine, dar si anumite funcții conservate in această familie. Gena *kipB* nu este esențială pentru creşterea vegetativă a fungului *A. nidulans*, iar meioza si formarea ascosporilor nu au fost afectate in Δ*kipB*.

S-a demonstrat în lucrarea de față ca proteina KipB este implicată în stabillitatea microtubulilor citoplasmatici în interfază, dar şi în mitoză, în stabilitatea microtubulilor astrali. Mutanții Δ*kipB* sunt mai puțin sensibili la o substanță cu proprietatea de depolimerizare a microtubulilor numită benomyl, iar structura microtubulilor celulelor in interfază aparținând tulpinei mutante apare modificată. Foarte interesant, poziționarea şi morfologia fusului de diviziune sunt puternic afectate in acelaşi mutant. Fusurile de diviziune au apărut in Δ*kipB* extrem de mobile, cu capacitatea de a se dispune in paralel unele față de altele in lungimea hifei, iar forma acestora a fost în 64% din cazuri sever cubată. Aceste observații au fost in contrast cu forma şi comportarea fusurilor de diviziune în mitoză din forma sălbatică de *A. nidulans*, în care fusurile se dispun în locuri fixe şi la distanțe egale unele de altele, iar forma lor este dreaptă şi fără curburi. Progresia în mitoză a fost întârzâiată în Δ*kipB*, în plus, un număr crescut de microtubuli citoplasmatici a rămas intact si nedepolimerizat in celulă. Tulpinile heterozigote Δ*kipB* împreună cu forma sălbatică au prezentat o instabilitate crescută a nucleilor diploizi pentru benomyl, ceea ce a demonstrat încă o dată implicarea proteinei KipB în mitoză, alături de interacțiunea genetică a Δ*kipB* cu mutantul termosenzitiv *bimC4*, BimC fiind altă kinezină implicată în mitoză in *A. nidulans*.

Localizarea subcelulară a kinezinei KipB s-a făcut prin intermediul unui construct genetic ce a constat in fuzionarea KipB cu o proteină-marker fluorescentă (GFP-green fluorescent protein). Semnalul fluorescent s-a localizat in formă discontinuă punctată impreună cu microtubulii citoplasmatici în interfază si cu microtubulii astrali în mitoză. Observațiile microscopice au indicat că punctele fluorescente se mişcă independent spre capătul plus (+) al microtubulilor. Aceasta a îndreptățit ipoteza că kinezina KipB poate prezenta procesivitate şi motilitate de-a lungul microtubulilor, sau că alte kinezine implicate în mişcarea biomoleculeor in celulă pot direcționa proteina KipB spre capătul plus (+) al microtubulilor. În cazul formelor de KipB incomplete în C-terminal, s-a observat un semnal GFP mai puternic, iar colocalizarea cu α-tubulină-GFP a arătat ca aceste forme marchează microtubulii citoplasmatici, mitotici şi astrali în toată lungimea lor. Aceasta a sugerat că regiunea C-terminală a kinezinei KipB este importantă pentru localizarea corectă şi pentru mişcarea ei de-a lungul microtubulior.

II. Introduction

A cell, like a metropolitan city, must organize and deal permanently with its restless macromolecule community. Designating meeting points and deciding the right timing for different molecules implicated in cell traffic are of fundamental importance in management of the processes inside the cell. Just as disruption of commercial traffic impairs the welfare of a city, defective molecular transport can result in developmental defects as well as cardiovascular and neuronal diseases (Vale & Milligan, 2000).

Within every living cell exists a complex highway system of motors that move along filamentous tracks. Biomotors and the tracks they move on are ubiquitous in the myriad processes occurring within the cell. They are responsible for muscle contraction, cell division, and transport of vesicles. They also power bacteria's flagella and the cilia within our lungs. These systems serve as host of other cellular functions, many of which we are only beginning to understand. Examples are the "highway systems" which serve structural, transport and motility purposes, and which also may provide a communication function across the intercellular environment. Interest in motor proteins has expanded enormously in recent years. They provide fascinating systems for understanding how proteins use ATP energy to power thermodynamically unfavourable events, like the unidirectional motion.

From a cell biological perspective, these motors are involved in virtually every imaginable cell biological process (Fig. II.1). Their function involves well-known mechanical activities, such as mitosis, cytokinesis and cell migration. However, there are also some recently discovered molecular motors with unanticipated roles, such as involvement in signal transduction pathways (Schnapp, 2003).

Landmark discoveries of cytoplasmic transport have been, and continue to be, made through advances in microscopy. The development of video-enhanced contrast microscopy in the early 1980s enabled the visualization of small membranous organelles (Allen et al., 1982) and large protein complexes (Kozminski et al., 1993). With this clearer view of the cell interior, the tremendous amount of directed cytoplasmic motion became apparent. The use of the green fluorescent protein for tagging organelles, proteins, and RNA led to another wave of discovery of

intracellular movement. In addition, recent genomic sequencing projects have uncovered the complete inventories of molecular motors in several organisms. Such data, combined with information from functional studies, are providing clues on the origins of the molecular motors and the intracellular transport strategies employed by various organisms. While prokaryotes contain cytoskeletal filaments, the cytoskeletal motors appear to be an early eukaryotic invention. The complexity of these so-called "Toolbox" motors expanded in higher eukaryotes through gene duplication, alternative splicing, and the addition of associated subunits, which enabled new cargoes to be transported. Remarkably, fungi, parasites, plants, and animals have distinct subsets of Toolbox motors in their genomes, suggesting an underlying diversity of strategies for intracellular transport (Vale, 2003).

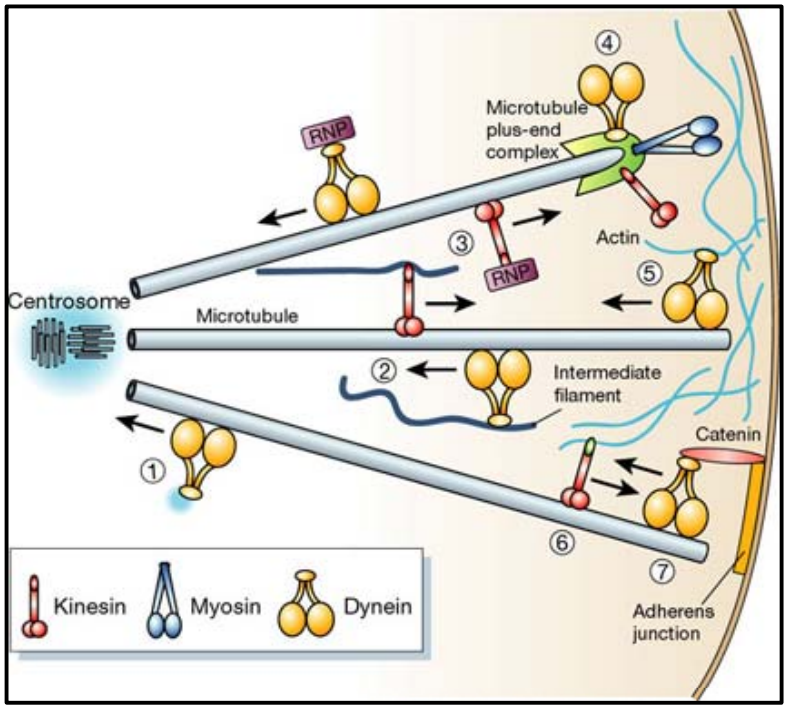

Fig. II.1: Summary of diverse roles of cytoskeletal motors. (1) Retrograde transport of centrosomal components. **(2)** Anterograde and retrograde transport of intermediate filaments. **(3)** Anterograde and retrograde transport of ribonucleoprotein (RNP) complexes. **(4)** Myosin, kinesin and dynein motors interact with components of the microtubule plus-end complex. **(5)** Anchorage of dynein at the actin-rich cell cortex. **(6)** Interaction of a kinesin-like protein with actin. **(7)** Catenin-mediated anchorage of dynein at adherens junctions. (Taken from Schliwa & Woehlke (2003))

1. Cytoskeleton

Cell movements are produced by large structures built of many different protein molecules, which together form the cytoskeleton. This is a distinct part of the cell: a cohesive meshwork of filaments formed by the self-assembly of protein molecules (Bray, 1992). The cytoskeleton of eukaryotic cells pervades the cytoplasm. It comprises three broad classes of proteins: actin filaments, microtubules and intermediate filaments. In addition to establishing cell and tissue shape, the cytoskeleton — along with associated motor proteins — influences a wide range of fundamental cellular functions, including cell migration, movement of organelles and cell division. The cytoskeleton is now no longer considered to be a rigid scaffold, but instead is viewed as a complex and dynamic network of protein filaments that can be modulated by internal and external cues. Because the present work analyses the function of a kinesin-like protein (KipB), which has strong influence onto the stability of microtubules in hyphae of *Aspergillus nidulans*, the following chapter will introduce briefly just this component of the cytoskeleton.

Microtubules

Microtubules are key actors in the cytoskeleton of eukaryotic cells. Together with actin filaments they play an important role in organising the spatial distribution of organelles within the cell and they can be either extremely stable as is the case in cilia and flagella or very dynamic as in the mitotic spindle. Microtubules are ~25 nm diameter hollow tubes with walls made from tubulin heterodimers (α- and β-tubulin) interacting head-to-tail to form protofilaments aligned lengthwise along the microtubule (Fig. II.2). Microtubules in eukaryotic cells consist of thirteen protofilaments, some exceptions to this rule being noted, as microtubules with 8 to 20 or more protofilaments in *Caenorhabditis elegans* (Savage et al., 1989). Microtubules have both a structural and a dynamic polarity. The structural polarity is conferred by the alignment of the tubulin heterodimer along the protofilament. During in vitro assembly, microtubules show a dynamic polarity with one end, called the plus end, growing and shrinking more quickly than the other. In the cell, microtubules grow out from the microtubule organizing centre (MTOC) towards the cell membrane with the plus end leading. They usually remain attached to the MTOC by their minus end. γ-

tubulin, a protein highly homologous to the α/β-tubulins is also localized at the MTOC and plays an important role in microtubule nucleation by interacting with α-tubulin (Oakley, 2004). Microtubules are highly dynamic, and exhibit a nonequilibrium behavior termed dynamic instability. In this process, microtubules undergo rapid stochastic transitions between growth and shrinkage, due to the association and dissociation, respectively, of tubulin dimers from the microtubule ends. The transition from growing to shrinking is termed a catastrophe, whereas the reverse behavior is referred to as a rescue (Desai & Mitchison, 1997; Howard & Hyman, 2003) (Fig. II.2).

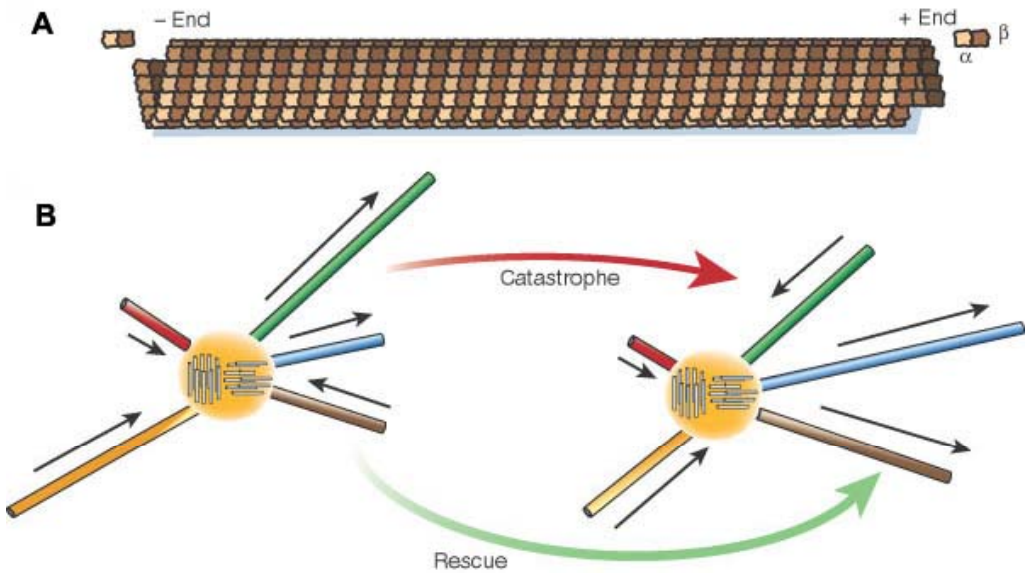

Fig. II.2: Microtubule structure and dynamics. **(A)** Microtubule lattice. The α-subunit of tubulin is at its minus end and the β-subunit at the plus end. **(B)** Dynamic instability of microtubules. Microtubules growing out from a centrosome switch between phases of growing and shrinking. The figure shows a hypothetical aster at two different times. The different colours represent different microtubules. The red and yellow microtubules are shrinking at both times. The blue microtubule is growing at both times. The green microtubule, growing at the first time, has undergone a catastrophe by the second time. The brown microtubule, shrinking at the first time, has undergone a rescue by the second time. (Revised after Howard et al., (2000)).

The microtubule networks provide directional pathways for dynein and kinesin and, together with these motors, engage in intracellular transport, the organisation of organelles in the cytoplasm and in cell division. (Wade et al., 1998). Microtubules function thus as (i) an internal scaffold that provides structural support and helps maintain the position of cytoplasmic organelles; (ii) the motile elements of cilia and flagella; (iii) a part of the molecular machinery that moves materials and organelles

from one part of a cell to another: (iv) active components in chromosome separation during mitosis and meiosis (Karp, 1996).

2. Motor protein superfamilies

Molecular motors are amazing biological machines that are responsible for most forms of movement we encounter in the cellular world. Three types of cytoplasmic motors, which form also three superfamilies are known: myosins, which move on actin filaments, and dyneins and kinesins, which use microtubules as tracks. The mechanism they use to convert chemical energy into mechanical work is both simple and ingenious. In all three motor classes, ATP hydrolysis causes a small conformational change in a globular motor domain that is amplified and translated into movement with the aid of accessory structural motifs. Additional domains outside the motor unit are responsible for dimerization, regulation and interactions with other molecules (Schliwa, 2003).

The founding member of the myosin family, filament-forming class II muscle myosin, was discovered nearly a century ago, and its role in muscle contraction has been studied extensively. Because of the large amount of knowledge acquired regarding the properties, myosin II is referred to as “conventional” myosin; all other types of myosin are referred to as “unconventional” (Schliwa, 2003). Dynein was first discovered in cilia in the early 1960s and later shown to be present in the cytoplasm of all eukaryotic cells. Kinesin was identified in squid and mammalian brain in the mid 1980s using *in vitro* motility assays (Vale et al., 1985).

The affiliation to a motor superfamily is amino acid identity within the motor domain, a region of the polypeptide, which is responsible for force generation and is situated at the N-terminus. Albeit there are defined “signature” motifs in the regions that contact nucleotide or polymer, which display even greater identity, the overall amino acid identity for this domain is 20-60%. In the case of myosin, the motor domain consists of a region of about 800 amino acids that includes actin- and nucleotide-binding sites. Dynein exhibits a less precise perimeter of the motor domain, but conservation between family members extends over most of its large ~ 4500 amino acids polypeptide chain. For kinesin, the conserved region containing the

microtubule- and nucleotide-binding regions is significantly smaller, and is represented by ~ 320 amino acids.

The non-motor regions or “tail” domains can differ considerably in size, structure and amino acid sequences, particularly among members of the kinesin and myosin motor superfamilies. These domains are thought to play roles in determining the biological functions of the motor proteins, and confer unique self-assembly properties (e.g. oligomerization or filament formation) as well as binding interactions, as the connection to cargoes or attachment of motors to the membranes (Kreis & Vale, 1999). However, relatively little is known about motor protein cargo, and even less is known about how motor proteins interact with their cargo or how this regulates transport. It is now well documented that motors can move many other types of cargo, including protein complexes and complexes of nucleic acids with proteins. The ability of motor proteins to transport such a wide array of cargo is due, in part, to the fact that the tail domains are quite divergent from one another. This has allowed them to evolve into adaptors, linking themselves to cargo through interactions with receptor proteins on the cargo surface (Karcher et al., 2002).

3. Kinesins

Although of the same importance and interest, dyneins and myosins will not be treated further in detail, because they do not represent the topic of this study. The focus will be instead oriented to the kinesin motor superfamily, with an emphasis on kinesin families in direct connection with the KipB kinesin analysed in the present work.

The microtubule motor protein kinesin, also known as conventional kinesin, was identified in 1985 as the motile force underlying movement of particles along the microtubules of the giant axon of the squid (Vale et al., 1985). Kinesin was shown to be capable of binding to microtubules and, in the presence of ATP, of moving towards the fast polymerizing/depolymerizing plus ends of microtubules, representing the first cytoplasmic microtubule motor protein to be discovered. Kinesin motor proteins have been found in all eukaryotes examined to date, including the protista, fungi, invertebrates, animals and higher plants. The number of kinesins identified to date in genomes that have been fully sequenced and at least partially annotated

varies from 6 in budding yeast to 19 in *C. elegans*, 24 in *Drosophila*, 45 in humans and 61 in *Arabidopsis* (Endow, 2003).

3.1. General structural features of kinesin motors

In 1990, the first hint of the existence of a kinesin superfamily emerged when genes were discovered in *S. cerevisiae* (Meluh & Rose, 1990) and *A. nidulans* (Enos & Morris, 1990) that contain a ≈350 amino acid region, which is 30-40% identical to the motor domain of the first discovered kinesin (termed conventional kinesin). Beyond the boundary of the motor domain, however, the sequences of these two kinesin-related proteins show no similarity to one another or to conventional kinesin. These findings suggested that a highly conserved motor domain had become combined with different non-motor domains that could target motors to different cargo within the cell and allow them to carry out unique force-generating functions. Motor domain refers to the force-producing element of the protein, which is itself divided into two major parts: one part, the globular catalytic core, is conserved throughout the superfamily and its three-dimensional structure has been solved. The second part termed the neck region is an adjacent ~40 amino acids found on either the N or C terminus of the catalytic core. The neck, which is conserved only within certain kinesin classes, appears to work in concert with the catalytic core to produce movement. Beyond the motor domain, many kinesin proteins contain a long α-helical coiled-coil domain termed the stalk. Finally, there is often an additional globular domain at the end of the stalk. This domain, the tail, is thought to target the motor to a particular cargo within the cell (Fig. II.3) (Vale & Fletterick, 1997).

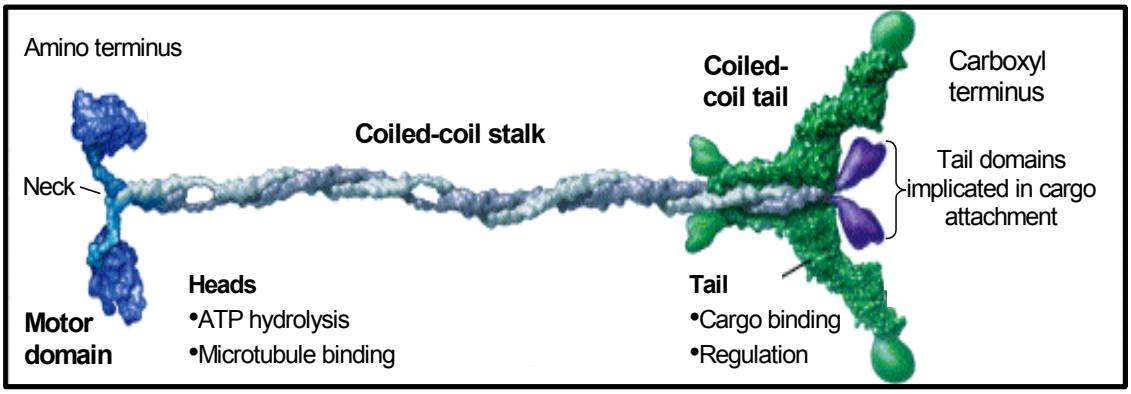

Fig. II.3: The "Toolbox" of cargo-transporting motor protein kinesin. The motor catalytic domains are displayed in blue, mechanical amplifiers in light blue, and tail domains implicated in cargo attachment are shown in purple. Tightly associated motor subunits (light chains) are shown in green (Modified after Vale, 2003).

3.2. Kinesin directionality and motility

Kinesin motors can be categorized on the basis of several features of their movement along microtubules. The first of these is directionality of movement. Minus-end kinesin motors move toward the more stable minus ends of microtubules, whereas plus-end motors move in the opposite direction, toward the dynamic plus ends. Most of the kinesin proteins, whose directionality has been determined, including conventional kinesin, are plus-end motors; *Drosophila* Ncd and other C-terminal motor kinesins are minus-end motors. To date, there is an absolute correlation between kinesin directionality and domain organization; all minus-end kinesins have their motor domain C-terminal to the coiled-coil stalk (Badoual et al., 2002). Directionality of kinesin movement is now believed to be a property associated with the neck. By constructing and analyzing chimeric motors between plus- and minus-end kinesins (Case et al., 1997; Endow & Waligora, 1998), or mutating the neck of native motors, researchers have shown that the neck of the Ncd motor is required for minus-end motor directionality. Not only can the Ncd neck confer minus-end directionality on a conventional kinesin catalytic domain (Endow & Waligora, 1998), but remarkably, mutation of a single neck residue of Ncd causes the motor to move in either direction on microtubules (Endow & Higuchi, 2000). So, disrupting the neck-motor interactions causes the motor to move in either direction along the

microtubule, indicating that the interactions are essential for directed movement of the motor to the microtubule ends.

A second property of motor movement that can be used to categorize kinesins is processivity. Processive motors take multiple steps along a microtubule before dissociating from the filament, whereas nonprocessive motors take only a single step before dissociation. Conventional kinesin is a highly processive motor that moves several microns along the microtubule before detaching, a distance corresponding to several hundred 8-nm steps (Svoboda et al., 1993). In contrast to conventional kinesin, the *Drosophila* motor Ncd is not only minus-end directed, but also is a nonprocessive kinesin protein (Endow & Barker, 2003).

3.3. Kinesin motors as molecular machines

Remarkably, motor proteins hydrolyze nucleotides and translocate along a filament, converting chemical energy from ATP hydrolysis directly into work without undergoing an intermediate heat or electrical conversion step, as do man-made machines.

Kinesin is expected to undergo several small conformational changes that may comprise several working strokes, culminating in 8 nm steps along the microtubule; thus understanding the mechanism by which the motor walks along the microtubule is essential to understand how the motor works. The nucleotide state of the two heads at each substep of the motor along the microtubule must be established, together with the conformational changes that occur and the changes that result in the force-generating strokes of the motor. The stepping mechanism of conventional kinesin is currently controversial: most workers favor a hand-over-hand mechanism in which the two heads of the motor bind alternatively to the microtubule and hydrolyze ATP (Fig. II.4, A, see also movie 1) (Schliwa, 2003). However, some researchers have proposed a model in which only one of the two heads hydrolyzes ATP and advances in an ‘‘inchworm’’ fashion along the microtubule, dragging the second head along (Fig. II.4, B and C) (Hua et al., 2002). The recent work found that some kinesin molecules exhibit a marked alternation in the dwell times between sequential steps, causing these motors to "limp" along the microtubule. Limping implies that kinesin molecules strictly alternate between two different conformations as they step,

indicative of an asymmetric, hand-over-hand mechanism (Fig. II.4, D) (Asbury et al., 2003).

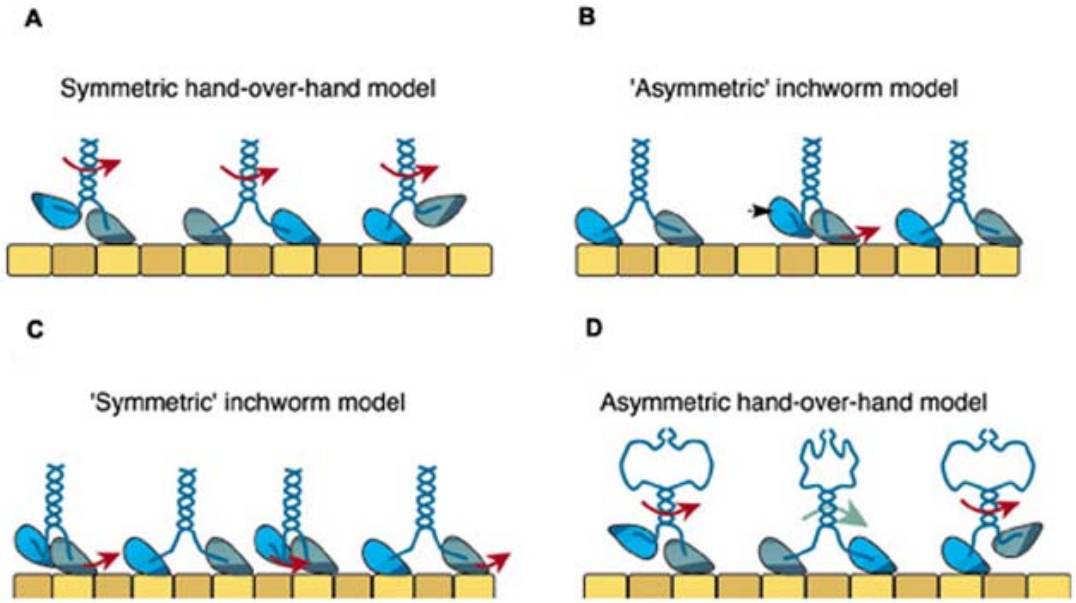

Fig. II.4: Models for kinesin stepping. (A) In the symmetric hand-over-hand model, the trailing head always passes the leading head on the same side (red arrows in front of the coiled-coil neck). **(B)** In the asymmetric inchworm model, only the leading head hydrolyses ATP while the trailing head is pulled up passively. Here, 'asymmetric' refers to ATP hydrolysis occurring only in one head. **(C)** In a symmetric inchworm model, both heads would hydrolyse ATP, and hydrolysis in the trailing head would push the leading head forward. **(D)** In an asymmetric hand-over-hand model, torsion generated during a step would be accommodated by the flexible hinge domain above the neck during one step (red arrow) and relieved by uncoiling in one of the next step(s), as shown by the green arrow behind the neck. (Taken from Schliwa, (2002)).

3.4. Cellular function of kinesins

Conventional kinesin and other members of the kinesin family bind ATP and microtubules at specific sites in their conserved motor domain, and use the energy from ATP hydrolysis to produce force and move along microtubules. The nonmotor region of the motor protein is believed to interact with other proteins or cellular components, enabling the motors to perform essential roles in vesicle and organelle transport, spindle function and chromosome motility, and regulation of microtubule dynamics. The large number of kinesin proteins in many organisms has given rise to the idea that different kinesin proteins could bind to specific vesicles or organelles and transport them between cellular compartments. The adaptor or receptor proteins

that couple kinesin motors to proteins associated with membrane-bounded cargo have recently begun to be identified using genetics, yeast two-hybrid screens, and coprecipitation by antibodies. Several of the adaptor or receptor proteins identified so far are components of large complexes that may include other receptor and signaling proteins, e.g. the AP-1 adaptor complex (Nakagawa et al., 2000), amyloid precursor protein (Kamal et al., 2000) and JNK signaling pathway interacting proteins (Verhey et al., 2001).

Besides their roles in vesicle and organelle transport, a large number of kinesin proteins have been implicated in chromosome distribution by their localization to the meiotic/mitotic apparatus or mutant effects on spindles or chromosomes. The motors can bind to and crosslink spindle fibers and use energy from ATP hydrolysis to move directionally along microtubules, performing essential roles in spindle assembly and maintenance, centrosome duplication, and attachment of centrosomes to poles. Several of the kinesin motors are associated with chromosomes and may play a role in mediating chromosome attachment to the spindle (Levesque & Compton, 2001) or congression to the metaphase plate (Wood et al., 1997).

Unexpectedly, some kinesin microtubule motor proteins have been found to destabilize or depolymerize microtubules, providing a link between regulation of microtubule depolymerization and assembly, and force-producing proteins associated with the spindle and chromosomes (Endow, 2003).

3.5. Kip3 family of kinesins

Kip3 kinesin was discovered as the sixth and the final kinesin-related gene in *S. cerevisiae* and is the founding member of a new kinesin family named Kip3 (Lawrence et al., 2002; West et al., 2001).

The Kip3 protein is involved in nuclear migration in *S. cerevisiae*, by moving the nucleus to the bud site in preparation for mitosis. Interphase nuclei are pushed around in the mother cell through growing and shrinking microtubules emanating from the spindle pole body. Prior to mitosis nuclei move towards the budding neck. This first movement depends on the function of Kip3 whereas the subsequent distribution of the two daughter nuclei is dependent on cytoplasmic dynein, microtubules and cortex-associated proteins as Num1, which is an essential element of the cortical attachment mechanism for dynein-dependent sliding of microtubules in

the bud. (DeZwaan et al., 1997; Heil-Chapdelaine et al., 2000, Miller et al., 1998,). Microtubules emanate from the spindle pole body and grow towards the cortex. Associated to the growing plus ends are several proteins, which are delivered at the cortex and in turn mediate contact between astral microtubules and the cortex (Gundersen & Bretscher, 2003; Maekawa et al., 2003). Deletion of Kip3 in *S. cerevisiae* did not impair vegetative growth and caused only a slight increase of binucleate mother cells at low temperature. These effects were much stronger in dynein (*dyn1)* deletion strains at low temperature and largely increased in *kip3/dyn1* double mutants at high temperature. These results suggested that Kip3 is responsible for spindle positioning in the absence of dynein and thus serves overlapping functions with this motor (Cottingham et al., 1999; Cottingham & Hoyt, 1997).

Recently, two other Kip3 homologous kinesins, Klp5 and Klp6, were characterized in the yeast *Schizosaccharomyces pombe*, with catalytic properties similar to those of KinI kinesins (Garcia et al., 2002; Garcia et al., 2002; West et al., 2002; West et al., 2001). The biological function of the KinI family members is less clear than in the case of conventional kinesin. The KinI family received this nomenclature due to the location of the motor domain and the structure of the protein (Ovechkina & Wordeman, 2003). Kinesins of this family are monomeric proteins and are not able to move along microtubules in the conventional sense but instead catalyse the depolymerization of microtubules *in vivo* and *in vitro* (Desai et al., 1999; Hunter et al., 2003; Moores et al., 2002). In mammals a KinI protein, CgMCAK localizes to the kinetochores in early prophase and MCAK deficiency results in chromosome segregation defects. This may be explained through an altered microtubule depolymerization rate. Overexpression of the gene resulted in depolymerization of cytoplasmic and spindle microtubules suggesting roles of this kinesin family also outside of mitosis (Maney et al., 1998). The studies of KinI kinesin family members in different organisms demonstrate that despite similar biochemical properties the cellular processes affected may be different. Hence, although the members of KinI and Kip3 families appear to have closely related functions, such as the microtubule depolymerization, the placement of their motor domains is different (central in KinI and N-terminal in Kip3), in consequence they are still described as separate entities until more data and phylogenetic analysis prove otherwise (Schoch et al., 2003).

In *S. pombe*, Klp5 and Klp6 are structurally very similar and deletion of either one or of both is not lethal (West et al., 2001). In contrast to *S. cerevisiae kip3* mutants, nuclear migration is not affected in Δ*klp5* or Δ*klp6* strains. However, microtubules are stabilized in both fungi and mitosis and meiosis are impaired in *S. pombe* (West et al., 2002). Klp5 and Klp6 are required for normal chromosome movement in prometaphase, although this function is not essential for successful mitosis. On the other hand the two kinesins are essential for meiosis (West et al., 2001). Klp5/6-GFP fusion proteins localized to spindle and cytoplasmic microtubules with no bias to either the plus or the minus end of the filaments (Garcia et al., 2002; West et al., 2001).

Other studies have also shown that in *klp5* mutants, spindle checkpoint proteins Mad2 and Bub1 are recruited to mitotic kinetochores for a prolonged duration, indicating that these kinetochores are unattached. Further analysis showed that there are kinetochores to which only Bub1, but not Mad2, localizes. These kinetochores are likely to have been captured, yet lack tension. Thus Klp5 and Klp6 appear to play a role in a spindle-kinetochore interaction at dual steps, capture and generation of tension. Two other proteins, Alp14 and Dis1, belonging to the TOG/XMAP215 family (its protein members play a positive role in microtubule stability by stimulating the growth rate at the plus end, are important for spindle formation, and localize to the spindle poles) are known to stabilize microtubules and be required for the bivalent attachment of the kinetochore to the spindle (Garcia et al., 2001). Despite apparent opposing activities towards microtubule stability, Klp5/Klp6 and Alp14/Dis1 share an essential function, as either *dis1klp* or *alp14klp* mutants are synthetically lethal, like *alp14dis1*. Therefore, it was proposed that Klp5/Klp6 and Alp14/Dis1 play a collaborative role in bipolar spindle formation during prometaphase through producing spindle dynamism (Fig. II.5) (Garcia et al., 2002).

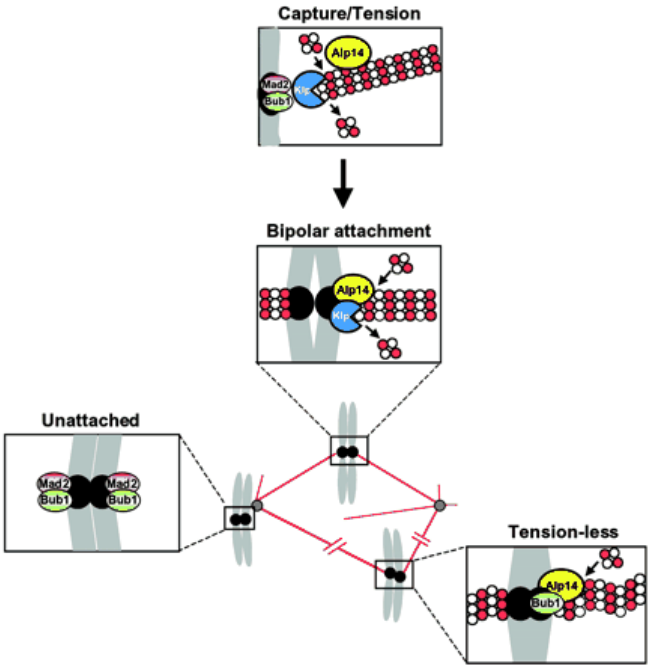

Fig. II.5: Role for Klp5/Klp6 and Alp14/Dis1 in the formation of bipolar mitotic spindles. Alp14 and Dis1 (shown as Alp14 in the figure) localize to both the mitotic spindles (shown by filaments consisting of tubulin dimers (white and red circles)) and the mitotic kinetochores (closed black circles). Klp5 and Klp6 (shown as Klp) also localize to the mitotic kinetochores. In their absence, the major defect is failure in the attachment of the kinetochores to which Bub1 and Mad2 localize. Furthermore, at least Klp5 and Klp6 have an additional role in generation of tension at the kinetochores upon attachment. In the absence of Klp5 and Klp6, the kinetochores fail to produce tension, as the spindles tend only to polymerize without the poleward force (depicted by wavy spindles). These tension-less kinetochores recruit Bub1, but not Mad2 (Taken from Garcia et al., (2002)).

A very recent report suggested that Klp5/6 cooperate with the Ras1-Scd1 pathway to influence proper formation of the contractile ring for cytokinesis (Li & Chang, 2003). Ras G proteins act as molecular switches for signal transduction pathways that are important for cell proliferation, differentiation, cell death, and organization of the cytoskeleton. Ras1 is the only Ras G protein in *S. pombe*, and has two distinct outputs. Ras1 activates Scd1, a presumptive guanine nucleotide exchange factor (GEF) for Cdc42 (a member of the Rho GTPase subfamily, which participates in many signalling pathways, but is particularly important in cytoskeletal remodelling (Etienne-Manneville & Hall, 2002)), to control morphogenesis and chromosome segregation, and Byr2, a component of a mitogen-activated protein kinase cascade, to control mating (Papadaki et al., 2002). Klp5/6 can form a complex with both Scd1 and Cdc42; furthermore, inactivation of Klp5/6 together with inactivation of the Ras1-

Scd1 pathway leads to abnormal cytokinesis. The abnormal cytokinesis appears to be caused by improper contractile ring formation, as the double-mutant cells frequently contain F-actin rings that are either mispositioned or fragmented in the cell cortex. Klp5 and Klp6 are thus likely to influence cytokinesis in a microtubule-dependent fashion and may act as plus-end motors to play a role in transporting cytokinesis regulatory proteins (Li & Chang, 2003).

Functional data for members of the Kip3 family are still limited in higher eukaryotes, excepting the *Drosophila* ortholog, Klp67A, which was shown as implicated in mitochondrial movement (Pereira et al., 1997). Recent functional analyses have demonstrated a requirement for Klp67A in the regulation of microtubule growth and stability during both *Drosophila* mitosis and male meiosis. Depletion of this microtubule plus end-directed motor increased the length and perturbed the morphology of spindle microtubules, beginning as early as prophase and extending through ana-telophase, and *Klp67A* mutations disrupted central spindle formation in both blastoderm embryos and spermatocytes and impaired centrosome separation. Therefore the proposed scenario was that Klp67A activity in *Drosophila* is required for spindle microtubules to interact properly during centrosome migration, metaphase spindle formation, chromosome segregation, and central spindle assembly, when microtubule ends must dynamically search and capture their appropriate targets (Gandhi et al., 2004).

Hence, the overall information currently available about the members of this family suggests that they are likely to conduct a conserved and important function in all fungal species (Schoch et al., 2003).

3.6. Kinesins in filamentous fungi

The characteristic growth form of filamentous fungi is the hypha. It is generated by germination of spores followed by continuous deposition of new cell material at the hyphal tip. As hyphal tips extend out into the medium, cytoplasm and various organelles migrate forward relative to the stationary cell walls (Chandra, 1996). Thus, filamentous fungi (such as *Aspergillus nidulans* and *Neurospora crassa*), rely on long distance organelle movement along microtubules to achieve fast tip growth, and the main players in this process are the motor proteins, among which kinesins are of a great importance.

In filamentous fungi, members of the kinesin superfamily of microtubule-associated motors are not only involved in long-distance transport of organelles and vesicles, but are also important for spindle formation and function. Analysis of fungal genomes indicates that there are at least 10 distinct kinesins in filamentous fungi (Table II.1), and several of these motors are not found in yeasts (Xiang & Plamann, 2003). Two kinesin subfamilies, KRP85/95 and MCAK/KIF2, clearly do not have any known fungal members, due probably to the fact that the kinesins belonging to those families are implicated in processes not existent in filamentous fungi (e.g. assembly and maintainance of ciliary and flagellar organelles, or roles in axonal transport in mammalian neuron cells) (Schoch et al., 2003).

Fungal kinesins show interesting differences in composition, structure and properties relative to conventional kinesins of higher eukaryotes. For example, the fungal kinesins apparently lack light chains that are typically part of conventional kinesin of higher eukaryotes (Kirchner et al., 1999). Fungal kinesins are also about four times faster in *in vitro* motility assays and show greater processivity when compared to human conventional kinesin (Kirchner et al., 1999; Lakamper et al., 2003). Studies have also shown that the fungal kinesin has a special neck domain directly adjacent to the motor domain. The presence of the neck region together with its adjacent motor domain containing the head and the neck-linker regions is not sufficient for dimerization, which is different from the case in higher eukaryotes (Kallipolitou et al., 2001).

Table II.1: Motor proteins in filamentous fungi
(Modified after Xiang & Plamann, (2003))

Family/Class	Possible functions
Conventional kinesin/KHC	Vesicle/organelle transport, nuclear positioning
Unc104/KIF1 (a long and a short version)	Vesicle/organelle transport
Chromokinesin/KIF4	Vesicle/organelle transport, DNA binding
BimC	Spindle assembly
C-terminal motor	Spindle assembly
Kip2/CENP-E	Microtubule stabilizing, kinetochore binding
Kip3	Microtubule dynamics
KID	Chromosome movement in metaphase
MKLP1	Spindle midzone organization and cytokinesis

3.7. Kinesin-like proteins of *Aspergillus nidulans*

The fungus *A. nidulans* is a useful model system for understanding the molecular basis of eukaryotic cellular morphogenesis as well as for asking more specific questions about several important motors required for nuclear distribution, mitosis or organelle movement. Genetic dissection of some of these processes identified a number of novel genes, among which three encoded kinesin–like proteins: BimC, KlpA and KinA.

The first member of the BimC family of kinesins was discovered in a genetic screen for temperature-sensitive lethal mitotic genes in *A. nidulans* as a mutant that was “blocked in mitosis” (Enos & Morris, 1990). Temperature-sensitive *bimC* mutants grown at the restrictive temperature failed to separate their duplicated spindle pole bodies during early stages of mitosis, resulting in mitotic defects such as abnormal spindle morphology and failure of nuclear division. The *bimC* gene proved to encode a 132 kDa, 1184 residue polypeptide with an N-terminal putative motor domain sharing 42% sequence identity with the motor domain of the kinesin heavy chain, providing the first direct evidence for the participation of a member of the kinesin superfamily in mitotic spindle function (Enos & Morris, 1990).

A motor with an opposing force is KlpA, a member of the C-terminal motor domain kinesin family. Deletion of this gene from the genome of *A. nidulans* causes a suppression of the *bimC4* mutation, suggesting that loss of KlpA function redresses unbalanced forces within the spindle induced by mutation in *bimC*. *klpA* could complement a null mutation in Kar3 (protein required for yeast nuclear fusion during mating and spindle formation (Page et al., 1994)), indicating that the primary amino-acid sequence conservation between tail domains of kinesin-like proteins is not necessarily required for conserved function (O'Connell et al., 1993).

The most recent report on kinesins in *A. nidulans* is about KinA, a homologue of conventional kinesin. Disruption of the gene led to a reduced growth rate and a nuclear positioning defect, resulting in formation of nuclear clusters with a dynamic behaviour. The mutant phenotypes are pronounced at 37°C, but rescued at 25°C. In addition, kinesin-deficient strains were less sensitive to the microtubule destabilizing drug benomyl, and disruption of conventional kinesin suppressed the cold sensitivity of an α-tubulin mutation (*tubA4*), suggesting that conventional kinesin of *A. nidulans* plays a role in cytoskeletal dynamics, by destabilizing microtubules (Requena et al.,

2001). It was also shown that KinA is involved in the localization of both cytoplasmic dynein and dynactin to the plus ends of microtubules in *A. nidulans*, because in the deletion mutant of *kinA*, the microtubule plus-end accumulation of both cytoplasmic dynein and dynactin are significantly diminished (Zhang et al., 2003).

The genetic tractability of filamentous fungi has made them excellent systems to study the function and regulation of the cytoskeleton and motor proteins. The recent availability of fungal genomes has revealed that many components of the cytoskeleton, including the cytoplasmic dynein pathway and the kinesin superfamily, are more closely related to those of higher eukaryotes than to those of the yeasts (Xiang & Plamann, 2003). Future studies are needed to further define specific roles for each motor, especially in the context when more proteins can function redundantly, and to address the interaction between them and the microtubule cytoskeleton for coordinated intracellular roles.

Started as an investigation for new roles of kinesin-like proteins of *A. nidulans* in nuclear migration, the present work analyses the role of a Kip3-like kinesin, KipB in mitosis and microtubule stability in *A. nidulans*. A combination of genetic, molecular and biochemical methods, fluorescence, time-lapse and confocal microscopy was chosen to examine KipB functions.

III. Materials and Methods

1. Equipment and chemicals

Chemicals were purchased from Sigma (Taufkirchen), Roth (Karlsruhe), Boehringer (Mannheim), Applichem (Darmstadt), Merck (Darmstadt), Biomol (Hamburg), ICN (Eschwege) and Difco Laboratories (Detroit, MI, USA). Restriction enzymes and other DNA-modifying enzymes were obtained from New England Biolabs (NEB, (Frankfurt), Amersham (Braunschweig), or Invitrogen (NV Leek, The Netherlands). The enzymes for PCR were bought from Promega (Mannheim) Qbiogene (Heidelberg) or Roche Diagnostics (Mannheim). The radionucleotide [α-^{32}P]-dATP was provided by Hartmann Analytics (Braunschweig). Autoradiographic films were from Kodak (Rochester, NY, USA) or Fuji (New RX, Fuji, Japan). The filter (Miracloth) was from Calbiochem-Novabiochem (Bad Soden/Ts.). Anti-HA antibody was purchased from Covance/Babco (Freiburg), anti-α-tubulin primary antibody and anti-mouse IgG (Fab specific) peroxidase conjugate secondary antibody, from Sigma (Steinheim), and anti-actin from ICN Boichemicals (Eschwege).

Table III.1: Equipment used in this study

Equipment	Type	Manufacturer
Centrifuge with rotors	SORVALL RC 5B plus (HB-6)	SORVALL, Bad Homburg
	SORVALL RC 28S	
	Centrifuge 5403	Eppendorf, Hamburg
Electroporation apparatus	Gene Pulser II, Pulse Controller	Bio-Rad, Munich
Electrotransfer apparatus	Mini Trans-blot Electrophoretic Transfer Cell	Bio-Rad, Munich
Hybridization oven	Personal Hyb™	Stratagene, Heideberg
PCR machine	Rapid Cycler	Idaho Technology, Idaho Falls, ID, USA
SDS-PAGE apparatus	Mini Protean II	Bio-Rad, Munich
UV-cross Linker	UV Stratalinker 2400	Stratagene, Heideberg
UV/Visible spectrophotometer	Ultrospec 3100 *pro*	Amersham Pharmacia Biotech, Freiburg

Table III.2: Kits used in this study

Kit	Manufacturer
BM Chemiluminescence Blotting Substrate (POD)	Roche, Mannheim
DNeasy Plant Kit	Qiagen, Hilden
Nucleobond® AX	Macherey-Nagel, Düren
RNeasy Mini Kit	Qiagen, Hilden
QIAEX® II Gel Extraction Kit (150)	Qiagen, Hilden
QIAquick® PCR Purification Kit	Qiagen, Hilden

2. Organisms used in this study and microbiological methods

2.1. Organisms

In this work were used the following *Aspergillus nidulans* and *Escherichia coli* strains:

Table III.3: *A. nidulans* and *E. coli* strains used in this study

Strain	Genotype	Source
SRF200	*pyrG89; ΔargB::trpCΔB; pyroA4; veA1*	(Karos & Fischer, 1999)
GR5	*pyrG89; wA3; pyroA4; veA1*	(Waring et al., 1989)
FGSC 26	*biA1; veA1*	FGSC*, Kansas, USA
GFP-*tubA*	*pyrG89; wA2; pyroA4; GFP::tubA::pyr4*	(Han et al., 2001)
MO62	*argB2; bimC4; nicA2*	V. Efimov (Piscataway, USA)
RMS011	*pabaA1, yA2; ΔargB::trpCΔB; trpC801, veA1*	(Stringer et al., 1991)
RMS012	diploid; *biA1; ΔargB::trpCΔB; methG1; veA1, trpC801 / pabaA1, yA2; ΔargB::trpCΔB; trpC801, veA1*	(Stringer et al., 1991)
SJW02	GFP-*tubA* x RMS011 progeny strain, *wA2; ΔargB::trpCΔB; pyroA4; alcA(p)::gfp::tubA*	J. Warmbold, Marburg
SNR1	*yA2; ΔargB::trpCΔB; pyroA4; veA1*; *kinA::pyr4*; (SRF200 transformed with pRF645 crossed to SAS7 (A. Singh, Marburg)	(Requena, et al., 2001)
SRS29	SRF200 transformed with pRS54 and pDC1 (*pyrG89; ΔargB::trpCΔB; pyroA4; veA1; gpd(p)::N-cit-1::gfp*)	(Suelmann & Fischer, 2000)

XX3	*pyrG89; nudA1, chaA1, veA1*	N. R. Morris, Piscataway, USA
SPR1	SRF200 transformed with pPR13, homologous integration (disruption construct) (*pyrG89*; *ΔkipB::argB; pyroA4; veA1*)	This study
SPR2	GR5 transformed with pPR11 and pRG1 (*wA3; pyroA4; veA1; alcA(p)::kipB::gfp)*	This study
SPR3	GR5 transformed with pPR12 and pRG1 (*wA3; pyroA4; veA1; kipB::HA*)	This study
SPR13	SPR1 x RMS011 progeny strain, *kipB* disruptant (*pabaA1, yA2; ΔkipB::argB; trpC801; veA1)*	This study
SPR22	SPR1 x RMS011 progeny strain, *kipB* disruptant (*pyrG89; ΔkipB::argB; trpC801; veA1)*	This study
SPR26	SPR1 x RMS011 progeny strain, *kipB* disruptant (*pyrG89; ΔkipB::argB; pyroA4*; *trpC801; veA1)*	This study
SPR30	SPR13 x GFP-*tubA* progeny strain, (*pyroA4; GFP::tubA::pyr4; ΔkipB::argB)*	This study
SPR36	SPR1 x SNR1 progeny strain, double mutant (*pyroA4, ΔkipB::argB; veA1; ΔkinA::pyr4*)	This study
SPR51	SPR1 x SNR1 progeny strain, Δ*kinA* mutant (*pyroA4, veA1; kinA::pyr4)*	This study
SPR55	GR5 x SPR13 progeny, diploid strain, (*ΔkipB/kipB; trpC801; veA1)*	This study
SPR60	SPR22 x SPR13 progeny, diploid strain, (*ΔkipB/ΔkipB, trpC801; veA1)*	This study
SPR80	SPR26 transformed with pRS54 (*ΔkipB::argB; pyroA4; trpC801; veA1; gpd(p)::N-cit-1::gfp*)	This study
SPR88	MO62xSPR13 progeny, double mutant *(ΔkipB::argB; yA2; bimC4; nicA2)*	This study
SPR90	MO62xSPR13 progeny, double mutant *(ΔkipB::argB bimC4; nicA2)*	This study
SPR93	RMS011 transformed with pDC1, wild type *(pabaA1, yA2, trpC801, veA1*)	This study
SPR96	SRF200 transformed with pPR38, homologous integration *(ΔargB::trpCΔB; pyroA4; veA1; alcA(p)::gfp::kipB)*	This study

SPR98	SRF200 transformed with pPR38, ectopic integration, *(ΔargB::trpCΔB; pyroA4; veA1; alcA(p)::gfp::kipB)*	This study
SPR99	SJW02 (GFP-*tubA*) transformed with pPND1 and pDC1, ectopic integration, *pyroA4; veA1; alcA(p)::mRFP1::kipB)*	This study
SPR101	SPR96 trasformed with pPND1, ectopic integration, *(pyroA4; veA1; alcA(p)::gfp::kipB*; *alcA(p)::mRFP1::kipB)*	This study
SSK13	SRL1xRMS011 progeny strain, *ΔkipA* mutant (*pabaA1; ΔkipA::pyr4; wA3; veA1*)	(Konzack et al., 2004)
SSK28	SSK13xSPR26 progeny strain, double mutant (*pabaA1; pyroA4; wA3; ΔkipA::pyr4; ΔkipB::argB; veA1*)	(Konzack et al., 2004)
SSK70	SSK44xSPR36 progeny strain, double mutant (*ΔkipA::pyr4; ΔkinA::pyr4; wA3; veA1*)	S. Konzack, Marburg
SSK73	SSK44xSPR36 progeny strain, triple mutant (*ΔkipA::pyr4; ΔkinA::pyr4; ΔkipB::argB; pyroA4; wA3; veA1*)	(Konzack et al., 2004)
SSK80	SSK44xXX3 progeny strain, double mutant (*pabaA1; ΔkipA::pyr4; wA3; nudA1, veA1)*	S. Konzack, Marburg
Escherichia coli		
XL1-Blue	*recA1, endA1, gyrA96, thi-1, hsdR17, supE44, relA1, lac* [*F'proABlacIQZ.M15::Tn10* (TetR)]	Stratagene, Heidelberg
Top10F'	F'[*lacIQ*, *Tn10* (TetR)] *mcrA* .(*mrr-hsdRMS-mcrBC*), O80 *lacZ .M15.lacX74*, *deoR, recA1, araD139.(ara-leu)7679, galU, galK, rpsL,* (StrR) *endA1, nupG*	Invitrogen, Leek, Netherlands

*FGSC: Fungal Genetic Stock Center, Kansas, USA

2.2. Cultivation and growing of microorganisms

Media for *E. coli* were prepared as previously described (Sambrook et al., 1989), (Table III.4) and supplemented in function of each experiment, with antibiotics and necessary reagents (Table III.5). Ingredients were added to ddH_2O water, poured into bottles with loosen caps and autoclaved 20 min at 15 lb/in^2. For solid media, 15 g agar per liter was added. Glassware and porcelain was sterilized in the heat sterilizer for 3 h at 180°C. Heat-sensitive solutions such as antibiotics, amino acids and vitamins were filer-sterilized with 0.22 um pore filter membrane (Millipore, France), and added to the media after autoclaving. Minimal and complete media for *A. nidulans* growth were prepared according to the protocols (Pontecorvo et al., 1953). For protoplast transformation of *A. nidulans,* 0.6 M KCl as osmoprotective substance

was added into minimal media (Table III.6). The supplemented vitamins, amino acids and nucleotides for auxotrophic *A. nidulans* strains were listed in Table III.7.

2.3. Growth conditions and storage of transformed *E. coli* and *A. nidulans* strains

Cultures of transformed *E. coli* strains were overnight cultivated on LB plates with appropriate antibiotics at 37°C. Liquid culture was inoculated from a single colony and incubated in LB medium containing appropriate antibiotics at 37°C with 180 rpm overnight shaking. For storage of *E. coli* strains, freshly grown bacterial suspension was adjusted to 15% end concentration of sterile glycerol and frozen at –80°C.

The *A. nidulans* strains were grown on minimal or complete medium plates. Colony pieces were cut from an agar plate and suspended in 15-20% sterile glycerol and stored at –80°C.

2.4. Determination of spore viability

For determination of the viability of spores, *A. nidulans* strains were freshly inoculated and grown onto appropriate agar plates for 2 days at 37°C. To obtain a clean suspension, sterile ddH_2O containing 0.02% Tween 20 was added to the plate, and the spores were harvested by gently scraping with a sterile inoculating wire the surface growth of the agar plate, followed by vigorously shaking until complete separation of the spores from the fruiting bodies and for breaking the spore clumps. Then, the dispersed fungal spore suspension was filtrated through sterile Miracloth into a sterile falcon tube (50 ml) 2-4 times to remove large mycelial fragments and clumps of agar which could interfere with the counting process. The final washed residue was diluted several times, in such a manner that the resultant spore suspension contained $1x10^3 \pm 2x10^2$ or $1x10^2 \pm 20$ spores per ml. The number of spores was determined with a Neubauer Improved counting chamber (depth 0.1 mm, square width: 0.05 mm) (Plan Optik GmbH, Elsoff), according to manufacturer protocols. Finally, agar plates were inoculated with different spore concentrations, incubated at 37°C for 2 days, and the number of colonies grown onto the plates was compared with the number of spores initially inoculated.

2.5. Induction of the *alcA* promoter

In this study, some of *A. nidulans* strains were carrying constructs expressed under the control of *alcA* promoter. For induction of this promoter, the strains were grown overnight (6-10 h) in medium with glucose, and then the medium was washed with sterile water, followed by a replacing with a medium containing 2% ethanol or 2% threonine (and lacking glucose), where the promoter can be induced. Also, especially for preparation of samples designated to be used for microscopy, the spores were inoculated overnight or for one day directly in the inducing medium and subsequently observed.

Table III.4: Media for *E. coli*

Medium	Ingredients (l liter)
LB	10 g Bacto-Trypton; 5 g Bacto-Yeast Extract; 10 g NaCl
SOC	20 g Bacto-Trypton; 1 g Bacto-Yeast Extract; 5 g NaCl; 0.185 g KCl; 2.03 g $MgCl_2$ x $7H_2O$; 2.46 g $MgSO_4$ x $7H_2O$; 3.6 g Glucose

Table III.5: Antibiotics and supplements for *E. coli* media

Substance	End concentration
Ampicillin (Ap)	100 µg/ml
Kanamycin (Km)	50 µg/ml
X-Gal	40 µg/ml
IPTG	8 µg/ml

Table III.6: Media and stock solutions for *A. nidulans*

Media or Stock	Preparation (per liter)
20 x Salt stock solution	120 g $NaNO_3$; 10.4 g KCl; 10.4 g $MgSO_4$ x $7H_2O$; 30.4 g KH_2PO_4
1000 x Trace elements stock solution	22 g $ZnSO_4$ x $7H_2O$; 11 g H_3BO_3; 5 g $MnCl_2$x 4H2O; 5 g $FeSO_4$ x $7H_2O$; 1.6 g $CoCl_2$ x 5H2O; 1.6 g $CuSO_4$ x $5H_2O$; 1.1 g $(NH_4)_6Mo_7O_{24}$ x $4H_2O$; 50 g Na_4 EDTA; adjust to pH 6.5-6.8 using KOH
Minimal medium (MM)	50 ml Salt stock solution; 1 ml Trace elements stock solution; 20 g Glucose; adjust to pH 6.5 using 10 N NaOH
Complete medium (CM)	Minimal medium with 2 g Peptone; 1 g Yeast extract; 1 g Casamino-acids; 1 ml Vitamin stock solution; 1 ml Trace elements stock solution; adjust to pH 6.5 using 10 N NaOH

Table III.7: Vitamins, amino acids and medium components

Component	Stock Concentration	Volume per liter
Biotin	0.05 %	1ml
PABA	0.1%	1ml
Pyridoxin-hydrochloride	0.1 %	1 ml
Arginine	500 mM	10 ml
Uracil	-	1 g
Uridine	500 mM	10 g

3. Genetic methods in *A. nidulans*

Genetic tests on *A. nidulans* strains were basically done after the commonly used protocols (Käfer, 1977); (Morris, 1976); (Pontecorvo et al., 1953); and (Clutterbuck, 1969).

3.1. Crossing of *A. nidulans*

The strains used for crossing were inoculated side by side onto CM plus appropriate markers plates for 2 days, until the mycelium of both strains fused at the borders. Small agar square blocks were cut from these fused edges and transferred to MM plates, where just the growth of a heterokaryon is possible. Plates were sealed with adhesive tape and incubated 10-14 days at 37°C or 30°C in a humid chamber. The fruiting bodies (cleistothecia) developed after this time were isolated with help of a sterile inoculating needle, rolled until completely clean from Hülle-cells on the surface of an agar plate, and smashed in an Eppendorf tube with 0.5 ml sterile ddH_20. An aliquot of the ascospore suspension obtained in this way was inoculated onto CM agar plates. After 3 days incubation, the grown colonies were transferred onto MM plates with different appropriate markers, to test for the missing auxotrophic marker. If more strains were analyzed, they were inoculated onto raster plates, which contained 20 colonies.

3.2. Construction of *A. nidulans* diploid strains

A. nidulans is a highly amenable organism for generation of diploid cells. The aerial hyphae of the fungus produce long chains of conidia (asexual spores). Each conidium has a single nucleus, and the phenotype of any individual spore is

dependent only of the genotype of its own nucleus, which makes certain kinds of selective techniques possible. If two haploid strains are mixed, the hyphae fuse and then both types of nuclei are present in a common cytoplasm, the heterokaryon. Following heterokaryon formation, some nuclei that are genetically the same will fuse, as well as those that are genetically different, so the diploid nuclei are formed. These nuclei will undergo mitosis, the crossing-over can occur, and the diploid segregants can be checked for chromosome loss by the degree of haploidization. The diploid strains are stable on minimal medium, but rather unstable onto benomyl plates, because this drug can cause mitotic instability, by destabilizing the spindle microtubules, and give rise to a random and fast haploidization.

To create diploid strains necessary for this study, a wild-type (GR5) and a *kipB* mutant strain (SPR13) were crossed, as well as two different mutant strains (SPR13 and SPR22). After the obtaining of the heterokaryon as described above, the spores were harvested by very gentle scrapping of the heterokaryon surface, suspended into sterile ddH_2O and filtered several times, until the complete separation from the fruiting bodies and traces of agar. Each time samples were taken from the filtrate and checked at the microscope, to prove the efficiency of the filtration. The spore suspension was then mixed with warm selective agar medium (MM) and plated. After the solidification of the medium, another layer of agar was poured onto the first one, in order to apply a selection pressure for spore germination, so that just spores containing the nuclei of both parental strains could grow further. The stable diploids obtained like that were inoculated onto benomyl-containing agar plates and were analyzed for the number of formed haploid sectors.

4. Molecular biological methods

4.1. Plasmids and cosmids

In this study the following plasmids and cosmids were used.

Table III.8: Plasmids and cosmids used in this study

Plasmids/ Cosmids	Construction	Source
pBluescript KS^-	Cloning vector	Invitrogen (NV Leek, The Netherlands)

pCR2.1-TOPO	TA-cloning vector for cloning of PCR fragments	Invitrogen (NV Leek, The Netherlands)
pCMB17apx	*alcA(p)::GFP, pyr4*; for N-terminal fusion of GFP to proteins of interest	V. Efimov (Piscataway, USA)
pDC1	*A. nidulans argB* gene in pIC20R	(Aramayo et al., 1989)
pHW-arg	A *Kpn*I–*Xho*I-released *argB* from pDC1 inserted into pBluescript KS–	(Wei et al., 2001)
pRG1	Contains *N. crassa pyr4*-gene	(Waring et al., 1989)
pRS31	*gpd(p)::gfp::stuA* into pBluescript KS–	(Suelmann et al., 1997)
pRS54	*gpd(p)::N-cit-1::gfp* into pBluescript KS–	(Suelmann & Fischer, 2000)
pPR5	*kipB* containing cosmid (*BamH*I short fragment, 3.3 kb) form pUI library	This study
pGR1	Subclone *BamH*I of *kipB* –short fragment- from pPR5 into pBluescript KS^-	This study
pPR7	3.6 kb *Sac*I-*Bam*HI fragment of *kipB* cloned into pBluescript KS-	This study
pPR11	*alcA(p)::kipB::sgfp, (kipB BamH*I fragment from pPR7) into pBluescript KS–	This study
pPR12	3xHA epitopes in *Not*I into pGR1, *kipB* natural promoter *(kipB::HA)*	This study
pPR13	*argB* gene with *Bam*HI sites cloned in *Bgl*II sites of *kipB* from pPR7 (disruption construct)	This study
pPR17	*kipB* containing cosmid (entire gene) from pUI library	This study
pPR19	4.3 kb *kipB Sac*I subclone from pPR17 cloned into pBluescript KS-	This study
pPR21	4.5 kb PCR product of *kipB* ORF from 5' end *Sac*I site, without the Stop codon	This study
pPR38	1.2 kb *kipB* from ATG, PCR product with *Asc*I and *Pac*I sites from pPR19 inserted into pCMB17apx	This study
pPND1	GFP replaced with mRFP1 (*Kpn*I-*Asc*I) into pPR38, *alcA(p)::mRFP::kipB, pyr4*	This study

4.2. DNA manipulations

4.2.1. Plasmid DNA preparation from *E. coli* cells

For isolation of plasmid or cosmid DNA (Sambrook et al., 1989) an alkali-lysis method was used. For DNA small volumes (miniprep), 2.5 ml of overnight liquid culture was centrifuged 1 min at 13000 rpm, the pellet resuspended in 200 μl Tris-EDTA Buffer, then 200 μl of Alkali-lysis buffer added and gently mixed, followed by addition of 200 μl neutralization buffer (Table III.9). After 10 min centrifugation, plasmid DNA-containing supernatant was precipitated with 0.7 vol. isopropanol, followed by 70% EtOH washing. The dried pellet was resuspended in TE buffer. For large DNA volumes (midipreps), plasmid DNA from 100 ml E. coli overnight liquid culture was extracted using a Macherey-Nagel Nucleobond® Plasmid DNA Purification Kit, according to the manufacturer protocols.

Plasmid DNA concentration was determined via absorption measurement with 260 and 280 nm in a spectrophotometer (Pharmacia LKB-UltrospecIII), with a quartz cuvette or by comparison between the intensity of ethidium bromide DNA bands on agarose gels and the intensity of defined standards.

Table III.9: Solutions used for plasmid extraction (miniprep)

Tris-EDTA buffer	5 ml 1M Tris-HCl (pH 7.5); 2 ml 0.5M EDTA (pH 8.0); 10 mg RNAse in 100 ml
Alkali-lysis buffer	0.2 M NaOH; 1% SDS
Neutralization buffer	1.5 M K-Acetate, pH 4.8
TE buffer	10 mM Tris-HCl; 1 mM EDTA; pH 8.0

4.2.2. Genomic DNA preparation from *A. nidulans*

Preparation of *A. nidulans* genomic DNA was done by inoculation in a 9 cm plastic Petri dish of around 20 ml fresh liquid minimal media with spore suspension from a colony grown on an agar plate, followed by incubation for 12-15 h at 37°C. Then, the mycelium was harvested with a spatula, pressed briefly until dry between paper towels, and frozen in liquid nitrogen. The frozen mycelium was grounded in liquid nitrogen or kept at –80°C until isolation. *A. nidulans* genomic DNA was extracted with

the DNeasy Plant Mini Kit (Qiagen, Hilden). To check DNA yield and quality, 5 μl extracted DNA was used via running a 1% agarose gel.

4.2.3. Digestion of DNA by restriction endonucleases

DNA samples (200 ng–1 μg) were digested by restriction endonucleases using corresponding reaction buffers. Generally, restriction digests were prepared in 20 μl total volume, with 0.5-1 μl restriction enzyme (1-20 U/μl) and incubated at 37°C from 1 h to overnight. In other cases, enzyme, DNA, buffer volumes and reaction times varied depending on the specific requirements. For enzyme inactivation, the sample was incubated at 65°C for 10 min. *A. nidulans* genomic DNA was generally digested overnight. In the case of different enzymes, the restriction digest was carried out first in the buffer with low salt concentration or the buffer compatible to both enzymes.

4.2.4. Dephosphorylation of digested DNA

After the digestion with restriction enzymes, the vector was dephosphorylated by Shrimp alkaline phosphatase (SAP) to remove the phosphate group at 5'-end, which prevented self-ligation of the vector. 0.1 unit / μM 5'-end with buffer was added to the sample. The mix was incubated 45 min at 37ºC. Less SAP and shorter incubation time were used for the protruding 5' termini than for recessed 5' termini. If two enzymes with incompatible termini were used, the dephosphorylation process was omitted.

4.2.5. DNA precipitation

Contamination by small nucleic acid fragment, protein and salt can be reduced to acceptable level by precipitating the DNA. In order to do this, 2.5 volume of ethanol and 1/10 3.0 M NaAc (pH 5.2) were added to the DNA solution. The sample was mixed, kept at –80ºC for 10 min and centrifuged for 10 min at 10.000 rpm. The supernatant was discarded and the pellet was washed with 70% EtOH, followed by centrifugation at 10.000 rpm for 5-10 min. The pellet of purified DNA was completely in a speed vacuum or at 50ºC for 10-20 min, and then dissolved in sterile water or TE buffer.

4.2.6. DNA ligation

DNA ligation was performed using T4 ligase (NEB, Frankfurt) at 16ºC or Fast Link™ System (Biozym, Hessisch Oldendorf) in a volume of 10-20 μl. Around 50 ng vector was used in one ligation. The ratio of vector to insert was 1: 2-3 and 1:5-10 respectively for cohesive and blunt end ligation. For the cloning of PCR products, restriction enzyme sites were added to both primers, or TA cloned. For TA cloning, the PCR products amplified with Expand (Roche, Mannheim) or other proof reading polymerases (e.g. Pfu, Promega, Madison, WI, USA) were cloned into pCR2.1 TOPO (Invitrogen, NV Leek, The Netherlands).

4.2.7. DNA agarose gel electrophoresis

The separation and identification of DNA fragments was done by running them through agarose gels (0.8-1.2%), which were prepared by boiling agarose into 0.5 or 1 x TAE buffer and pouring it into gel chambers. DNA samples were mixed with 1/10 10 x DNA Loading buffer. As standard DNA marker an *Eco*130I-cut λ DNA (MBI Fermentas, St. Leon-Rot) was used, and gels were run for 30 min - 4 h in gel chambers with 0.5 or 1x TAE buffer. Then, the gel was stained for 15-30 min in 0.5 x TAE buffer with ethidium bromide (1 μg/μl). The DNA bands were visualized in the gel at 302 nm UV light. Photos were taken using a camera (INTAS, Goettingen) connected to a video printer.

50 x TAE buffer (pH 8.0)	40 mM Tris-Acetate; 1 mM EDTA; pH 8.0
10 x Loading buffer	20% Ficoll 400; 0.1 M Na_2EDTA (pH 8.0); 1% SDS; 0.25% Bromphenol blue; 0.25% Xylene cyanol

4.2.8. PCR

Polymerase chain reaction (PCR) was performed with Taq (Qbiogene, Heidelberg), Expand (Roche, Mannheim) or Pfu (Promega, Madison, WI, USA) polymerases according to manufacturer protocols. Oligonucleotides synthesis was made by MWG Biotech (Ebersberg) and the concentration used for a PCR reaction volume of 10-100 μl was 5-20 pM. As DNA template were used plasmid or cosmid DNA (0,2-10 ng) and genomic DNA (10-20 ng). The PCR reactions were carried out in a capillary Rapid Cycler (Idaho Technology, Idaho Falls, ID, USA). The

polymerization duration and annealing temperatures varied in function of each application. PCR programs were generally used with 30-40 cycles, at a denaturation temperature of 94°C, and a polymerization temperature of 68-72°C. In the case of oligonucleotides containing restriction sites, the PCR reaction was first carried out for 4-5 cycles at a lower annealing temperature (5-10°C) then the melting temperature of the primers. RT-PCR was carried out using SUPERSCRIPT^{TM} II RNase H^{-} Reverse Transcriptase (Invitrogen) according to the manufacturer protocol.

Standard PCR reaction in a Rapid Circler	
1 µl	2.5 mM dNTP
1 µl	DNA template
1 µl	10 x buffer
1 µl	50 mM $MgCl_2$
1 µl	10 x BSA
1 µl	10 x Ficoll
1 µl each	5 µM Primer A and B
0.2 µl	Taq DNA polymerase
1.8 µl	Autoclaved ddH_2O

Oligonucleotides used in this study (Table III.10) were synthesized by MWG Biotech (Ebersberg).

Table III.10: Primers used for PCR in this study

KipB_A	5'-CCGACAACCATCCGACGC -3'
KipB_B	5'-CAATTCCGTATGCTTCTCGC-3'
KipB_C	5'-GCGAGAAGCATACGGAATTG-3'
KipB_D	5'-CGGATTCCCTCTGCTGCG-3'
KipB_E	5'-GTCGACGCAGCAGAGGGAATC-3'
KipB_F	5'-CTCGTATCGAATTACTTGAAGTTG-3'
KipB_G	5'-GAATCGGTGAGGCTCTGG-3'
KipB_K	5'-GCGCGCGGTCTAAAGG-3'
KipB_L	5'-TTAGATCTGGGTTGTCGTGAATTGAG-3'
KipB_M	5'-GCGCAAGGTCTTAACATTGCCT-3'
KipB_N	5'-AGAGACACTGATGTTATTGTG-3'

KipB_Z	5'-CCTTCCATCGAACGCTCC-3'
KipB_T1	5'-CGATGTTCACCGCGCAAG-3'
KipB_T2	5'-GAAACCGCCAATAGCACTC-3'
KipB_T3	5'-CTCGCCGTCGTAAGATGG-3'
KipB_T4	5'-GAGGGCCTAGGACAGCAG-3'
KipB-Ngfp-fwd	5'-GGCGCGCCCGGGATGGGGGCCTCAAGCGAC-3'
KipB-Ngfp-rev	5'-CGCTTTGAGTTCGTTAATTAATGCC-3'
KpnI_mRFP1_fwd	5'-CGGTACCATGGTCTCCTCCGAGG-3'
AscI_mRFP1_rev	5'-CGGCGCGCCGGCGGTGGA-3'
KipB-TOPO-GFPfwd	5'-CGAGCTCCTGGGTCTAGG-3'
argB-3'raus	5'-GACTCTCCTCATTCCATAC-3'
sGFP-Xba-2F	5'-ATCTAGAAATGGTGAGCAAGGGCGAG-3'
sGFP-Xba-2R	5'-ATCTAGAATTTGTACAGCTCGTCCATG-3'
M13(-20)Forward	5'-GTAAAACGACGGCCAG-3'
M13Reverse	5'-CAGGAAACAGCTATGAC-3'

4.2.9. Spore PCR

Extraction of DNA from filamentous fungi for PCR analysis is usually time consuming and generally expensive, especially when is done in order to check a great number of transformants for different mutations. To avoid this, conidia of *A. nidulans* were used directly for PCR analysis, without isolation of DNA. The PCR assay was performed with conidia obtained from freshly grown colonies on agar plates, at 37°C or 30°C for 2 days. The spores were harvested by gently scrapping the colony surface with a sterile wire and transferred to the lid of an Eppendorf cup filled with 100 μl sterile water. Collection of medium by this harvest it was avoided, since agar may inhibit the PCR reaction. The samples were strongly vortexed, and appropriate spore concentration was adjusted for a reaction tube (10^4-10^6 spores per reaction), followed by freezing them for 10-15 min. at –80°C. Alternatively a master mix was prepared as for a normal PCR reaction, with the special addition of 0.1% Triton X-100. The mix was added proportionally to the samples and they were generally subjected to the following PCR conditions: denaturation at 95°C for 5 min., 30 cycles of 95°C for 1 min. / appropriate annealing temperature and times/ 72°C for 2-5 min., followed by 72°C for 5-10 min.

4.2.10. DNA isolation from agarose gel

For isolation of DNA fragments, 0.8%-1% “low melting” gel was often used. The low melting gel separated by gel electrophoresis at 50 V was stained in 0.5-1 x TAE with ethidium bromide. The appropriate DNA bands were cut out under UV light. The DNA purification was carried out according to the protocol of Wizard^{TM} PCR Preps DNA Purification System (Promega, Madison, WI, USA). Alternatively, the DNA from normal agarose gels was isolated with the QIAEX II Gel Extraction System (Qiagen, Hilden).

4.2.11. DNA sequencing

DNA sequencing was done by commercial sequencing (MWG Biotech, Ebersberg).

4.2.12. Transformation of *E. coli*

The transformation of electrocompentent *E. coli* cell was done as described (Ausubel et al., 1995). After dialyzation of ligation reaction, 2 μl ligation solution and 50 μl *E. coli* electrocompetent cells were mixed and filled into a transformation cuvette (PEQLAB, Erlangen). The plasmids were transformed by electroporation (Gene-Pulser, Bio-Rad) into electrocompentant *E. coli* cells XL1-Blue (Stratagene, La Jolla, USA). Alternatively, chemical competent *E. coli* strain TOP10 F’ (Invitrogen, Leek, Netherlands) was used according to the distributor protocols.

4.2.13. Transformation of *A. nidulans*

Standard procedures of *Aspergillus* protoplast transformation were used (Yelton et al., 1984). Spores were harvested from freshly grown plates (~10^9 conidia), inoculated in 500 ml volume minimal medium with appropriate components, and shaked at 30ºC in water bath for 12-16 h until spores germinated. The culture was filtered through sterile Miracloth followed by washing using Wash solution. The washed mycelium was collected on ice in a sterile 100 ml Erlenmeyer flask with 5 ml of Osmotic medium. After addition of GlucanX (Novozyme) (200 mg/ml sterile water) and 5 min. incubation on ice, BSA (6 mg/0.5 ml sterile water) was added into the flask. Subsequently, the digestion mixture was incubated at 30ºC in water bath for 1-3 h until enough protoplasts became free. Then, it was transferred into a 30 ml Corex tube and 10 ml of Trapping buffer was slowly added, followed by a centrifugation at

5000 rpm for 15 min using HB-6 rotor. The obtained protoplast band was transferred into a new sterile tube, followed by washing two times using STC with centrifugation at 7000 rpm for 8 min. The protoplast pellet was gently resuspended in 200-1000 μl STC for transformation (for the solutions used, see Table III.11).

100 μl protoplasts in STC and 100 μl DNA (10 μg DNA filled up to 100 μl STC) were mixed and incubated 25 min at room temperature in a falcon tube. Then, 2 ml PEG was added and the tube was rolled until the mixture was homogeneous, followed by 20 min incubation at room temperature. Finally, 8 ml STC was added and the entire mixture was spread onto osmotically stabilized medium (MM + 0.6 M KCl) with appropriate selection markers. The plates were incubated at 37ºC until colonies were formed after 3-4 days.

Table III.11: Solutions used for *A. nidulans* transformation

Mycelium wash solution	0.6 M $MgSO_4$
Osmotic medium	1.2 M $MgSO_4$, 10 mM Na_3PO_4 buffer, pH 5.8
Trapping buffer	0.6 M sorbitol, 0.1 M Tris-HCl, pH 7.0
STC	1.2 M sorbitol, 10 mM $CaCl_2$, 10 mM Tris-HCl, pH 7.0
PEG	60% PEG 4000, 10 mM $CaCl_2$, 10 mM Tris-HCl, pH 7.0

4.2.14. DNA-DNA hybridization (Southern blot analysis)

DNA-DNA hybridization (Southern blot analysis) was performed using radioactive α-^{32}P-dATP (Sambrook et al., 1989). The preparation of radioactive probes was made by means of random priming (USB, Freiburg). The DNA samples isolated through agarose gel were transferred by capillarity to the positively charged nylon filter (Biodyne A, Pall, Ann Arbor, MI, USA). The filter was cross-linked under UV radiation with a dose of 1.2 x 10^5 μJ (UV Stratalinker 2400, Stratagene, Heidelberg). The probe was purified through prespin MobiSpin S-300 Column (Mo Bi Tec GmbH, Göttingen). The membrane was then prehybridized in Hybridization solution or QuickHyb commercially prepared hybridization solution (Stratagene Europe, Amsterdam, The Netherlands) supplemented with 100 μg/ml Salmon sperm DNA 1-2 h, and respectively 45 min. at 68ºC and then hybridized 2-3 h with the probe at 68ºC, followed by stringent washing at 68ºC. The first washing step consisted in 2 times of 2 x SSC / 0.1% SDS 2 x washing solution for 10 min, and then the second step of 2

times each 10 min 0.1-0.2 x SSC / 0.1% SDS 0.2 x washing solution. The detection was accomplished by mean of autoradiography using the films from Kodak (Rochester, NY, USA) or Fuji (New RX, Fuji, Japan). If the filter was reused, a process of striping was carried out in 0.5% SDS at 95ºC for 2-4 times. The striping result was radioactively checked (for the solutions used, see Table III.12).

Table III.12: Solutions used for Southern blot

Hybridization solution	5 x SSC; 1% skim milk; 0.1% lauroylsarcocine sodium salt; 0.02% SDS
Acidic solution	0.25 M HCl
Denaturation solution	100 g NaOH; 438.3 g NaCl in 5 l
Neutralization solution	242 g Tris; 347 g NaCl in 4 l; pH 7.2
20 x SSC	441.3 g Na_3Citrate; 876.3 g NaCl in 5 l, pH 7.0
2 x Washing solution	100 ml 20 x SSC; 10 ml 10% SDS in 1 l
0.2 x Washing solution	10 ml 20 x SSC; 10 ml 10% SDS in 1 l

4.2.15. Colony hybridization

For colony hybridization, colonies of *E. coli* were transferred to nylon membranes (Hybond^{TM}-N, Amersham, Braunschweig) and treated according to manufacturer specifications. DNA was fixated to the membrane through UV cross-linking and analysed in a Southern blot experiment as described at point 4.2.14.

4.3. RNA manipulations

4.3.1. Isolation of total RNA from *A. nidulans*

For isolation of total RNA, 500 ml CM liquid culture inoculated with spore suspension from one plate was shaken at 200 rpm for 14 h at 37ºC. The overnight grown mycelium was harvested, dried between paper towels, frozen in liquid nitrogen and grounded in a mortar. RNA isolation from grounded mycelium powder was carried out with TRIZOL (Gibco or Invitrogen) according to manufacturer protocol. The RNA was finally dissolved in 40-50 μl sterile DEPC H_2O with 0.5 U/μl RNase inhibitor (Promega, Mannheim). The RNA concentration was measured in a photometer (Pharmacia LKB, UltrospecIII). The RNA samples were diluted to 1 μg/μl with DEPC H_2O containing RNase inhibitor. The samples were kept at –80°C.

4.3.2. DNA-RNA hybridization (Northern blot analysis)

DNA-RNA hybridization (Northern blot) was accomplished as described (Sambrook et al., 1989). The RNA was denatured with formamide and separated in denaturing formaldehyde agarose gel, followed by capillary transfer to a positively charged nylon membrane (Biodyne Plus, Pall, Ann Arbor, MI, USA). The size estimation was done with the RNA marker of Promega (Mannheim). The membrane was cross-linked as for Southern blot. It was stained afterwards with Methylene blue (0.03%) and washed using H_2O, after which clear rRNA bands appear. A photo of the gel was taken via a camera (INTAS, Göttingen) and a video printer. The filter was subsequently destained in Destaining solution. The prehybridization was performed in Northern hybridization solution with 100ug/ml Salmon sperm DNA 1-2 h at 42°C and then hybridized overnight with the probe at 42°C, followed by stringent washing at 65-68°C, 1 time in 2 x SSC / 0.1% SDS for 10 min, and then 2 times each, 10 min in 0.5 x SSC / 0.1% SDS. The detection was carried out with radioactive labeled probes as for Southern Blot (for the solutions used, see Table III.13).

Table III.13: Solutions used for Northern blot

DEPC water	0.1% DEPC, stir overnight, autoclave
10 x MOPS	0.4 M MOPS (pH 7.0); 0.1 M sodium acetate; 0.01 M EDTA, autoclave
RNA sample buffer	100 µl formamide, 38 µl 37% formaldehyde, 20 µl 10 x MOPS, 42 µl DEPC water, 20 µl RNA loading Buffer
RNA loading buffer	80% formamide; 1 mM EDTA; 0.1% bromphenol blue; 0.1% xylene cyanol
Northern staining solution	0.03% methylene blue in 0.3 M Na-Acetate
Northern destaining solution	1% SDS; 1 x SSC
100 x Denhardt solution	10 g ficoll 400; 10 g polyvinylpyrrolidone; 10 g BSA (Pentax fraction V); H_2O to 500 ml, filter and store at –20˚C in 25 ml aliquots
Prehybridization / Hybridization solution	5 x SSC; 1% SDS; 5 x Denhardt solution; 50% formamide
Northern running buffer	100 ml 10 x MOPS, 20 ml 37% formaldehyde, 880 ml DEPC Water
Northern mini gel	0.36 g Agarose, 21 ml DEPC water, boiling, after reaching 70˚C, add 6 ml 37% formaldehyde and 3 ml 10 x MOPS

4.4. Description of DNA constructs (plasmids)

4.4.1. Cloning of the *kipB* gene

The partial sequence obtained from Cereon Genomics LLC (Cambridge, USA) was used to design primers (KipB_A, B or KipB_C, D) for amplification of a specific *kipB* fragment. This fragment was used to identify two cosmids carrying a part of the gene (pPR5) and its entire length (pPR17), from a cosmid library pUI. From the first cosmid, a 3.3 kb *kipB* containing (short fragment) *BamH*I restriction fragment was subcloned into the pBluescript KS- (Invitrogen (NV Leek, The Netherlands) (pGR1). Because the sequencing of this plasmid revealed that the 3' *Bam*HI site was introduced artificially through construction of the cosmid library and the translation of the DNA insert continued into the pGR1 plasmid, the second cosmid was used for subcloning of 4.3 kb *Sac*I fragment of *kipB* into pBluescript KS- (pPR19). Whereas the ORF also did not finish within the *Sac*I fragment, the 3' end of the gene was amplified by PCR, with genomic DNA as template (KipB-TOPO-GFPfwd, KipB_T2) and the entire ORF of *kipB* was subsequently cloned into the pCR2.1 TOPO vector (Invitrogen (NV Leek, The Netherlands) (pPR21).

4.4.2. Cloning of the *kipB* disruption construct (pPR13)

A *Bam*HI–*Bam*HI-released *argB* fragment from pHW-arg (Wei et al., 2001) was cloned into the *Bgl*II sites of *kipB* gene (short version, plasmid pPR7), in order to disrupt the motor domain of the protein (for scheme see results, Fig. IV.6). This plasmid was cut finally with *Bam*HI, which releases the entire construct. Homologous integration of the construct (pPR13) in *A. nidulans* would lead to a deletion of 18 bp of the *kipB* gene. In addition to the deletion, the *argB* gene disrupts the coding region of *kipB*. The disruption construct was transformed into the arginine-auxotrophic *A. nidulans* strain SRF200.

4.4.3. GFP labeling of KipB (pPR11; pPR38)

For the C-terminal construct of the KipB::GFP fusion protein the plasmid pGR1, which contained 3.3 kb *kipB*-including ORF *Bam*HI short fragment was used. This led to a truncated version of the protein, in which the first 690 amino acids were fused to GFP. The *alcA* promoter was cloned upstream of *kipB* as a *Kpn*I-*Xho*I fragment and *sgfp* as an *Xba*I restriction fragment downstream into the polylinker of pBluescript

KS- (pPR11). For the N-terminal construct, a 1.2 kb (starting from ATG) fragment of *kipB* from pPR19 was amplified with the primers: KipB-Ngfp-fwd with an *Asc*I site added in 5' and KipB-Ngfp-rev and cloned into pCMB17apx plasmid (kindly provided by V. Efimov, Piscataway, USA) into *Asc*I-*Pac*I sites (pPR38). Homologous recombination of this construct into the *kipB* locus would lead to a N-terminal GFP fusion of the entire KipB protein under the control of the *alcA* promoter and a truncated 5'-region under the natural promoter. First construct (pPR11) was transformed into *A. nidulans* strain GR5 and the second one (pPR38) into the strain SRF200.

4.4.4. mRFP1-labeling of KipB (pPND1)

mRFP1 (red fluorescent protein monomer) was amplified with the primers KpnI_mRFP1_fwd and AscI_mRFP1_rev, and cloned into the *Kpn*I-*Asc*I sites of pPR38 plasmid, replacing the sGFP. This resulted into a N-terminal mRFP1 fusion of 1.2 kb (starting from ATG) fragment of KipB, under control of the *alcA* promoter. The construct was transformed into *A. nidulans* strains SJW02 and SPR96.

4.4.5. HA-labeling of KipB (pPR12)

The HA epitope was cloned downstream of *kipB* as a *Not*I restriction fragment into the polylinker of pGR1 (same truncated version of the protein as for pPR11). This construct led to an HA fusion of KipB truncated protein expressed under the natural promoter. The plasmid (pPR12) was transformed into *A. nidulans* strain GR5.

5. Biochemical methods

5.1. Isolation of protein from *A. nidulans*

For protein extraction, spores were incubated overnight in liquid media at 37°C shaking with 200 rpm. The grown mycelium was filtered, dried and grounded in liquid nitrogen as for genomic DNA extraction. Then, it was resuspended in the same amount of a protein extraction buffer (20 mM TrisCl pH 8.0; 0-0.2 % Triton X-100; 150-300 mM NaCl, 10 µl Protease Inhibitor Cocktail, SIGMA, Taufkirchen). The slurry was centrifuged at 13.000 rpm at 4°C for 5-10 min and the total protein concentration of the supernatant measured according to Bradford (Bradford, 1976). After centrifugation, the supernatant was stored at -80°C or aliquots selected for analysis

were heated at 95°C for 10 min together with loading buffer (240 mM Tris/HCl, pH 6.8; 8 % SDS; 40 % Glycerol; 12 % DTT; 0.004 % Bromophenole blue) prior to loading.

5.2. Determination of protein concentration (Bradford Assay)

Protein concentration was determined according to Bradford (Bradford, 1976) using the Bio-Rad protein assay (Bio-Rad, München). This measurement is based upon Coomassie® Brilliant Blue G-250 dye-binding assay. Acryl-cuvettes (Sarstedt, Nümbrecht) were used for the determination of protein concentration. 200 µl Bio-Rad Protein Dye (Bio-Rad) were added to samples and standard (BSA, bovine serum albumine) (0-50 µg / 0.8 ml H_2O with diluted sample isolation buffer), afterwards they were gently mixed to avoid bubbles. After 10 min, the measurement was carried out in the photometer (Pharmacia LKB, UltrospecIII) at 595 nm.

5.3. SDS-Polyacrylamide gel electrophoresis (SDS-PAGE)

For immunodetection of the proteins a Western blot was performed. The SDS-PAGE gel consisted of a resolving gel topped by a stacking gel. The separating gel was casted between the glass plates using Bio-Rad Mini Protean II equipment and overlayed with a thin layer of ddH_2O. After gel polymerisation, the water was removed and the gel chamber was filled up with stacking gel. The protein samples were diluted to appropriate concentrations using 4 x Laemmli sample buffer, heated at 95ºC for 10 min and loaded onto the gel. Electrophoresis took place at room temperature, first at 50 V until the sample moved out from the wells and then 100-120 V until tracking dye reached the bottom of separating gel (for the solutions used, see Table III.14).

Table III.14: Solutions used for polyacrylamide gels preparation

Solutions	Stacking gel	Separating gel		
	4%	6%	10%	12%
Acrylamid / Bisacrylamid 40%	0.36 ml	1.1 ml	1.9 ml	2.25 ml
1 M Tris-HCl pH 6.8	0.45 ml			
1 M Tris-HCl pH 8.8		1.88 ml	1.88 ml	1.88 ml
H_2O	2.8 ml	4.4 ml	3.6 ml	3.25 ml

10% SDS	36 µl	125 µl	125 µl	125 µl
10% APS	15 µl	40 µl	40 µl	40 µl
TEMED	3 µl	5 µl	5 µl	5 µl

10 x Electrophoresis running buffer	30.3 g Tris; 144 g Glycine; 2 g SDS in1 liter of ddH_2O.

5.4. Western blotting

After electrophoresis, the proteins were transferred from the gel to Hybond ECL nitrocellose membrane (Amersham-Pharmacia Biotech, Freiburg). Electroblotting was performed in a "sandwich" assembly in Transfer buffer for 3 h to overnight at 60 V at 4°C using Mini Trans-Blot Apparatus (Bio-Rad, Munich). After transfer, the membrane was stained for 5 min in Ponceau S solution, and then washed with water until the protein bands were distinctly visible. The membrane was washed in TBS-T solution 4 x 5 min, blocked in Blocking solution for 1 h, then hybridized for 1-2 h at room temperature or overnight at 4°C with the primary antibody diluted in Blocking solution. Afterwards, the membrane was washed again 4 x 5 min in TBS-T, incubated with the secondary antibody for 1 h at room temperature, followed by 4 x 5 min washing in TBS-T (for the solutions used, see Table III.15). HA epitope was detected with a monoclonal anti-HA antibody (IgG1, developed in mouse, Babco, Freiburg), and a secondary antibody (anti-mouse IgG, peroxidase conjugate, SIGMA, Taufkirchen). The detection was done with the BM chemiluminescence kit from Roche (Mannheim).

Table III.15: Solutions used for Western blot

10 x Transfer buffer	30.3 g Tris; 144 g Glycine in 1 liter of ddH_2O.
Transfer buffer	800 ml H_2O, 100 ml 10 x Transfer buffer, 200 ml methanol
Ponceau S	0.1% Ponceau-S in 1% Acetic acid, reusable
10 x TBS	24.2 g Tris, 80 g NaCl in 1 liter of ddH_2O, pH 7.6
TBS-T	1 x TBS, 0.1% Tween 20 (100%)
Blocking solution	TBS-T with 3% BSA

6. Fluorescence microscopy, live-cell image acquisition and analysis

Cells were grown in glass bottom dishes (World Precision Instruments, Berlin) in 2 ml of MM + glycerol + pyridoxine and/or arginine or MM + 2 % ethanol + pyridoxine and/or arginine medium. For time lapse studies, cells were incubated at 30°C for 15 hr or at RT for 24 hr and images were captured at RT, with an Axiophot microscope (Zeiss, Jena), a Planapochromatic 63X or 100X oil immersion objective lens, and a 50 W Hg lamp. In the case of DAPI staining for visualization of nuclei, strains (FGSC26 and SPR1) were grown for 8 hr at 37°C onto coverslips with 500 μl appropriate medium, and subsequently fixed for 30 min at 37°C in 4% formaldehyde in PME buffer (50 mM PIPES, 5 mM EGTA, 1 mM $MgSO_4$ (pH 6, 9)). The cells were then digested with 4 mg/ml glucanase, 2 mg/ml yeast lytic enzyme and 11 mg/ml driselase (InterSpex Products) for one hour at room temperature. This was followed by three washes with PME buffer, and for staining of the nuclei mounting media with Vectashield DAPI (Vector Laboratories Inc., Burlingame CA) was used.

Images were collected and analyzed with a Hamamatsu Orca ER II camera system with optional RGB modus, and Wasabi software (version 1.4). Time-lapse series were obtained with an automated Wasabi program that acquires series of images with 3, 10 or 20 s of pause time, 0.5 or 0.75 s exposure time, and about 40 exposures in a sequence. Image and videos processing was done with Photoshop 6.0 (Adobe) and freeware programs as ImageJ and VirtualDub.

IV. Results

1. Cloning of the *kipB* gene

To gain insights into the organization and function of *Aspergillus nidulans* kinesins, the genomic DNA database at Cereon Genomics LLC (Cambridge, USA) was analysed, and partial sequences of putative kinesin motors were obtained (Fig. IV.1, C: 1-2). One of them was localized on chromosome III, was 788 bp in length and encoded a peptide with high homology to the Kip3 kinesin from *Saccharomyces cerevisiae*, being called *kipB*. This partial sequence was used to design primers to isolate two correspondent cosmids from the pUI library (kindly provided by B. Miller, Idaho, USA). One of them (pPR5) contained a 3.3 kb *Bam*HI fragment of the *kipB* gene (called later "short fragment"), which was subcloned (pGR1) and sequenced (Fig. IV.1, C: 3-4). Sequencing revealed that the 3' *Bam*HI site was introduced artificially through construction of the cosmid library. In addition, translation of the DNA insert continued into the pGR1 plasmid, suggesting that pPR5 did not contain the entire *kipB* gene, therefore a second cosmid (pPR17) was isolated and a 4.3 kb *Sac*I restriction fragment was subcloned and sequenced (pPR19) (Fig. IV.1, C: 5-6). Since the ORF did also not finish within the *Sac*I fragment, the 3' end of the gene was amplified by PCR, with genomic DNA as template (from the 5' *Sac*I site until the Stop codon), cloned into pCR 2.1 vector (Invitrogen, NV Leek, The Netherlands) and sequenced (pPR21) (Fig. IV.1, C: 5-7). All sequences were assembled to the final *Sac*I-*Nru*I fragment, compared to the sequence available at Whitehead Center for Genome Research (Cambridge, USA) after the public release of *A. nidulans* genome sequence, and considered as the final genomic locus.

In order to deduce a putative kinesin protein sequence and the intron-exon borders, a correspondent cDNA sequence was amplified by RT-PCR and compared with the genomic DNA sequence. The determination of intron positions was done by PCR amplification with the same primers of overlapping fragments covering the entire ORF and having as template cDNA and genomic DNA. By running the PCR products in 1% agarose gels, a shift was detected between the cDNA and the genomic DNA amplified with the primers KipB_A and KipB_B (Fig. IV.1, A and B). This revealed one 56 bp intron, located at the N-terminus of the predicted protein

(Fig. IV.1, A, B and C). The position of the intron is conserved in comparison to *Schizosaccharomyces pombe* kinesin genes *klp5* and *klp6*. Using a promoter prediction program (http://www.fruitfly.org/seq_tools/promoter.html), a putative promoter could be identified, with the start of transcription 78 bp upstream of the translation start (Fig. IV.1, C). A *kipB* specific probe hybridized in a northern blot to a 3.5 kb transcript (Fig. IV.2, A). After the removal of the intron sequence, the open reading frame consisted of 989 amino acids, with a predicted molecular mass of 108.7 kDa and a calculated isoelectric point of 9.9.

To detect the KipB protein in crude cell extracts the initial construct containing the first 690 amino acids was used (plasmid pGR1, with short version of KipB), because at that time the artificial *Bam*HI site was thought to belong to the gene and the Stop codon was situated very close to it. The 3.3 kb *Bam*HI fragment from pGR1 was tagged C-terminally with 3 HA epitopes under the control of the *alcA* promoter, and the plasmid (pPR12) was transformed into wild type strain GR5. One of the transformant strains (SPR3 – truncated KipB-HA) with 2 integrations was selected and was processed for a Western blot (Fig. IV.2, B). A specific band of about 76 kDa could be detected, which was in good agreement with the short putative KipB protein with a deduced molecular mass of 76.7 kDa. The full length KipB protein has not been analyzed by western blot yet.

Fig. IV.1: Locus of *A. nidulans* kinesin *kipB*. (A) Scheme of the *kipB* gene locus. The open reading frame and the transcript are indicated by arrows and the intron position is marked with a white box. **(B)** Agarose gel photo with determination of the intron position by PCR amplification of overlapping fragments covering the entire ORF and having as template cDNA and genomic DNA. First and last lanes for each primer combination represent genomic DNA from wild type and *kipB*-containing cosmid (pPR17) and the middle lane shows the cDNA. The white arrow points to the PCR product that displays a shift between the genomic and the cDNA, and which contains the intron. The DNA marker used: Gene Ruler^{TM} 100 bp DNA Ladder, from MBI Fermentas, Germany. Primers positions are depicted in (A). **(C)** Genomic sequence of the *kipB* gene, with the deduced protein sequence. The segment of 4771 bp from chromosome III includes the ORF (2973 bp), and one intron of 56 bp, in the N-terminal region of *kipB*. An asterisk above the putative promoter sequence indicates the predicted start of transcription. Between ① - ②: the initial Cereon sequence; ③ -④: *BamH*I short fragment (pGR1); ⑤-⑥ : SacI subclone (pPR19) from the cosmid pPR17; ⑤- ⑦: PCR amplified full open reading frame (pPR21).

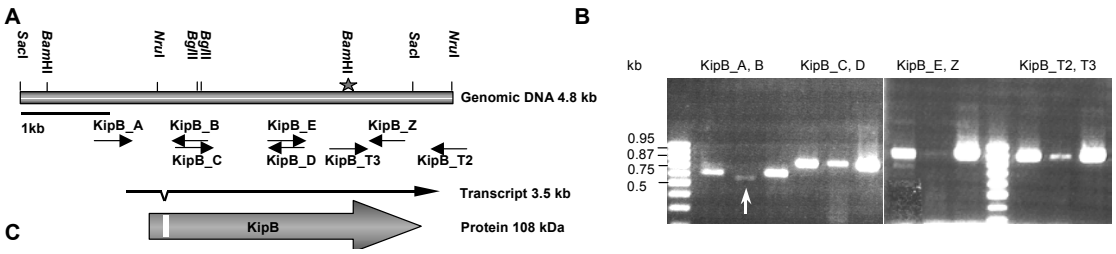
A
SacI
BamHI
NruI
BglII
BglII
BamHI
SacI
NruI
Genomic DNA 4.8 kb
1kb
KipB_A
KipB_B
KipB_C
KipB_E
KipB_D
KipB_Z
KipB_T3
KipB_T2
Transcript 3.5 kb
C
KipB
Protein 108 kDa
B
kb
KipB_A, B
KipB_C, D
KipB_E, Z
KipB_T2, T3
0.95
0.87
0.75
0.5

```
                                                
```

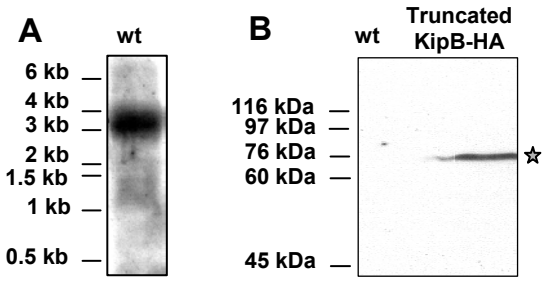

Fig. IV.2: Detection of the *kipB* transcript and the KipB protein (A) Northern blot analysis of *kipB*. RNA was isolated from mycelia of FGSC26, incubated at 37°C, harvested after 16 h of vegetative growth, and hybridized to a *kipB*-specific probe. **(B)** Protein extracts (RMS011 (wt) and SPR3 (truncated KipB (690 aa.)-HA)) were subjected to Western blot analysis and probed with anti-HA antibodies. The asterisk at the right of the panel marks the position of the protein and the absence of the signal for the wt (FGSC26).

2. Analysis of the protein sequence

Examination of the domain morphology of the KipB protein revealed the characteristic pattern of a kinesin. The highly conserved motor domain starts about 60 amino acids downstream of the initiation codon, and consists of about 320 amino acids. It contains an ATP-binding motif (or P-loop) near aminoacid position 130 (GxxxxGKT), and the C-terminal half of the motor domain displays the highly conserved regions termed switch I (SSRSH) and switch II (DLAGSE), which are involved in microtubule-binding (Fig. IV.3 and IV.4, A) (Song et al., 2001). Comparison with other Kip3-like proteins revealed 45.7 % identity with *Neurospora crassa*, 33.5 and 35.3 % identity with *S. pombe* Klp5 and Klp6 respectively, and 30.4% with *S. cerevisiae* Kip3. The identity between the proteins is much higher in the motor domains: 85% with *N. crassa*, 68% with Klp5 and 59% with Klp6 from *S. pombe* and 61% with Kip3 from *S. cerevisiae*. The N-terminal region starts with a short nonmotor sequence of 65 amino acids. The latter one displays after the first 6 amino acids a sequence of 18 aa, which is conserved among the compared proteins (Fig. IV.3 and IV.4, A). The significance of the 18 amino acid motif is yet unknown (West et al., 2001). The nonmotor, COOH-terminal 600 amino acids exhibited very low sequence similarity to the nonmotor regions of the other kinesin-related proteins, or to proteins in the current DNA, protein and EST databases. Also, in the COOH-terminal domain short regions with a significant probability for a coiled-coil formation were detected, similar to the proteins from *S. cerevisiae* and *S. pombe* (Fig. IV.4, B).

The positions of these regions are conserved (DeZwaan et al., 1997), (West et al., 2001), and they can potentially mediate protein multimerization.

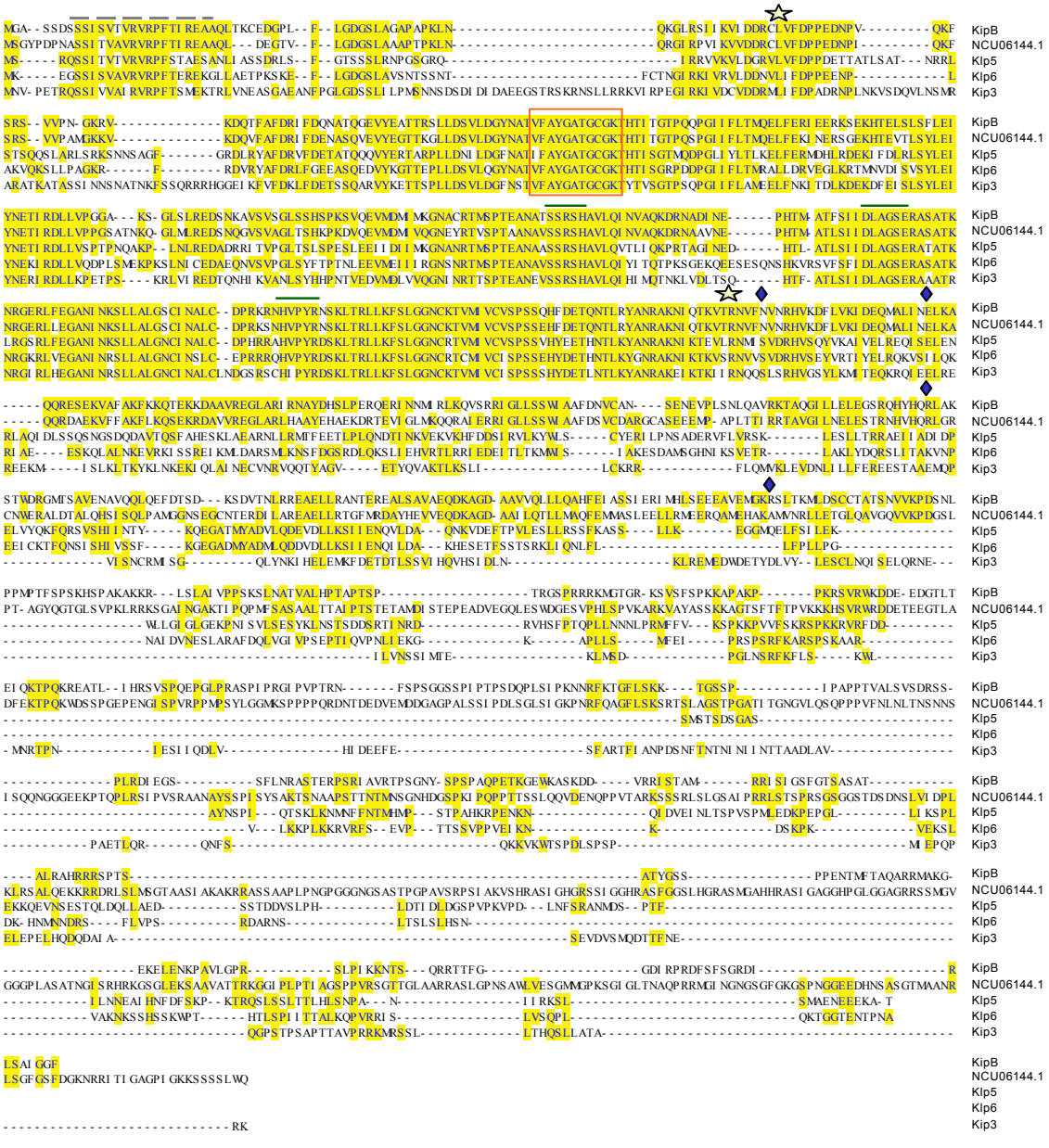

Fig. IV.3: Alignment of *A. nidulans* KipB with homologous kinesin sequences from *N. crassa* (NCU06144.1), *S. pombe* (Klp5 and Klp6) and *S. cerevisiae* (Kip3). The alignment was done with DNAstar using MEGALIGN (CLUSTAL) with a window size of 5 and a gap length penalty of 10. The beginning and the end of the highly conserved motor domains are indicated by asterisks above the sequences. The ATP-binding motif is boxed (orange) and the putative microtubule binding pocket is indicated by lines (green) above the sequences. The 18 amino acid motif at the N-terminus, which is conserved among the compared proteins is highlighted by a dashed line (grey) above the sequences. The putative coiled-coil domains are marked by the diamond (blue) above the sequences.

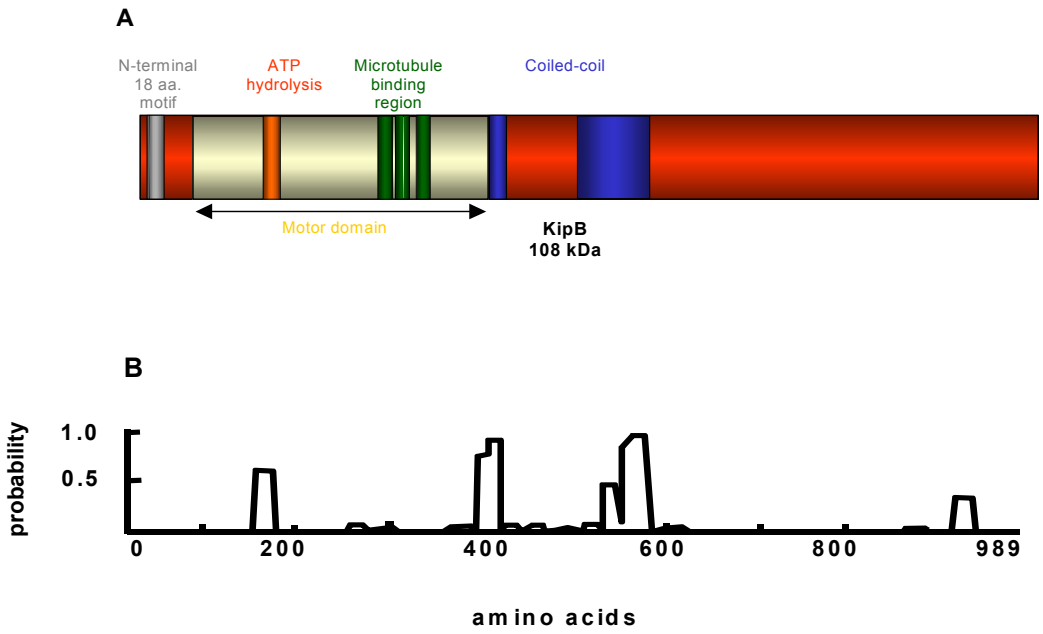

Fig. IV.4: Domains and coiled-coil prediction for the KipB protein. (A) Schematic drawing of different domains, with correspondent colour display onto the protein alignment from Fig IV.3. **(B)** Coiled-coil prediction (Lupas et al., 1992) for KipB (window size 14). Significant coiled-coil probability was found between amino acids 390-408, and 500-600.

The sequence of *A. nidulans kipB* was deposited in the EMBL database and is available under the accession number AJ620863.

After obtaining the full length *kipB* gene sequence, the question which rose was if there are other *kipB* kinesin homologues in *A. nidulans* genome, as it was described for *klp5* and *klp6* in *S. pombe* (West et al., 2001). Upon completion of the *A. nidulans* genome sequencing project at the Whitehead Center for Genome Research (Cambridge, USA), the public databases were thus searched using the BLAST program available at this site (http://www-genome.wi.mit.edu/annotation/fungi/aspergillus/index.html) for kinesin-like proteins (Fig. IV.5) (study realized in collaboration with Sven Konzack, Marburg). The motor domain of *A. nidulans* KipB protein was used to identify eleven putative kinesin motors.

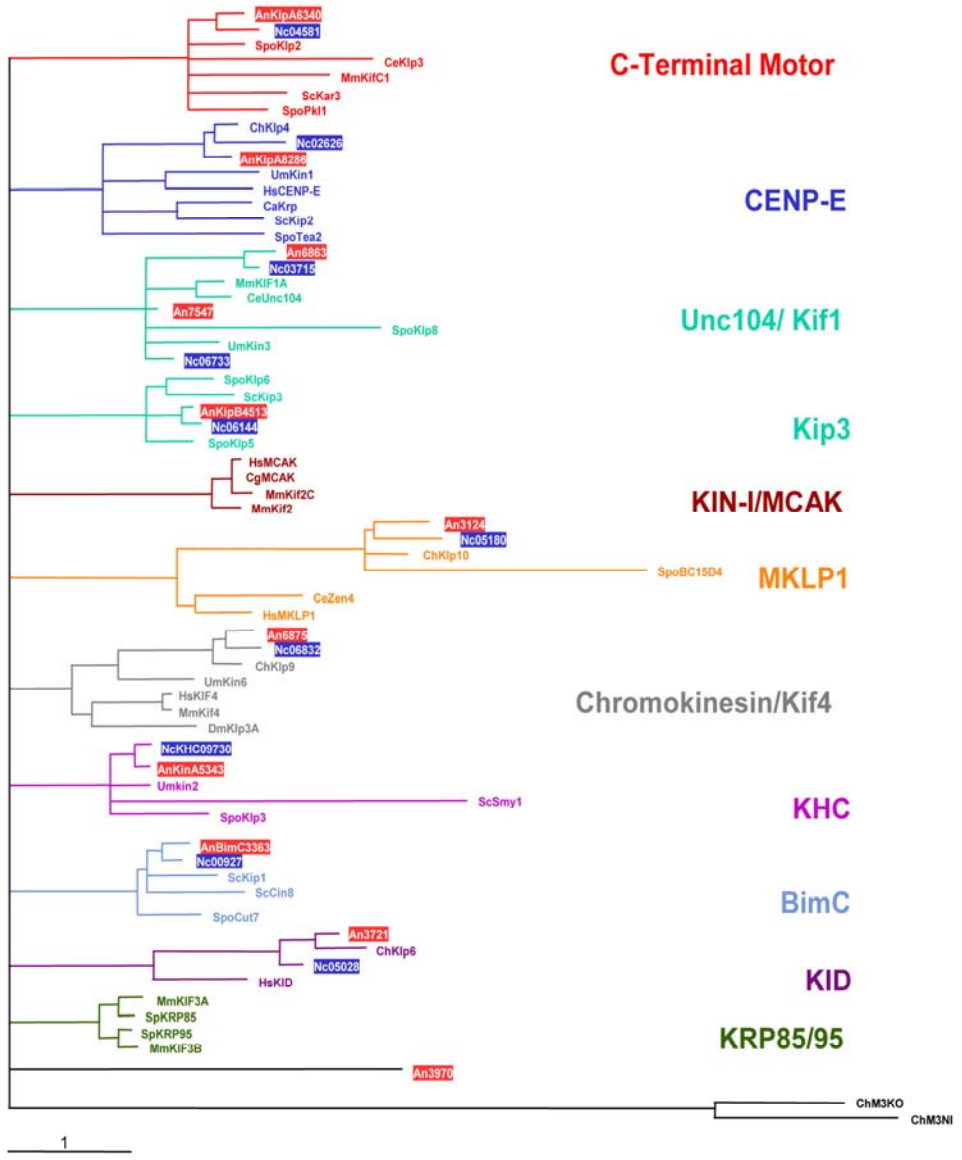

Fig. IV.5: Relatedness analysis of the eleven *A. nidulans* and the ten *N. crassa* kinesins. A most likely phylogenetic tree of 74 kinesins was built with Treepuzzle (http://www.tree-puzzle.de/) using a maximum-likelihood algorithm. For evaluation of statistical significance of the topology 25.000 replicating puzzling steps were performed. The substitution model Whelan-Goldman 2000 was used because it produced a consensus tree, which was in good agreement with the published data (Schoch et al., 2003). For the construction of the tree we have chosen fungal kinesin sequences and additional kinesins from other organisms characteristic for the different families. It has to be noted that for *A. nidulans* exon/intron boarders were only experimentally determined in the case of BimC, KlpA, KinA, KipA and KipB. In the case of *N. crassa* only the conventional kinesin NcKHC has been analyzed experimentally. The other primary structures of the proteins of *A. nidulans* and *N. crassa* are based on the predictions in the annotation process at the Whitehead Institute. The *N. crassa* Kip3 homologue was annotated manually. The origin of the kinesin sequences was abbreviated: An = *A. nidulans*; Nc = *N. crassa*; Spo = *S. pombe*; Ce = *Caenorhabditis elegans*; Mm = *Mus musculus*; Um = *U. maydis*; Sc = *S. cerevisiae*; Ch = *Cochliobolus heterostrophus*; Hs = *Homo sapiens*; Ca = *Candida albicans*; Dm = *Drosophila melanogaster*; Cg = *Cricetulus griseus*; Sp = *Strongylocentrotus purpuratus*. The *A. nidulans* and the *N. crassa* sequences were boxed.

They grouped into nine of the eleven families, two kinesins being found in the Unc104 family and one did not fall into any of the known families. The ten *N. crassa* kinesins (identified through similar procedure of motor domain search at http://www-genome.wi.mit.edu/annotation/fungi/neurospora/index.html were closely related to the *A. nidulans* proteins. In comparison, in the single cell organisms *S. cerevisiae* reside six and in *S. pombe* nine kinesins (Schoch et al., 2003).

3. Molecular analysis of *kipB* functions

3.1. *kipB* disruption

The cellular function of *kipB* was investigated through the construction of a null mutant by homologous recombination (Fig. IV.6, see also Chapter III). The motor domain was disrupted by insertion of the nutritional marker gene *argB* (Fig IV.6, A). Colony purified arginine prototrophic transformants of strain SRF200 were tested for the integration event at the *kipB* locus by Southern blot analysis using different restriction digests (Fig. IV.6, B, left) and by PCR tests (with primers: forward at the 3' end of *argB* and reverse at the 3' end of *kipB*) (Fig. IV.6, B, right). Two of 43 strains harboured the knock-out situation. In a cross with an *argB* deletion, *kipB* wild type strain (RMS011) the *kipB* disruption (Δ*kipB)* co-segregated with the *argB* marker. Two strains obtained in the cross (SPR13 and SPR22) were chosen for further phenotypic analysis with respect to polarized growth, mitochondrial movement and nuclear distribution. Observation of colony growth on plates at different temperatures (permissive temperature, 37°C and two restrictive temperatures, 30°C, 42°C) revealed no difference for the mutant strain, in parameters as colony diameter, growth speed or polarized growth (Fig. IV.7).

In *S. cerevisiae* several studies have shown that Kip3, the KipB homologue is required for migration of the nucleus to the bud site in preparation for mitosis (DeZwaan et al., 1997). The distance over which the nucleus has to migrate from the center of the cell is rather short and the mitotic machinery contributes significantly to this distribution process. In filamentous fungi, nuclei migrate long distances to follow the growing hyphal tip. During the migration process nuclei divide and individual nuclei are left behind to populate the entire mycelium (Suelmann & Fischer, 2000). Therefore the analysis of nuclear movement in *A. nidulans* can reveal insights into a very complex machinery driving organelles within the cell. Since the *kipB* gene

appeared as a real candidate in this process, its putative role in nuclear migration in *A. nidulans* was studied. Thus, the movement of GFP-labeled nuclei has been followed in living hyphae by fluorescence microscopy. Time-lapse studies of nuclear migration in both wild type and mutant indicated no particular phenotype for Δ*kipB*, except a slight tendency of nuclei to remain clustered for short periods after their exit from mitosis. After that, they distributed normally in the same even pattern as in the wild type (Fig. IV.8 and movies 2 and 3).

The interest in studying mitochondrial dynamics and morphology came after a report was published about two similar kinesin-related proteins (KRPs) from the higher plant *Arabidopsis*, named MKRP1 and MKRP2 (for mitochondria-targeted KRP), and which contained an N-terminal mitochondrial targeting signal (MTS). They were considered to represent a new subclass of KRPs that might work within mitochondria (Itoh et al., 2001). To check if KipB could be implicated in this process, a plasmid (pRS54) containing the green fluorescent protein (GFP) targeted to mitochondria of *A. nidulans*, by its translational fusion to 76 amino acids of the N-terminus of citrate synthase (from *A. niger*; Acc. No. 63376), which harbor the signal sequence required for mitochondrial import (Suelmann & Fischer, 2000), was transformed into a Δ*kipB* mutant (SPR26). The transformant strains were screened for fluorescence, one of them (SPR80) and a wild type strain containing the same plasmid (SRS29) were chosen for further analysis. Fluorescence microscopy investigation of mitochondrial morphology and movement revealed the same tubular structures within the hyphae, mainly oriented in the longitudinal axis of the cell (Fig. IV.9 and movies 4 and 5) (Suelmann & Fischer, 2000).

A

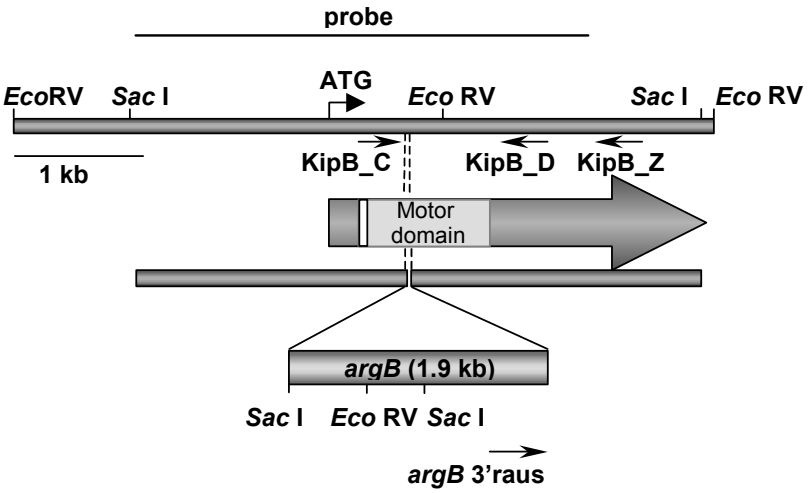

B

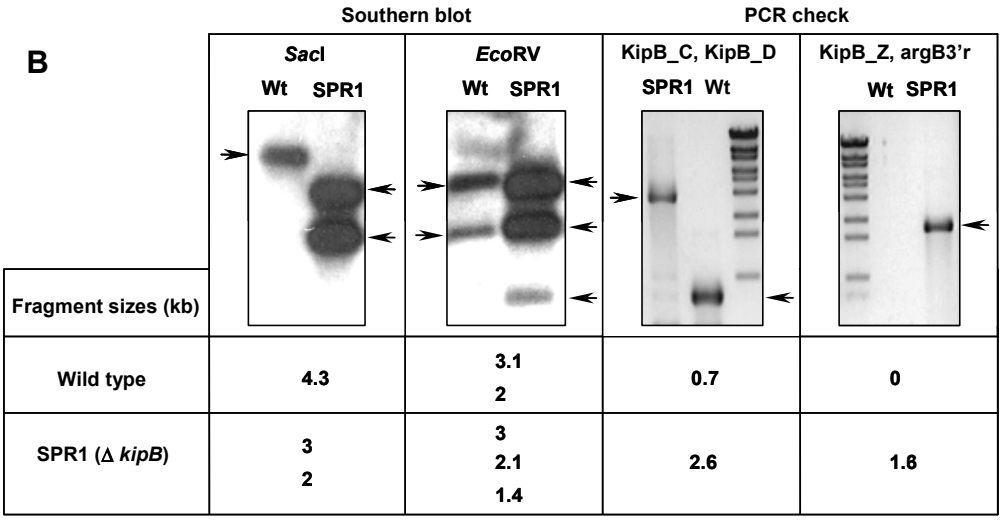

Fragment sizes (kb)	*Sac*I	*Eco*RV	KipB_C, KipB_D	KipB_Z, argB3'r
Wild type	4.3	3.1 2	0.7	0
SPR1 (Δ *kipB*)	3 2	3 2.1 1.4	2.6	1.8

Fig. IV.6: Disruption of the *kipB* gene. (A) Scheme of the strategy. The nutritional marker gene *argB* was inserted into *kipB* and thereby deleted 18 bp. **(B, left)** Southern Blot analysis of a *kipB* disruption strain (SPR1). Genomic DNA of a wild type (FGSC26) and the kinesin disruptant strain were isolated, restricted with *Sac*I (left) and *Eco*RV (right), separated on a 1% agarose gel, blotted and hybridized with the probe indicated in A. **(B, right)** PCR check of the same wild type and mutant strains, with the primers indicated in **(A)**. The DNA marker used: Lambda DNA/*Eco*130I (*Sty*I), from MBI Fermentas, Germany.

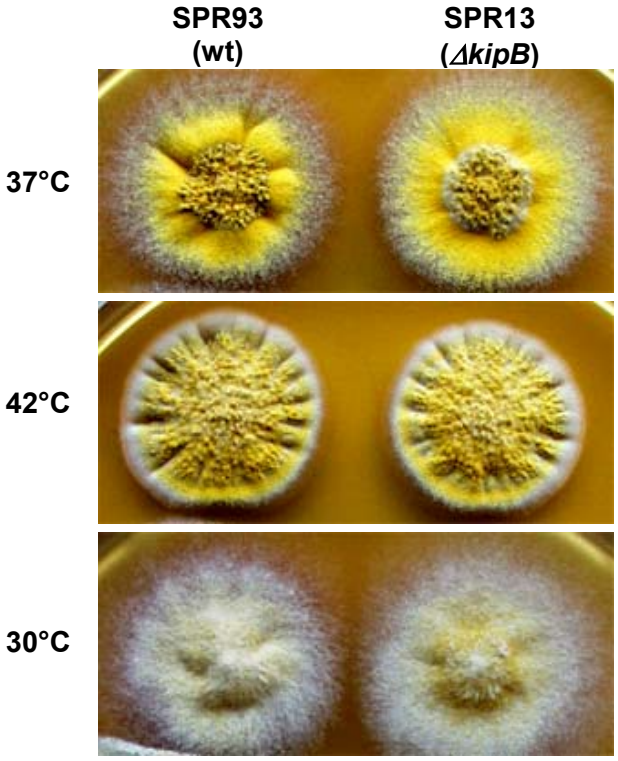

Fig. IV.7: Colony growth of wild type (SPR93) and the *kipB* disruptant (SPR13). Strains were inoculated on agar plates at different temperatures (37°C, 42°C and 30°C).

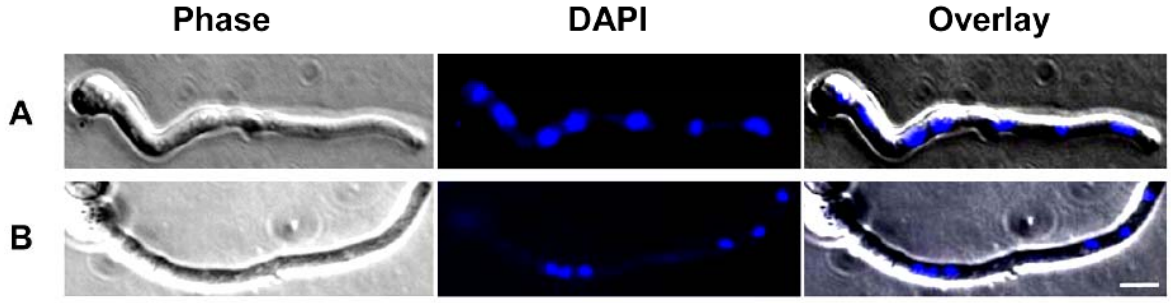

Fig. IV.8: Nuclear distribution in a wild type and a Δ*kipB* mutant strain. Conidia of a wild-type strain (FGSC26) and a kinesin mutant strain (SPR1) were germinated on microscope coverslips, at 37°C overnight, fixed with 4% formaldehyde, mounted with VECTASHIELD® mounting medium with DAPI and observed by fluorescence microscopy. **(A)** wild type (FGSC26), **(B)** Δ*kipB* strain (SPR1). Scale bar 5μm.

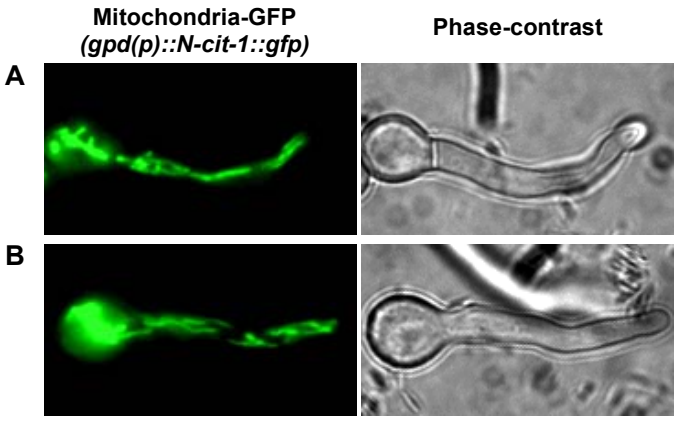

Fig. IV.9: Mitochondrial morphology in a wild type and a Δ*kipB* mutant strain. A wild-type strain (SRS29) and a kinesin mutant strain (SPR26), which were transformed with a sGFP construct targeted to mitochondria (pRS54) (Suelmann & Fischer, 2000), were selected and compared for mitochondrial morphology. **(A)** wild type (SRS29); **(B)** Δ*kipB* mutant strain (SPR80).

The absence of differences between the wild type and the Δ*kipB* mutant strains in all the features analysed above suggests that KipB is not involved in those processes or other kinesin motors are able to substitute for the function of KipB.

3.2. Disruption of *kipB* affects microtubule stability

The next step for investigation of KipB function was to look for a role of the protein in the organization of the microtubule cytoskeleton. Early reports about homologous genes as *kip3* in *S. cerevisiae* and *klp5* and *klp6* in *S. pombe* proposed roles for them in microtubule stability and organization. In order to assess this function, the sensitivity to the microtubule-destabilizing drug benomyl for both the wild type and mutant was analysed. While the wild type failed to grow at concentrations between 0.75-0.9 μg/ml, the Δ*kipB* mutant was still able to grow and was only inhibited at concentrations above 0.95 μg/ml (Fig. IV.10). The difference in benomyl-sensitivity was independent of the growth temperature. These results suggest that the kinesin KipB destabilizes microtubules in *A. nidulans*.

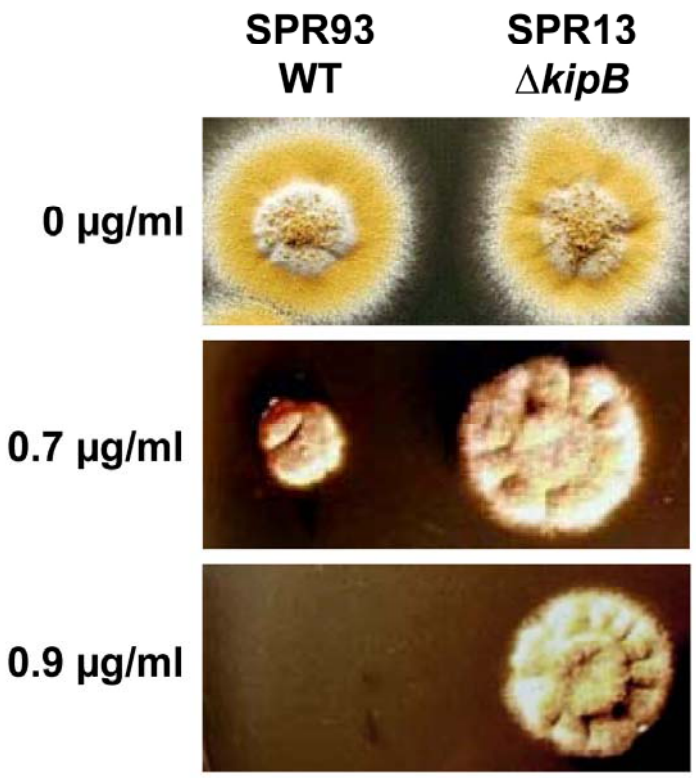

Fig. IV.10: Effect of different benomyl concentrations on colony growth of wild type (SPR93) and the *kipB* disruptant (SPR13). Strains were inoculated on agar plates at 37°C supplemented with the indicated benomyl concentrations dissolved in DMSO.

To study directly an effect of the *kipB* mutation on microtubule stability, the microtubule cytoskeleton in wild type and a Δ*kipB* mutant strain (SPR30) where alpha-tubulin was labeled with GFP was compared. In single cell yeasts such as *S. cerevisiae* or *S. pombe* the effect of mutations of genes encoding microtubule-destabilizing components can be easily documented since the cytoplasmic or astral microtubules in those strains elongate even after contacting the cortex. As a result microtubules appear bent along the cortex (Behrens & Nurse, 2002). In filamentous fungi differences in the cytoplasmic microtubule network were rarely reported (Requena et al., 2001). Likewise, in the Δ*kipB* mutant only a slight effect in comparison to wild type interphase cells could be detected. Microtubules appeared more curved, which could be due to continuous growth after reaching the hyphal tip (Fig. IV.11, A). However, it is difficult to follow a single MT along the entire length through the compartment. A striking difference in microtubule organization became obvious when mitotic cells were analysed. During mitosis cytoplasmic microtubules

are almost entirely depolymerized to provide tubulin subunits for the assembly of the mitotic spindle and the formation of astral microtubules (Ovechkina et al., 2003). In the Δ*kipB* mutant strain, however, several cytoplasmic microtubules were observed during mitosis (Fig. IV.11, B). In addition, astral microtubules grew to long filaments.

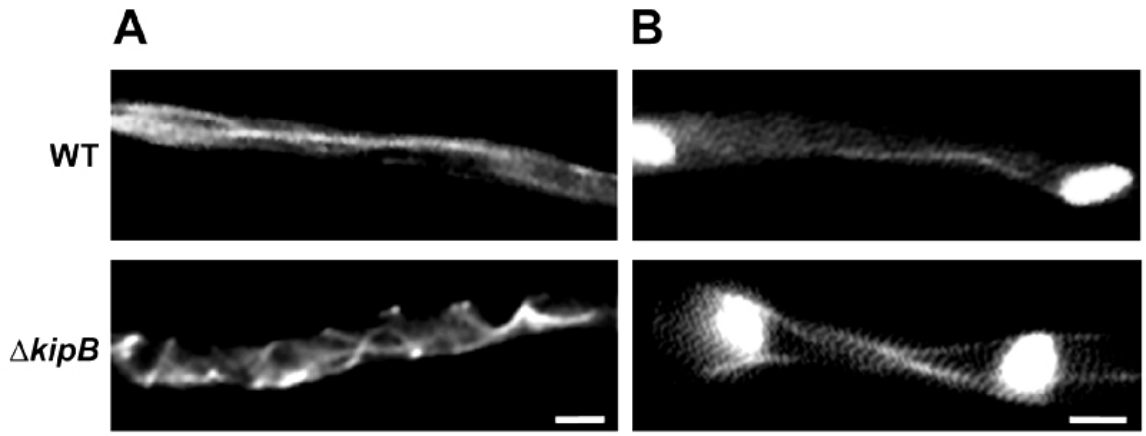

Fig. IV.11: Morphology and microtubule organization in a Δ*kipB* mutant strain and wild type. Microtubules were observed as α-tubulin-GFP by fluorescence microscopy (see Materials and Methods). Upper row: wild type; lower row: Δ*kipB* strain. **(A)** Cytoplasmic microtubules. In wild type they are long and straight, while they display a curved pattern in Δ*kipB.* **(B)** Two mitotic spindles can be seen. In wild type one cytoplasmic MT remained while in the Δ*kipB* strain three filaments are visible. Scale bar equals 5 μm.

3.3. KipB is involved in the positioning and morphology of mitotic spindles

During the course of the analysis of mitotic cells, it was noticed that the mitotic spindles were not properly distributed in hyphae. Mitosis in wild type is almost synchronous in one hyphal compartment (see movie 6) and since nuclei are evenly spaced before entering mitosis, mitotic spindles remain distributed and fixed at their

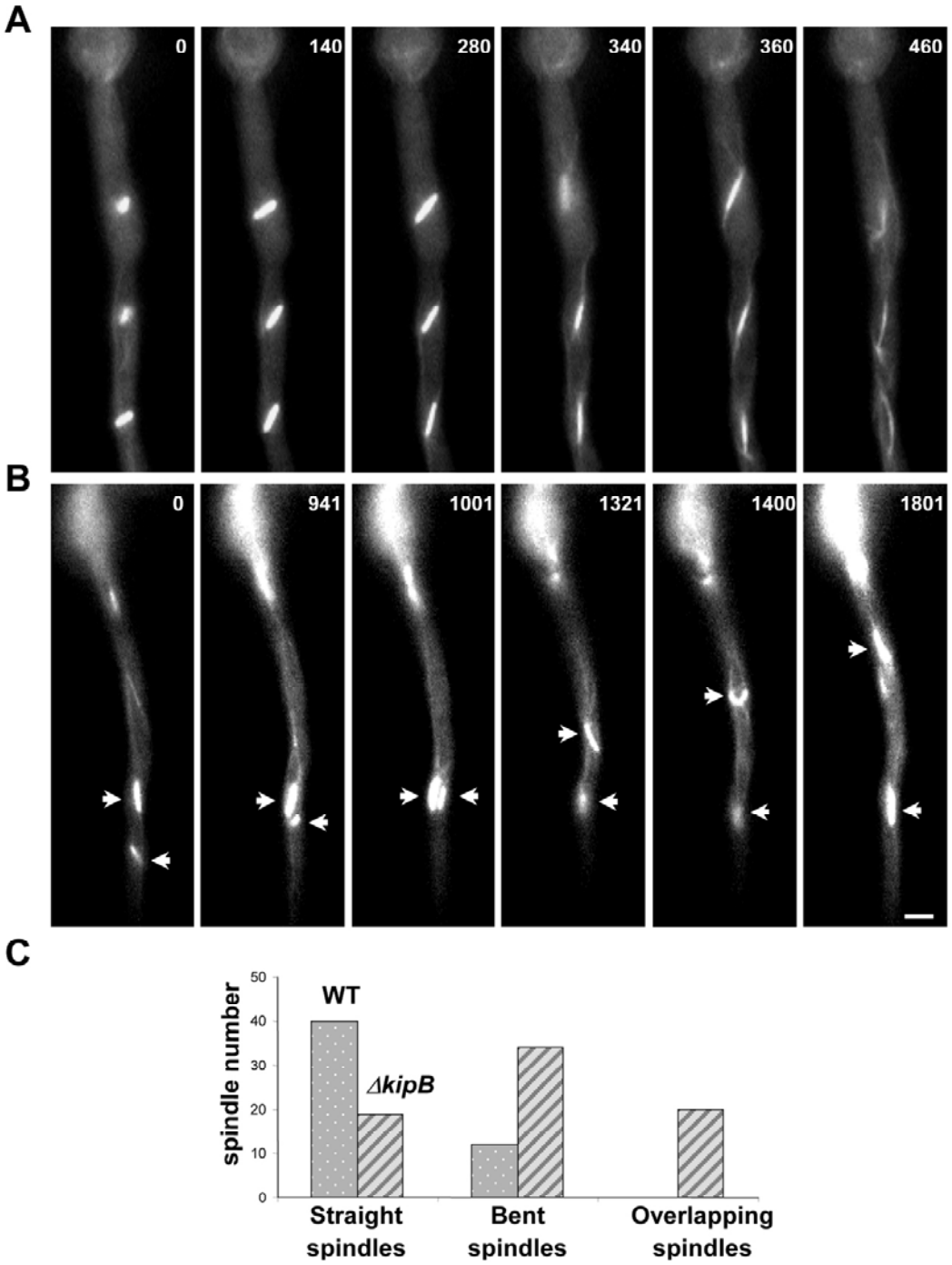

Fig. IV.12: Positioning of mitotic spindles in wild type and Δ*kipB* disruptants. Images from a time-lapse series are displayed (times in seconds are indicated in the upper right of each panel). **(A)** Wild type synchronized mitoses, with evenly distributed spindles along the length of the hypha (see movie 6). **(B)** Mitosis in the Δ*kipB* mutant strain, with defects in spindle positioning, morphology (sharp angled bow-like structures) showing high mobility through the cytoplasm, which leads to overlapping of the spindles (arrows) (see movie 7). Scale bar equals 5 μm. **(C)** Quantification of different spindle morphologies and spindle behaviour in wild type and the Δ*kipB* mutant strain.

positions (Fig. IV.12, A). In contrast, mitotic spindles of Δ*kipB* mutants were highly mobile, overpassed each other and frequently moved long distances through the cytoplasm (Fig. IV.12, B, and movie 7). However, interphase nuclei were again evenly distributed.

During their migration process 64 % of the spindles appeared with a bent shape (53 spindles, two independent strains were analyzed). In wild type such a shape was only observed in 23 % of the cases (52 spindles analyzed). Time-lapse studies revealed that the some longer astral filaments radiating from one pole of the spindle could make contact backward of the connection point of the asters from the opposite pole, thus pulling the entire spindle structure and bringing the opposite poles in the same plane, and thus sharply bending the spindle structure. In a Δ*kipB* mutant strain where spindle pole bodies (SPBs) were visualized through ApsB-GFP tagged protein (ApsB was shown to associate with SPBs, (Veith et al., 2004)), it was observed the situation when the SPBs reversed direction momentarily and consequently they were drawn closer together (Fig. IV.13, see also movies 8 (wild type) and 9 (mutant)). This often resulted in severely curved spindles, which sometimes could be rescued by the dragging of the disturbed pole back to its initial position, this probably through the action of another emerging astral microtubule, capable to attach to the first position at the cortex.

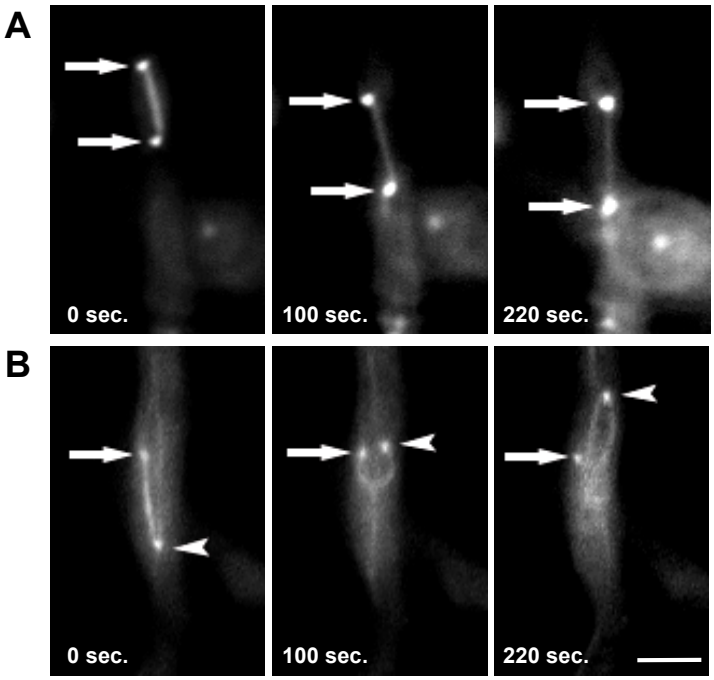

Fig. IV.13: Morphology of mitotic spindles in wild type and Δ*kipB* disruptants. (A) Elongation of the mitotic spindle during mitosis in wild type. Spindle pole bodies (SPBs, marked with arrows) remain at the opposite poles of the spindle. **(B)** Bending of the spindles in Δ*kipB* mutant. One of the SPBs remained at a fixed position (arrow), while the opposite one migrates backwards (arrowhead), arriving in the same plane with the first SPB. See also movies 8 (wild type) and 9 (mutant). Scale bar equals 5 μm.

3.4. *kipB* disruption causes a delay in mitotic progression

To determine if any stage of mitosis is affected in the Δ*kipB* mutant, spindle behaviour in both wild type and the mutant was compared by live-imaging. In fungi, mitosis starts with an early prophase, when the SPB's divide and separate towards opposite sites, generating a half-spindle. In metaphase the bipolar spindle is completely formed and the chromosomes are attached to the spindle microtubules via the kinetochores. The chromosomes are usually scattered over the middle one-third to one-half of the spindle rather than arranged in a metaphase plate. Anaphase occurs in two stages. During anaphase A, the chromatids are separated and migrate asynchronously along the entire length of the spindle to the respective spindle poles, and the astral microtubules are starting to be developed. During anaphase B, the spindle elongates rapidly between the two SPB's and the astral microtubules reach their maximal length (Aist & Morris, 1999). The first stage (prophase to metaphase) had a short duration (60-80 sec). Then, the mutant exhibited a much longer anaphase A, with duration of 400-600 sec, in comparison to wild type with 160-200 sec (Fig. IV.14) (see movies 10 (wild type) and 11 (mutant)).

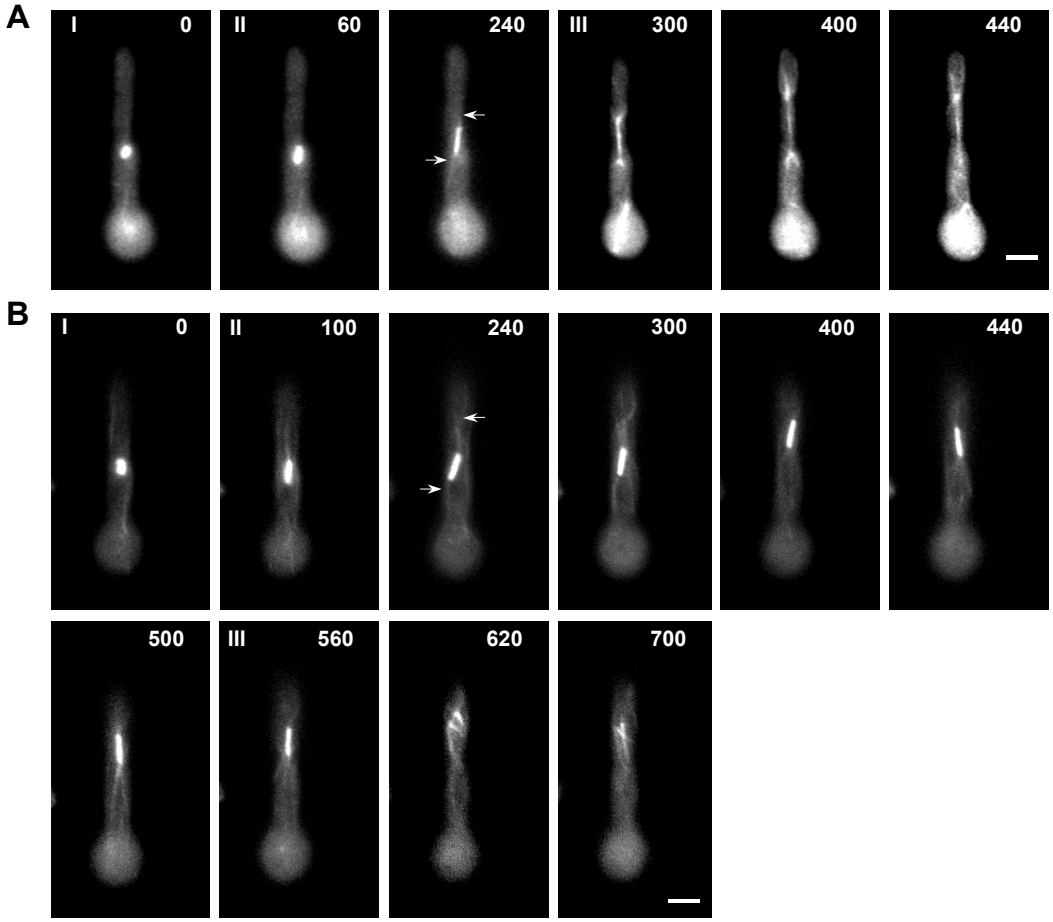

C

Strain	Prophase (I) (sec)	Anaphase A (II) (sec)	Anaphase B (III) (sec)
WT	60-80	160-200	160-200
ΔkipB	60-100	300-600	160-200

Fig. IV.14: *kipB* disruption causes a delay in mitotic progression. Time-lapse analysis of mitosis in germlings of wild type (strain GFP-*tubA*) (see movie 10) **(A)** and Δ*kipB* mutant (SPR30) (see movie 11) **(B)**. Microtubules were labeled with GFP. The stages of mitosis are indicated in the upper left corner of the pictures. Prophase to metaphase (= I)(short spindle); anaphase A (= II)(spindle elongates very slowly, appearance of astral microtubules (indicated by arrows)), anaphase B (= III)(spindle elongates rapidly and doubles or triples in length). Cells were grown overnight at 30°C and were observed at room temperature. Images were taken every 20 sec., a selection of which is displayed here. The time points (in sec) are indicated in the upper right corner of the pictures. Scale bar equals 5 μm. **(C)** Summary of the time intervals of different mitotic phases in wild type and Δ*kipB* mutant strain. (see also movies 10 (wild type) and 11 (mutant)).

3.5. Genetic interaction of Δ*kipB* with *bimC4*

Since KipB appeared to play a role in mitosis, the Δ*kipB* mutation was tested for genetic interaction with a temperature sensitive kinesin motor mutation*, bimC4.* The first member of the BimC family of kinesins was discovered in a genetic screen for temperature-sensitive lethal mitotic genes in *A. nidulans* as a mutant that was "blocked in mitosis". The proteins belonging to the BimC family are bipolar motor proteins that exert their function by crosslinking and sliding apart antiparallel microtubules (Kashina et al., 1997). A cross between a Δ*kipB* mutant (SPR13) and a temperature sensitive *bimC4* strain (MO62) was performed. Two *bimC4/*Δ*kipB* double mutant strains (SPR88 and SPR90) were selected and their growth was compared with the growth of strains with corresponding single mutations (Fig. IV.15). This assay was performed at permissive (30°C), at restrictive (42°C) and at semi-permissive temperature (37°C) for *bimC4*. The double mutant displayed increased temperature sensitivity compared with the two single mutants. At intermediate temperature the double mutant showed a stronger growth defect than the *bimC4* mutant, suggesting genetic interaction of the two kinesins (Fig. IV.15).

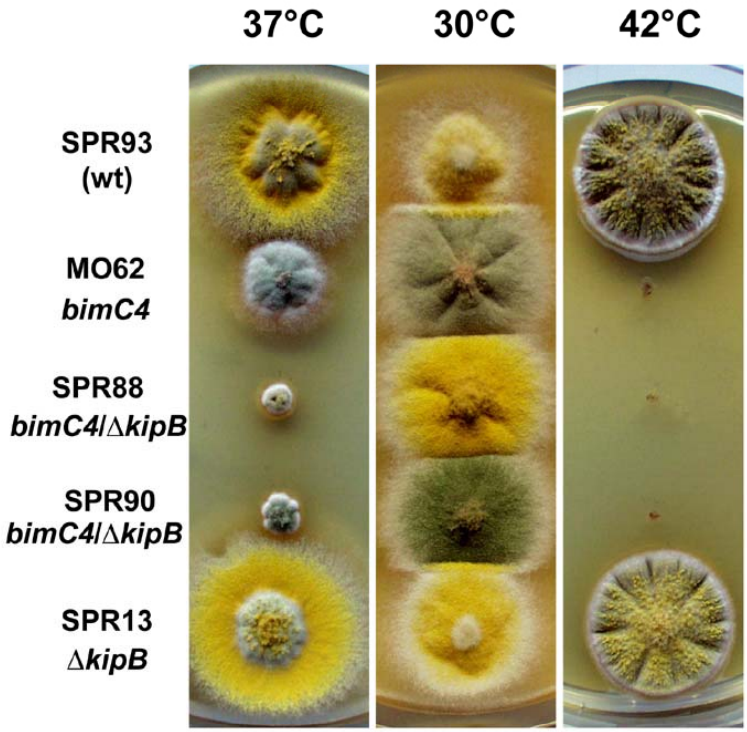

Fig. IV.15: Disruption of *kipB* is synthetically lethal with *bimC4*. Comparison of colony growth of SPR93 (wt), MO62 (*bimC4*), SPR13 (Δ*kipB*) and two double mutants (SPR88 and SPR90), at 37°C, 42°C for 3 days and 30°C for 5 days.

3.6. Gene dosage of *kipB* determines the frequency of chromosome loss in a diploid strain

To further investigate the effect of the Δ*kipB* mutation on nuclear division, a wild type and the Δ*kipB* mutant were compared for chromosome loss during mitosis. Since conidiospores of *A. nidulans* are haploid, any loss of one of the eight chromosomes would lead to the death of the spore and thus a germination defect. However, no difference in the viability of conidiospores harvested from the two strains was found, suggesting a more subtle effect of the mutation. Therefore it became interesting to study putative chromosome loss in diploid strains (Fig. IV.16, A). Those strains can be obtained from conidiospores generated in a heterokaryon. With a low frequency diploid spores are formed and can be stably maintained when a selection pressure is applied. If they loose one chromosome during mitosis, they reduce the number to the haploid set of chromosomes and in the absence of the selection pressure they can grow to mature colonies (Käfer, 1977). If strains with green spores were used in combination with strains with yellow spores for the construction of the diploid or strains with white spores in combination with strains with yellow spores, haploidization can be easily visualized through the colors of a colony and sectors with different colors. Chromosome-loss can be stimulated by the application of low benomyl concentrations. Diploid strains between the *kipB* mutant (yellow spores) (SPR13) and a wild type (white spores) (GR5) and a homozygous Δ*kipB* diploid strain (yellow and green spores in the haploid parents) (SPR13 and SPR22) were constructed and compared the frequency of haploidization with a diploid wild type strain (RMS012). The frequency of sectors with different colors was very low in wild type and increased with increasing benomyl concentrations. In comparison diploids heterozygous for the *kipB* mutation (*kipB/*Δ*kipB)* (SPR55) formed more haploid sectors than the wild type. Interestingly this frequency decreased with increasing benomyl concentrations. A Δ*kipB* homozygous diploid (Δ*kipB/*Δ*kipB*) (SPR60) appeared to have an even lower frequency of haploidization than the wild type (Fig. IV.16, B).

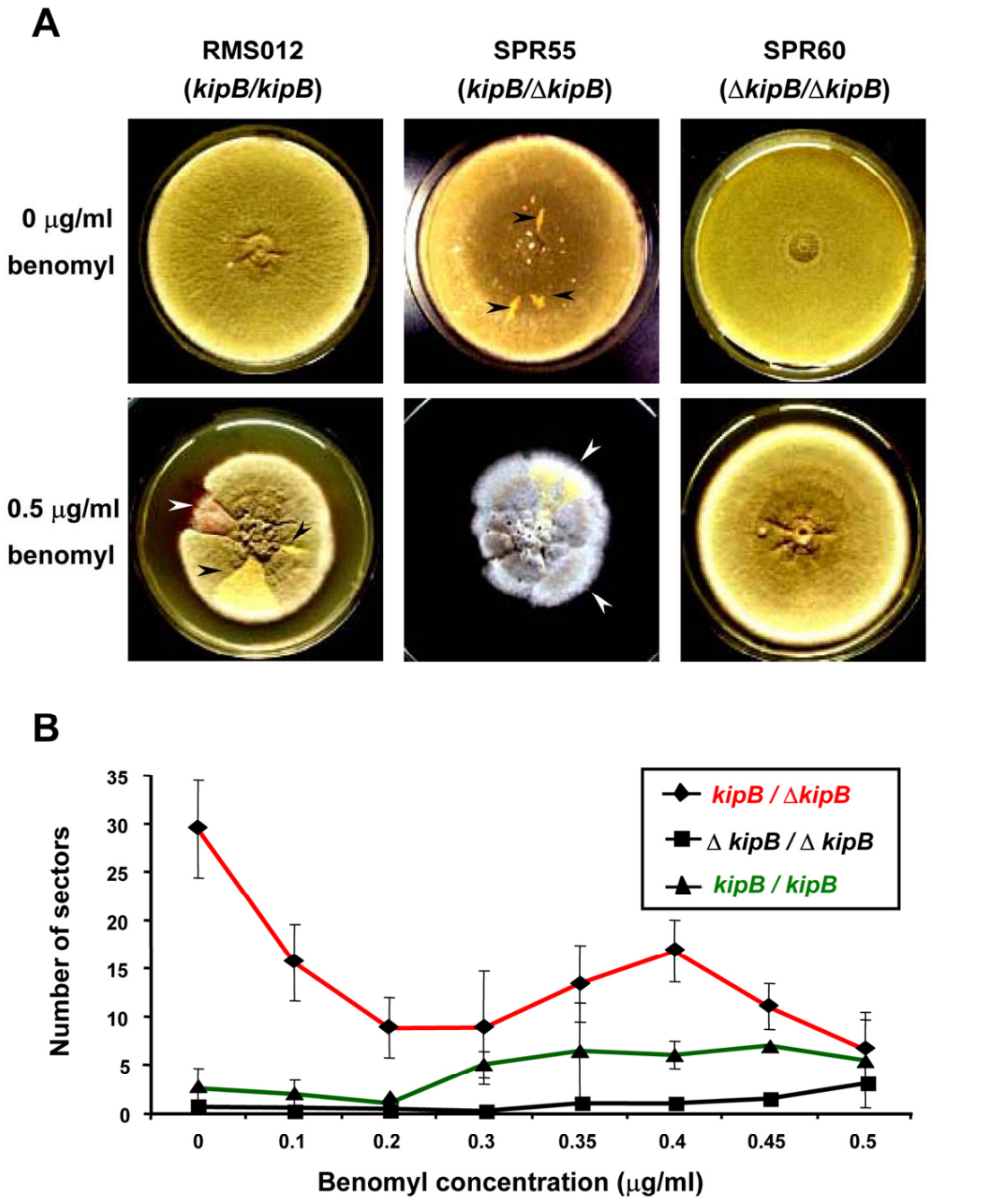

Fig. IV.16: Haploidization of diploids of *kipB/kipB* (wild type, RMS012), Δ*kipB/kipB* (heterozygous, SPR55) and Δ*kipB*/Δ*kipB* (homozygous, SPR60). (A) Colony growth on plates without benomyl (upper row) and with 0.5 µg benomyl/ml (lower row). The arrows point to haploid sectors. **(B)** The number of haploid sectors was counted for the three strains denoted in (A). For the homozygous Δ*kipB* situation were analyzed 10 diploid strains, for the heterozygous 6 and for the wild type 1 strain. The average numbers of sectors are shown.

In contrast to the effect on mitosis and chromosome segregation in the diploid, there is no evidence for a role of KipB in meiosis. Crosses between different strains did not show any abnormality and the number of ascospores per ascus as well as the viability of the spores was not altered.

3.7. Genetic interaction of Δ*kipB* with other motor protein mutants

Because Δ*kipB* mutant exhibited very subtle phenotypic differences in comparison with the wild type strain, the question that rose was about the existence of partially redundant pathways for some of the phenomena presented above (nuclear migration, mitochondrial dynamics, polar growth, etc.). Thus, it was intriguing to know whether other motor protein mutations would show genetic interactions with Δ*kipB.* To carry out this analysis, crosses were performed with strains bearing deletions in some of the kinesin-related genes along with several other relevant genes required for nuclear positioning, microtubule integrity, and/or polar growth. These genes were: *kinA* (conventional kinesin) (Requena et al., 2001), *kipA* (*A. nidulans kip2* homologue) (Konzack et al., 2004), *nudA1* (cytoplasmic dynein heavy chain temperature sensitive mutant) (Xiang et al., 1994), and *bimC4* (temperature-sensitive mutant of a kinesin related protein, see also Chapter 3.6) (Enos & Morris, 1990). The viability and growth characteristics of the resulting double or triple mutant strains were then used as an indicator for possible genetic interactions. Table IV.1 summarizes the results from the crosses, and Fig. IV.15 depicts a cross in which a synthetic growth defect was found. Another test performed with all the mutants described above was to grow them at two different temperatures (37°C and 30°C) in the presence of different benomyl concentrations, to compare the effect of double or triple mutations with the single ones on microtubule stability. The study of this phenotypic feature was chosen because it represented a striking phenotype for the Δ*kipB* mutant. Fig. IV.17 illustrates the outcome of this experiment. The double mutants exhibited the dominant phenotype of one of the parents (see also Table IV.1).

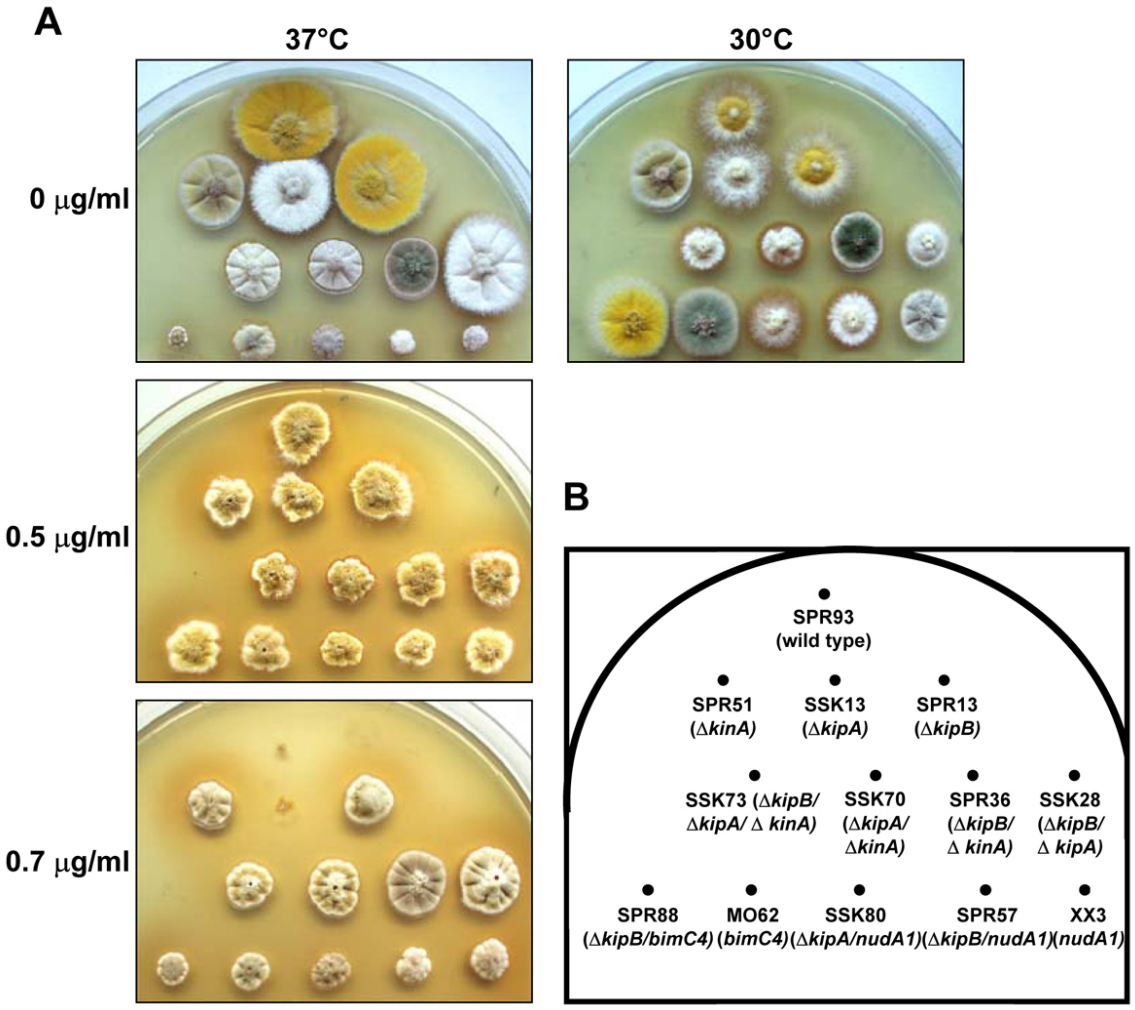

Fig. IV.17: Effect of different benomyl concentrations on colony growth of various mutant combinations with the *kipB* disruptant (A). (B) Strain identity for the plates depicted in (A). Strains were inoculated on agar plates at 37°C and 30°C and supplemented with the indicated benomyl concentrations dissolved in DMSO (the strains SSK13, 28, 70, 73 and SSK80 were constructed by S. Konzack, Marburg).

Table IV.1. Viability of double and triple mutants in combination with Δ*kipB*

Mutant combinations	Viability of double or triple mutants	Dominant phenotype (growth characteristics)
Δ*kipB*/Δ*kinA* (SPR36)	viable	Δ*kinA* (compact colony) (Requena et al., 2001)
Δ*kipB*/Δ*kipA* (SSK28)	viable	Δ*kipA* (polar growth defect) (Konzack et al., 2004)
Δ*kipB*/*nudA1* (SPR57)	viable	*nudA1* (dynein t.s. mutant) (Xiang et al., 1994)
Δ*kipB*/*bimC4* (SPR88)	synthetically lethal at semi-permissive temperature	-
Δ*kipB*/Δ*kipA*/Δ*kinA* (SSK73)	viable	Δ*kipB*/Δ*kinA* and Δ*kipB*/Δ*kipA*

Here is important to specify that for Δ*kipB,* Δ*kinA,* Δ*kipA* the permissive temperature is 37°C, while *bimC4* and *nudA1* are temperature sensitive mutants, for which 30°C and 42°C are permissive and restrictive temperatures, respectively. In Fig. IV.18 the variation of colony diameter with increased concentrations of benomyl, after 3 days growth at 37°C is shown.

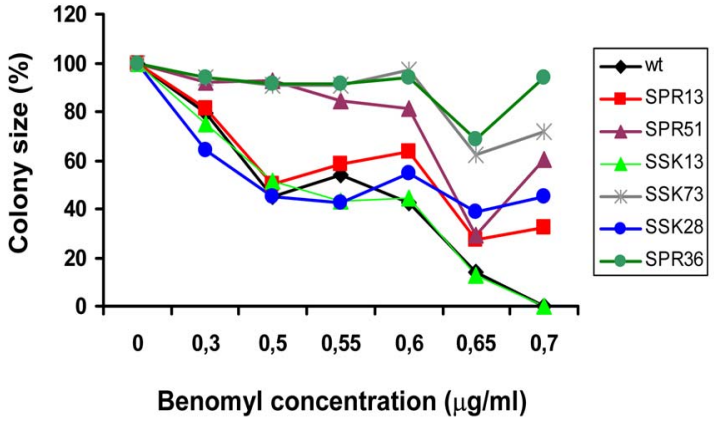

Fig. IV.18: Effect of benomyl onto colony growth of different mutant combinations with Δ*kipB*. The colony diameter was measured after 3 days of growth at 37°C at different benomyl concentrations (for genotype of the strains see Fig. IV.16, B).

First, the Δ*kipB* mutant was crossed to a mutant that also destabilizes microtubules, Δ*kinA* (SPR51). The double mutant (SPR36) was found viable, and expressing the Δ*kinA* mutant phenotype, with compact colonies at 37°C and 30°C, and increased resistance to benomyl like either of the parental strains. In contrast, the double mutant (SSK28) with Δ*kipA* (SSK13) displayed a compact colony growth at 30°C, suggesting cold temperature sensitivity and possible partially redundant functions. Also, the same double mutant showed enhanced resistance to high benomyl concentrations in comparison with the Δ*kipA* single mutant, indicating that the Δ*kipB* mutant phenotype was dominant, and rescued the high benomyl sensitivity of the *kipA* mutation. The double mutant (SPR57) of Δ*kipB* in combination with the dynein temperature sensitive mutant (XX3) was viable at permissive temperature (30°C) and exhibited no visible differences in growth compared with the single dynein conditional mutant. Furthermore, the triple mutant Δ*kipB*/Δ*kipA*/Δ*kinA* (SSK73) was indistinguishable in size from the Δ*kipB*/Δ*kinA* colony at 37°C, and from Δ*kipA*/Δ*kipB* double mutant at 30°C, and displayed no enhanced benomyl resistance as SPR36 (Δ*kinA*/Δ*kipB*), but it was slightly more stable to benomyl as SSK28 (Δ*kipA*/Δ*kipB*) (double and triple mutants of Δ*kipB* with Δ*kipA* were constructed by S. Konzack, Marburg).

3.8. KipB localizes to mitotic, astral and cytoplasmic microtubules

To localize KipB in *A. nidulans,* a N-terminal fusion protein with GFP was constructed. Approximately 1.2 kb from the 5' region of the coding sequence was cloned downstream of GFP. The chimeric gene was expressed under the control of the inducible *alcA* promoter (pPR38) (Fig. IV.19, A). *A. nidulans* SRF200 was transformed with the circular plasmid pPR38 and transformants were screened for GFP fluorescence under inducing conditions (threonine as carbon source). These strains were analysed for the integration of the plasmid and a strain with a single ectopic integration as well as a strain with a single homologous integration was chosen for further analysis (glycerol and/or ethanol as carbon source) (Fig. IV.19, B). The ectopic copy results in an aberrant, non-functional fusion protein, whereas homologous integration results in a duplication of the region where the plasmid integrated. The full-length KipB protein is N-terminally tagged with GFP.

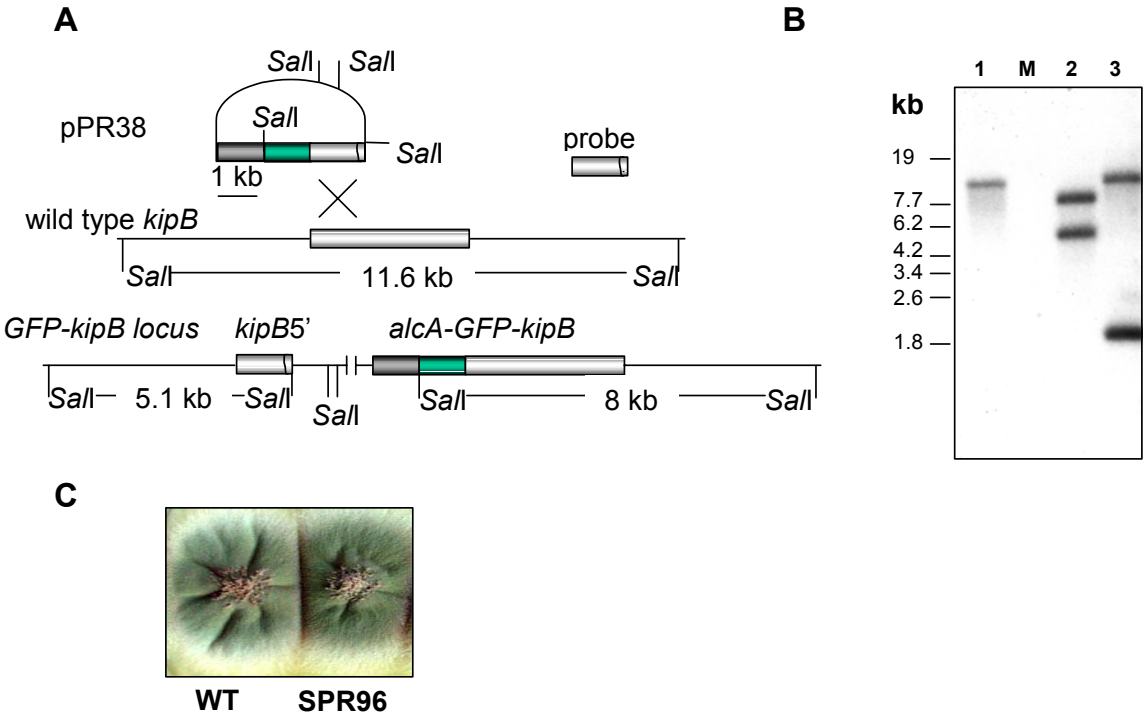

Fig. IV.19: Construction of the *GFP-kipB* strain. (A). Illustration of the pPR38 plasmid, the wild-type *kipB* locus and the *kipB* locus after homologous integration of the pPR38 plasmid (*GFP-kipB*). The green box represents GFP and the grey box its upstream *alcA* promoter. The open box represents the *kipB* gene. *kipB*5' indicates the 5' end 1.2 kb region of the *kipB* gene. A "cross'" sign indicates homologous recombination. **(B)**. Southern blot analysis indicating that the pPR38 plasmid integrated into the wild-type *kipB* locus as expected, and another strain with an ectopic integration. Genomic DNA from a wild type (lane 1), the *GFP-kipB* homologous integration strain (SPR96) (lane 2) and ectopic integration strain (SPR98) (lane 3) were digested with the restriction enzyme *Sal*I and subjected to Southern blot analysis with the 1.2 kb DNA fragment from the 5' end of the *kipB* gene as a probe. **(C)** The growth phenotype of the *GFP-kipB* homologous integration strain SPR96 compared with its parental wild-type strain SRF200 on a MM + glycerol + pyridoxine + uridine + uracil + arginine plate. The plate was incubated at 37°C for 2 days.

Both strains displayed normal growth on plates (Fig. IV.19, C). The KipB-GFP protein localizes to cytoplasmic microtubules in interphase cells and to spindle and astral microtubules during mitosis (Fig. IV.21) (see movies 12 (spindle) and 13 (cytoplasmic)). However, the protein displayed a discontinuous pattern along the microtubules. The spots disappeared or stopped when benomyl was added (Fig. IV.20, B) (see also movies 14 (microtubule-GFP dynamics on benomyl) and 15 (KipB-GFP spots behaviour on benomyl)).

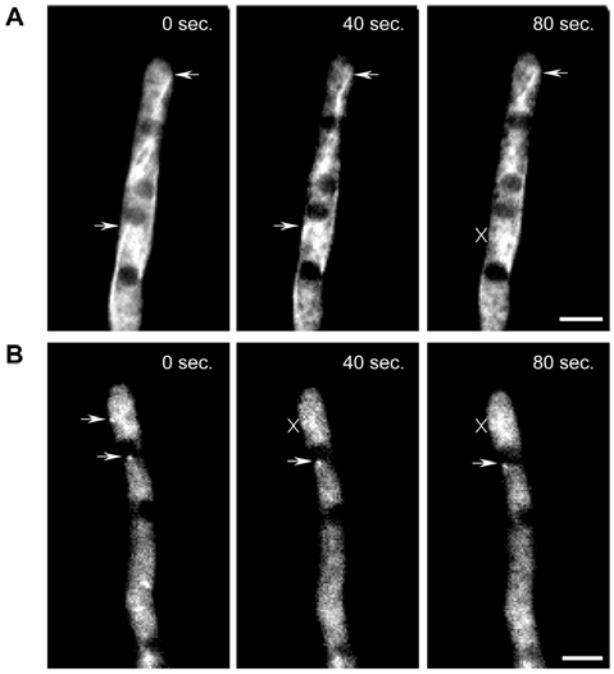

Fig. IV.20: Comparison of the behaviour of both microtubule-GFP and GFP-KipB spots in hyphae treated with 0.35 μg/ml benomyl. (A) Images of GFP-microtubules (strain SPR30, see movie 14) and **(B)** of GFP-KipB spots in low-concentration benomyl-treated cells (strain SPR96, see movie 15). Arrows point to **(A)** a nondynamic microtubule end and **(B)** nonmotile GFP-KipB spots. The "cross" sign marks the disappearance of one of the microtubules and one of the spots. Cells were grown overnight at 30°C before being treated with benomyl. All of these images were taken within 4.5–6 min after the cells were treated with 0.35 μg/ml benomyl. Scale bar equals 5μm.

Speckles of GFP-KipB appeared to be aligned in the cell and time-lapse studies revealed that the spots were moving independently along microtubules. In the hyphal tip, where microtubules are oriented with their plus ends towards the cortex, the spots moved only towards the tip. In the middle and the rear of the hyphal tip compartment, where microtubule polarity is mixed (Konzack et al., 2004), GFP-KipB spots moved into both directions (see movie 16). To discriminate between the two possibilities that GFP-KipB spots are transported together with the growing plus end or that the spots move along microtubules independently of the plus ends, we studied the dynamics of plus ends and compared it to the behaviour of the GFP-KipB spots. Whereas the microtubule plus ends grew with a speed between 9 +/- 3 μm/min., the KipB spots showed a greater range of speeds and no pronounced peak. Also, colocalization by time-lapse analysis between full-length KipB protein tagged N-terminally with GFP and the truncated version of mRFP1-KipB, which evenly stains the microtubules showed that the spots are situated onto the microtubules, but they move independently of microtubules plus ends (Fig IV.22, see also movie 17). These two results together suggest that KipB-GFP moves towards the microtubule plus end.

In the case of the truncated GFP-KipB protein a stronger GFP signal was obtained. The colocalization of this truncated version with α-tubulin-GFP revealed that the GFP-KipB fusion protein uniformly stains cytoplasmic, mitotic and astral

microtubules (Fig. 21, c and d) (see movie 18 (mitotic) and 19 (cytoplasmic)). Any abnormality of the microtubules, which could be caused by a dominant negative effect of the truncated protein, was not observed. A similar result was obtained with a construct where GFP was fused to the C-terminus of KipB replacing about 300 amino acids (Fig. 21, e and f).

A truncated KipB-HA fusion protein was also constructed (pPR12) and detected in Western blot (Fig. IV.2, B), but its subcellular detection by immunostain was not possible. That could be explained by the instability of the C-terminal HA fusion protein because it did not contain the Stop codon, or by the fact that the HA epitope was shielded in the C-terminus by protein folding, and so unaccessible for antibody binding.

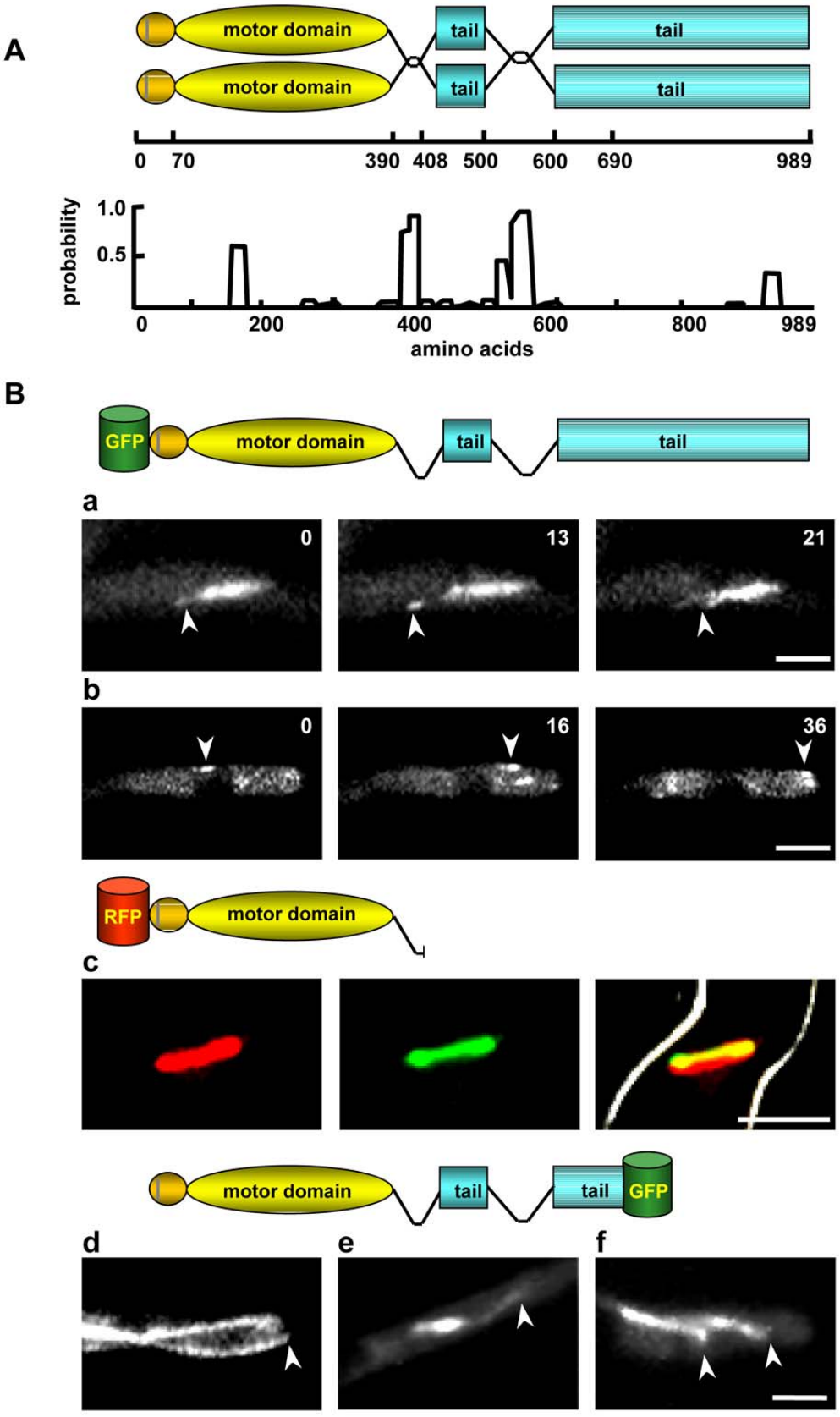
A
motor domain
motor domain
tail
tail
tail
tail
0
70
390
408
500
600
690
989
probability
1.0
0.5
0
200
400
600
800
989
amino acids
B
GFP
motor domain
tail
tail
a
0
13
21
b
0
16
36
RFP
motor domain
c
motor domain
tail
tail
GFP
d
e
f

Fig. IV.21: Localization of GFP-KipB fusion proteins. **(A)** Coiled-coil prediction (Lupas et al., 1992) for KipB (window size 14). Schematic draw of domains for the KipB protein: globular heads (in yellow), with the amino-terminal motif of 18 amino acids (in grey), the coils (curved lines), and the tail domain (in blue). The amino acid positions are represented on the line below. **(B)** Localization of different GFP-KipB fusion proteins. (a, b) Time-lapse analysis of full-length KipB protein tagged N-terminally with GFP (see above each series of photos the schematic drawings of the different constructs). Strain SPR96. (a) Localization of GFP-KipB onto spindle and astral microtubules, the arrows point to the plus end of the astral microtubules. (see movie 12) (b) spots of GFP-KipB moving onto cytoplasmic MTs (see movie 13). (c, d) Colocalization between a truncated version of mRFP1-KipB and mitotic spindles (see movie 18). Strain SPR99. left: mRFP1-KipB; middle: α-tubulin GFP; right: merged images of the first two photos. (d) localization to cytoplasmic MTs (see movie 19). Arrow points to the plus end of the MT in the hyphal tip. (e, f) C-terminal fusion of KipB with GFP. Strain SPR2. Localization onto mitotic, astral (arrow) (e) and cytoplasmic microtubules (arrows) (f). Scale bar equals 5 μm.

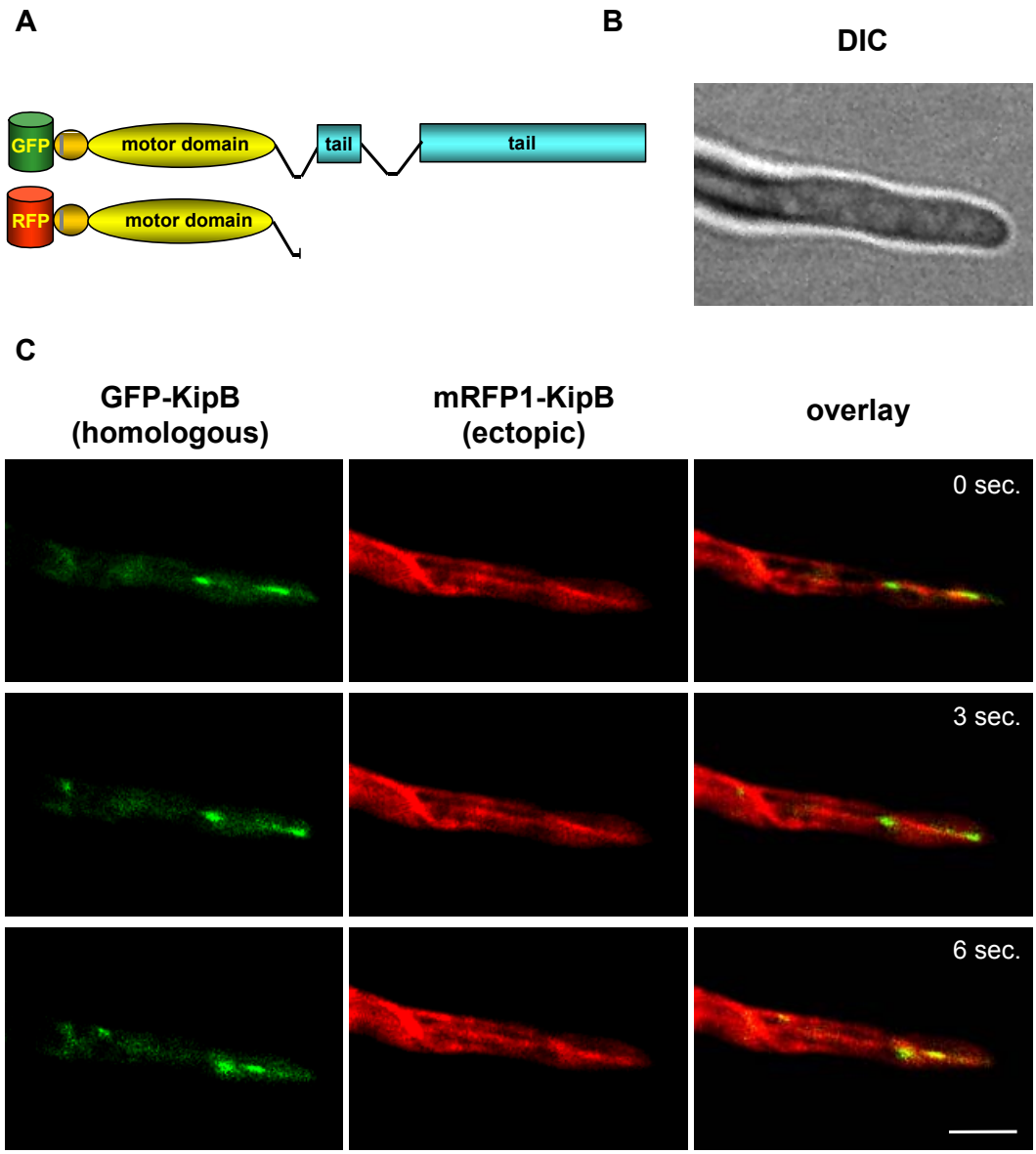

Fig. IV.22: Colocalization of GFP-KipB fusion protein with microtubules (A) The GFP-KipB constructs used for colocalization (as in Fig. IV.21). **(B)** DIC image of the germling depicted in (C) **(C)** Colocalization by time-lapse analysis between the full-length KipB protein tagged N-terminally with GFP and a truncated version of mRFP1-KipB, which evenly stains the microtubules (see also movie 17). Strain SPR101. left: GFP-KipB, homologous integration; middle: truncated mRFP1-KipB, ectopic integration; right: merged images of the first two photos. Scale bar equals 5 μm.

V. Discussion

Despite great progress in understanding the internal order established by eukaryotic cells using protein motors to transport molecules and organelles along cytoskeletal tracks, there remain many open questions about the roles of motor proteins and microtubule dynamics in processes like mitosis, intracellular organelle transport or membrane trafficking. How are the force-generating properties of dynamic microtubules and motor proteins coordinated? What are the precise roles of molecular motors in intracellular transport or in temporal and spatial morphogenesis of the mitotic spindle? How are they integrated and regulated? Inhibiting motors (via complete deletion or diverse mutations) and visualizing microtubule dynamics, along with genetic or biochemical manipulations and quantification of the mechanical and force-generating properties of both the tracks and the motors are some of the currently used approaches to gain important knowledge regarding this field (Schliwa, 2003).

The fungi, with relatively "simple" kinesin inventories, and ease of functional analysis, are premier model systems for investigating these questions (Schoch et al., 2003). Filamentous fungi, in particular, have provided model studies of the cytology and genetics of motor proteins and cytoskeleton, including important advances in the study of mitotic forces, microtubule-associated motor proteins, and mitotic regulatory mechanisms (Aist & Morris, 1999).

In the present study a new kinesin, KipB of *A. nidulans* was characterized. Several lines of evidence show that it is involved in the turnover of all populations of cellular microtubules, interphase cytoplasmic, mitotic and astral microtubules: (i) Δ*kipB* mutants are less sensitive to the microtubule-destabilizing drug benomyl, (ii) the microtubule cytoskeleton of interphase cells appears altered, (iii) spindle positioning is affected, (iv) mitotic progression is delayed, (v) an increased number of cytoplasmic microtubules remains intact during mitosis, (vi) spindle morphology is altered, and (vii) Δ*kipB* heterozygous strains show an increased instability of diploid nuclei.

1. KipB is a member of the Kip3 kinesin family

Initially, Goodson et al. (1994) grouped kinesins into five clearly defined subfamilies and subsequent analyses with expanded data sets yielded up to ten subfamilies plus a number of ungrouped "orphans" (Goodson et al., 1994; Hirokawa, 1998; Kim & Endow, 2000). More recent phylogenetic comparisons including a study of human kinesins, grouped them into 14 subfamilies by means of maximum parsimony (Miki et al., 2001) and a comparison by means of maximum likelihood delineated 11 subfamilies from a spectrum of eukaryotic kinesins, placing some, previously classified as orphans, into known subfamilies (Lawrence et al., 2002). A last study referring to filamentous fungal kinesins grouped them into nine from the total eleven kinesin families by comparison with well-characterized kinesins from other eukaryotes (Schoch et al., 2003). And, the latter re-evaluation of the kinesin microtubule motor protein family based on the recent completion of the genome sequences of humans and several model organisms, revealed the emergence of several new groups consisting only of *Arabidopsis thaliana* proteins, which suggests that the kinesin motors may have a broader range of functions in higher plants than in other organisms (Dagenbach & Endow, 2004).

In this work we identified eleven kinesin motors in *A. nidulans.* This is in good agreement with the number of kinesins in other fungi ranging from six in *S. cerevisiae*, ten in *N. crassa* to twelve in *Cochliobolus heterostrophus* (Schoch et al., 2003). Interestingly, two kinesins of *A. nidulans* and *N. crassa* were found in the Unc104 family, whose members are involved in vesicle transportation. This may reflect the importance of the requirement for fast tipward vesicle movement in fast growing filamentous fungi. Not surprisingly, *S. cerevisiae* does not have any related kinesin of this family. In addition, *S. cerevisiae* kinesins are lacking from the Chromokinesin/Kif4, the MKLP1 and the KID family, whereas *A. nidulans* and *N. crassa* do have representatives in these groups. Since these kinesins are involved in mitotic processes, this may reflect different mechanisms of nuclear division in *S. cerevisiae* and the two filamentous fungi (Schoch et al., 2003): The possibility of various mechanisms employed in mitosis by different organisms (e. g. yeasts and filamentous fungi) was also one of the reasons why we conducted our analysis onto KipB kinesin in *A. nidulans*.

The characterization of specific family members from a spectrum of eukaryotes has shown that phylogenetic analysis of large groups of kinesins based on motor domain alignments can successfully group kinesins of similar function. Additional areas of the primary amino acid sequence, such as the unique sequences of the neck region and binding sites in the tail have also provided clues to protein function (Schoch et al., 2003). We used the same main criteria for building our relatedness kinesin tree, and thus KipB kinesin grouped to Kip3 family, along with its other homologues, already reported to belong to this family. There are several shared characteristics that define members of this kinesin family. First and foremost, there is considerable sequence similarity in their motor domains and in their general domain structure and organization. Second, Kip3, Klp5, and Klp6 localize also all to cytoplasmic and spindle microtubules, as KipB kinesin (DeZwaan et al., 1997; West et al., 2001). Furthermore, Klp5, Klp6 and Kip3 share with KipB an activity that fosters microtubule disassembly, as evidenced by the unusually stable microtubules found in the Δ*kipB* mutant (Cottingham & Hoyt, 1997; DeZwaan et al., 1997; Miller et al., 1998; West et al., 2001). Microtubule-disassembling activity has also been described for the KinI kinesin subfamily (including MCAK, XKCM1), in which the motor core is located *I*nternally within the polypeptide sequence (Desai et al., 1999; Maney et al., 1998; Miller et al., 1998; Walczak et al., 1997). Likewise, KinIs localize principally to the mitotic spindle of dividing cells and are essential during mitosis (Moores et al., 2002). A report including a study of Kip3 as a protein with opposing activities to Stu2 (a protein from Dis1 family of microtubule-associated proteins, which localize to the microtubule-organizing center and spindle during mitosis) recalculated a phylogenetic tree from a multiple sequence alignment of the kinesin superfamily using only the sequence of the kinesin motor domain, and showed that the Kip3 family did congregate with the MCAK/Kif2 (KinI) subfamily (Severin et al., 2001). Also, another phylogenetic analysis of kinesin families based on maximum likelihood methods, grouped Kip3 and KinI families in the same clade, together with Chromokinesin, CENP-E, Unc104 and MKLP families, taking into consideration that they share a common function (accomplished through different mechanisms), namely mitosis and chromosome movements (Lawrence et al., 2002). Separate proteins from human and fly that group with both subfamilies have already been shown in other phylogenetic analyses (Iwabe & Miyata, 2002; Miki et al., 2001). There is, however, no obvious sequence similarity between members of the Kip3 subfamily and

the other kinesins with "exotubulase" activity (see KinI mechanism of microtubule depolymerization discussed below). It is possible that each kinesin subfamily uses a different mechanism to promote microtubule disassembly or that there is conservation in protein structure that is not apparent from the amino acid sequence (West et al., 2001).

The present work reveals several functions of KipB in *A. nidulans*, as the effect on microtubule stability and its role in spindle positioning and morphology, that, besides the kinesin relatedness study, which used KipB sequence similarities to other motors in the databases, placed this protein into the group of the Kip3 family, thus supporting the distinction between the KinI family, consisting of higher eukaryotic kinesin depolymerases, and the fungal Kip3 family.

2. Microtubule organization in the Δ*kipB* mutant

In filamentous fungi, microtubules are essential for both nuclear division and nuclear migration, together with several motor proteins. Microtubules form spindles in the nucleus during mitosis and cytoplasmic tracks during interphase (Xiang & Fischer, 2004). During mitosis, microtubules assemble and are organized into a functional spindle within the nuclear envelope, which does not break down. At mitotic onset, tubulin moves rapidly into the nucleus reaching a level 3 times greater than in interphase and the spindle begins to assemble seconds later, coincident with early prophase. As mitosis proceeds, the spindle gradually increases in length, containing about 34-50 microtubules. About half of the microtubules terminate at each spindle pole body. In late stages of mitosis (anaphase A and B), mitotic asters composed of cytoplasmic and SPB-associated microtubules are being developed. In anaphase B the spindle elongates, becomes visibly thinner, and the mitotic asters reach their maximal length. The spindles are often so long that their astral microtubules end by overlapping each other, and sometimes are forced to bend as they reach the cell periphery. Tubulin is removed rapidly from the nucleus at the end of mitosis, after spindle disassembly (Aist & Morris, 1999; Jung et al., 1998).

Microtubule's building blocks, the α- and β-tubulin heterodimers, are arranged in a head-to-tail fashion in a protofilament, which gives a microtubule its inherent polarity, with β-tubulins at its plus end and α-tubulins at its minus end (Nogales et al., 1999). The microtubule plus ends are highly dynamic, with alternate growing and shrinking

phases. In most interphase cells, the minus ends of microtubules are located at the microtubule organizing center (MTOC) near the nucleus whereas the plus ends face the cell periphery (Han et al., 2001). A parallel study in our lab found MTOCs in the cytoplasm close to nuclei but also at different places in the cytoplasm of *A. nidulans*. In addition, very active MTOCs were detected at the septa. These MTOCs give rise to a mixed polarity of microtubules in compartments of *A. nidulans*. Nevertheless, microtubule formation from the tip occurred only very rarely, indicating that there is no true MTOC in this region. Microtubule filaments merge in the hyphal tip and appear fixed at a central point until the occurrence of a next catastrophe event. A catastrophe event does not lead to complete disassembly of the entire microtubule but only of some filaments. New filaments can then grow along the still existing filament, so it can be speculated that microtubules are bundles of several filaments, with individual dynamics (Konzack et al., 2004).

The changes in the dynamics of microtubules could have effects on various dynamic processes in the cell, so examination of the microtubule cytoskeleton can provide essential details about their dependence on the the KipB protein.

Growth-tests done for both the wild type and Δ*kipB* mutant regarding sensitivity to the microtubule-destabilizing drug benomyl and microscopic investigation of microtubule cytoskeleton indicated that KipB kinesin could play an important role in stability of interphase and mitotic microtubules. Two experiments supported this hypothesis. First, disruption of the *kipB* gene rendered the *kipB* mutant strains less sensitive towards the microtubule-destabilizing drug benomyl. Second, observations done onto strains containing GFP-tagged tubulin revealed that microtubule organization in kinesin mutants was slightly impaired in interphase, when the microtubules appeared more curved, and significantly modified during mitosis, with several permanently present cytoplasmic microtubules and long and very stable astral filaments.

These results indicate that KipB protein could promote microtubule disassembly in the cell and is necessary for proper microtubule organization in *A. nidulans*, otherwise a sheared feature among the Kip3 family members. Also, these data are consistent with those reported for MCAK (Maney et al., 1998) and support the notion that Kip3-like kinesins show strong connection with those belonging to KinI family, which act as microtubule-destabilizing factors, probably at the plus end of microtubules, as proposed in higher eukaryotes (Hunter et al., 2003). At this moment,

it is unclear whether the mechanism of microtubule destabilization by Kip3 kinesins is different from that of KinIs. KinI proteins are described as capable to bind to the sidewall of the microtubule and exhibit one-dimensional diffusion along the lattice; also they are able to target and depolymerize microtubules from both ends. When the protein reaches the end, binding to a high-affinity site would stimulate ATP-ase activity and it would result in a conformational change in the microtubule lattice. Consequently, KinI protein would processively remove approximately 20 dimers before dissociating from the end of the microtubule (Fig. V.1). However, it is still uncertain why a KinI enzyme needs to be processive, given intrinsic tubulin dynamics, being acknowledged that a key feature of dynamic instability is that microtubules catastrophically depolymerize (Walczak, 2003). Of course, in this light it is still possible that with dynamic microtubules KinI would release one tubulin dimer and then dissociate from it, as it was originally proposed (Desai et al., 1999).

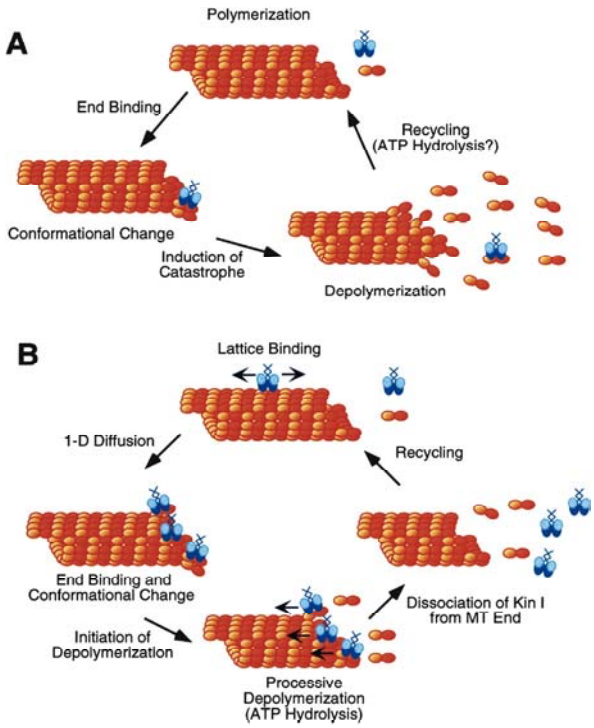

Fig. V.1. Models for KinI depolymerization of microtubules. For simplicity, in both models only one end of the MT is shown, although the depolymerization by KinI occurs at both ends. (A) During polymerization, KinI targets to the MT end. Upon binding, it induces a conformational change in the MT that is sufficient to cause a catastrophe that results in depolymerization of the MT. KinI is released from the MT in a complex with a tubulin dimer, and hydrolysis of ATP is involved in dissociating the tubulin dimer from KinI so that it can be recycled. (B) During polymerization, KinI targets to the MT lattice and reaches the MT end by one-dimensional diffusion. Upon reaching the end of the MT, ATP hydrolysis is coupled to processive depolymerization of the MT. After removal of approximately 20 tubulin dimers, KinI dissociates from the MT end and is recycled (Taken from Walzack, (2003)).

Detailed analysis of the microtubule destabilizing activities of Kip3 kinesins *in vitro* could bring new insights in elucidation of the molecular mechanism of Kip3-mediated microtubule depolymerization and in finding a boundary and/or connection between Kip3 and KinI functions in this mechanism.

3. KipB is involved in spindle architecture, positioning and mitosis

Another process that implicates the activity of KipB kinesin is nuclear division and mitosis. In *A. nidulans* this process has been extensively dissected at the genetic level, with some novel insights into its regulation in eukaryotes in general. However, there remains a lot of useful information to be gleaned from the knowledge about the genes identified in previous screens or from the existing, but incompletely characterized, mutants (Martinelli & Kinghorn, 1997).

The nuclear division cycle occurs in a set order and takes about 75-120 minutes, depending on growth conditions. At 37°C mitosis (M) is estimated to last about 5 minutes; G2, 30 minutes; S-phase (DNA synthesis), 25 minutes and G1, 15 minutes. The morphological events of nuclear replication have been described at both light and electron microscope levels (Martinelli & Kinghorn, 1997). Among the most important reported features of mitosis in filamentous fungi are: mitosis is intranuclear (therefore the term of “closed mitosis”), bipolar spindles are formed from half-spindles, spindles are composed of fine-to-coarse filaments, metaphase chromosomes are usually scattered over the middle one-third to one-half of the spindle rather than arranged in a metaphase plate, and the strung-out arrangement of anaphase A chromatids along the entire length of the spindle derives from asynchronous disjunction of chromosomes that were scattered on the metaphase spindle (Aist & Morris, 1999). Thus, one of the most intriguing aspects of mitosis is the formation and behaviour of the highly ordered segregation structure represented by the mitotic spindle. Assembly and organization of the spindle requires counteracting motors, which function to build up tension within the spindle rather than moving a cargo (Steinberg, 2000).

Based on spindle length, the mitotic phase can be divided into three distinct stages, phase 1 (equivalent to prophase, during which the spindle elongates until the two spindle pole bodies (SPBs) are separated to the opposite sides of the nucleus, forming the intranuclear, bipolar spindle, phase 2 (metaphase/anaphase A; when

spindle length remains constant between the two poles and mitotic asters are being developed), and phase 3 (anaphase B, during which the spindle is elongated rapidly between the two SPBs and doubles or triples in length, as the asters reach their maximal size) (Aist & Morris, 1999; Garcia et al., 2002).

In order to visualize mitotic spindle behaviour in germlings of *A. nidulans*, GFP tagged tubulin strains were used for wild type and Δ*kipB* mutants. Time-lapse studies of mitosis in Δ*kipB* mutant strains revealed that individual mitotic spindles moved within the cytoplasm although most of the spindles were positioned like in wild type (Fig. V.2, A-1, (wild type)). In wild type cells spindles are likely to interact through astral microtubules with the cortex. Cortical proteins such as ApsA are probably required for the contact (Farkasovsky & Kuntzel, 2001; Fischer & Timberlake, 1995; Xiang & Fischer, 2004). In the Δ*kipB* mutant astral microtubules are stabilized and are likely to reach the cortex and subsequently extend further along it. They could then make contact to cortical proteins at a distance from their "own" attachment site and pulling forces could then cause the movement (Fig. V.2, A-3, 4). The spindle movement phenotype was striking and raises the question why we did not observe an effect on nuclear distribution in interphase cells. This finding suggests that besides nuclear separation through mitosis, other mechanisms exist which further distribute nuclei (discussed below) (Xiang & Fischer, 2004).

The longer and more stable astral microtubules are perhaps also the reason why we saw perturbed spindle architecture in late stages of mitosis of Δ*kipB* mutants, represented by sharply bent spindles. This phenotype might be caused by a mispositioning of one or both of the SPBs, because time-lapse studies of a Δ*kipB* mutant strain where SPBs were visualized through ApsB-GFP tagged protein, confirmed that sometimes the very long astral filaments were able to extend from one pole of the spindle and to migrate backward of the junction point of the asters from the opposite pole, thus pulling the entire spindle structure and bringing the opposite poles in the same plane (Fig. V.2, A-2, see also movie 9)

Furthermore, sometimes the twisted spindle structure could be detected during early stages of mitosis (prophase to metaphase, when the spindle elongates slowly), and that may be due to the inaccurate or incomplete SPB's separation. Changes in dynamics and disproportionate microtubule growth could induce an improper behaviour of the plus ends of astral microtubules, preventing the microtubule-cortex

interactions and/or accurate cross-linking of anti-parallel spindle microtubules, at the beginning of bipolar spindle formation from the half spindles, both having as result abnormal SPB migration to the opposite poles of the nuclear envelope. That aspect was described for another Kip3 homologue, Klp67A from *Drosophila*, which plays a distinct role in centrosome separation, *Klp67A*^{322b24} mutant displaying so-called "banana-shaped" spindles explained by the reduction of astral pulling forces and consequently incomplete centrosome separation (Gandhi et al., 2004). However, monopolar spindles were not observed in Δ*kipB* mutants, so if an impaired disjunction of SPBs is the reason of the bending of the spindles, they eventually became bipolar and could successfully complete mitosis. A further argument supporting this hypothesis is the additive growth defect observed for the *kipB* deletion with the temperature-sensitive kinesin motor mutation*, bimC4* at the semi-permissive temperature 37°C (see discussions at Chapter V.4).

Nevertheless, spindle bending was shown to be a natural, albeit infrequent and momentary, occurrence in living fungal cells. It was thus proposed that spindle actually elongated while bending, demonstrating that there is an elongation force intrinsic to the spindle that can push the ends of the spindle against the SPBs during anaphase B. But, it has to be specified that only during very brief moments this spindle pushing force is actually manifested (as smooth spindle bending), so during anaphase B spindle is almost always under tension from the astral pulling force, rather than being primarily under compression from the spindle pushing force, and this tension consequently contributes substantially to the rate of spindle elongation (Aist & Morris, 1999). Hence this resumes again the initial hypothesis, which stipulates the influence of KipB protein onto the stability of astral and spindle microtubules as a cause of severe spindle bending in Δ*kipB* mutant.

Besides the effect of the Δ*kipB* mutation on spindle positioning and morphology, we found a defect in mitosis, represented by a delay in mitotic progression. Separation of chromosomes requires the coordinated action of motor proteins and microtubule dynamics. Normally, mitotic microtubules are known to be much shorter and less stable then interphase microtubules. Studies with *Xenopus* egg extracts have indicated that the mechanism for this change in microtubule stability is an increase in the frequency of transitions from microtubule polymerization to depolymerization at the microtubule plus ends (Desai & Mitchison, 1997). Thus, the

mitotic progression delay observed in Δ*kipB* mutant strains may be explained by either a direct or indirect effect of the motor deletion on the dynamics of microtubules and thus a disruption of the balance of forces exerted on the kinetochores (Garcia et al., 2002; Garcia et al., 2002; West et al., 2002). The absence of microtubule-destabilizing KipB could lead to spindle and astral microtubules stabilization and, as a result, to the loss of the poleward force and tension at the kinetochores (Fig. V.2, B-1 and 2). Forces both away from and towards the pole are vital for chromosome congression. The defect in the poleward force would lead to imbalance at the centromeres, which results in a tension-less state at these kinetochores (Garcia et al., 2002). Together, these observations may suggest that dynamic instability allows the microtubule plus ends to search and capture appropriate anchorage sites such as the kinetochores or specialized sites at the cell cortex, and KipB could be one of the proteins implicated in regulation of this dynamic instability.

The delay in mitotic progression observed in Δ*kipB* mutant could be also seen as a consequence of the activation of spindle checkpoint components, which can block sister chromatid separation and mitotic exit. When the timing of mitotic events is perturbed, or the mitotic spindle is damaged, the spindle assembly checkpoint inhibits the normal succession of mitotic events. This situation was in fact proven for the two KipB homologues in fission yeast, Klp5 and Klp6, as mutations in either Klp5/Klp6 activated the common Mad2-dependent checkpoint (Garcia et al., 2002). Therefore, the two genes were proposed to play a crucial role in mitotic progression by contributing to bipolar spindle formation at dual steps, first being the attachment and second the generation of tension upon capture (Fig. V.3, B) (Garcia et al., 2002). Further analysis is required to clarify this important point, but from the present results it appears that KipB and Klp5/6 play an analogous role in mitosis, suggesting that their mitotic functions are conserved within the Kip3 family.

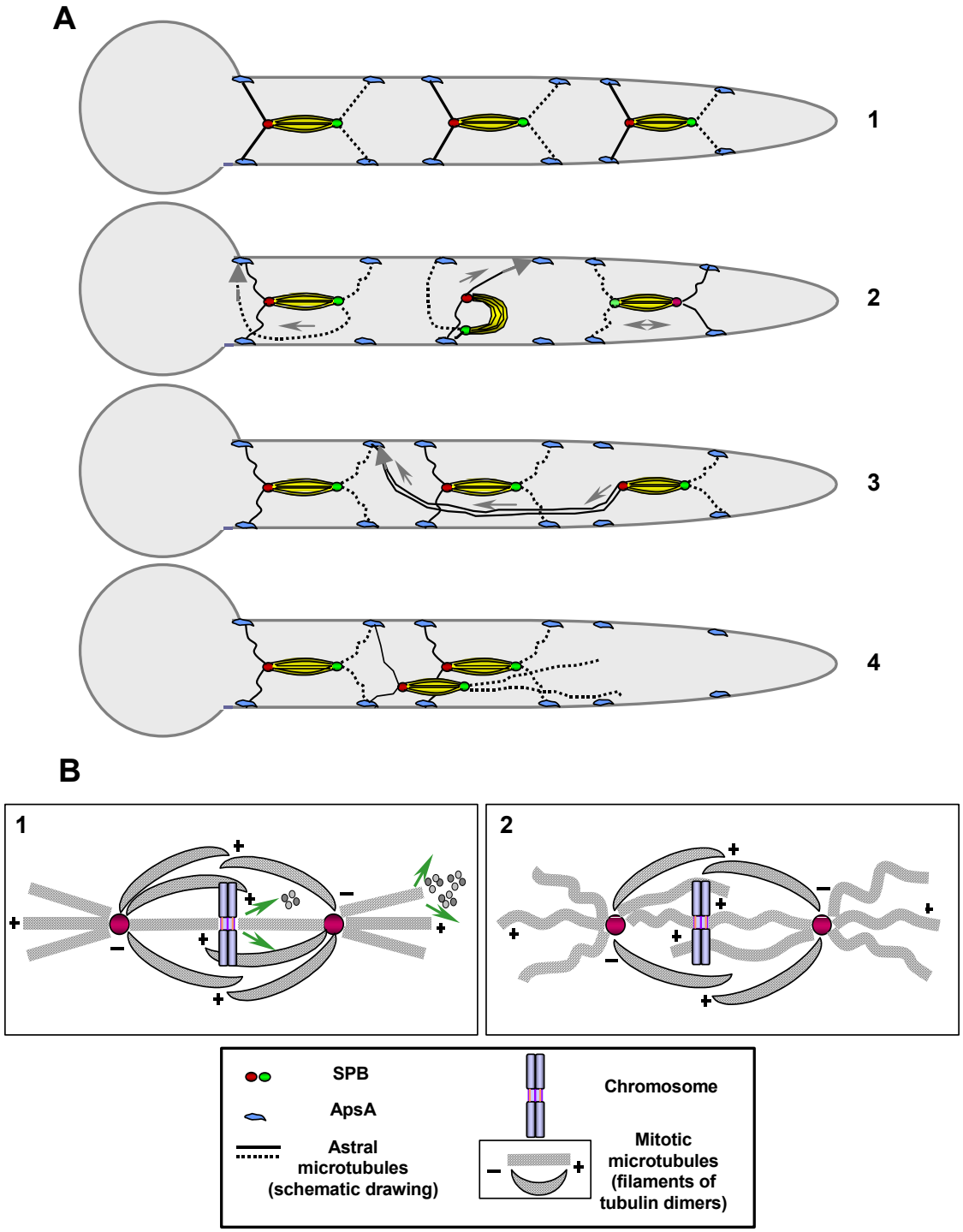

Fig. V.2. Two possible models of mitotic defects in Δ*kipB* mutants. (A) Defects in spindle morphology and positioning. (1) Wild type situation, where spindles are evenly distributed along the hypha. (2)-(4) Δ*kipB* mutant. (2) Spindle modified architecture, with bending and SPB reversing orientation (red dot-left SPB changing position with the right

SPB-green dot) due to the longer astral microtubules (depicted as lines, in schematic drawing), which can make possibly contact with ApsA (blue patches) at the cortex (arrows show direction of astral microtubules orientation, and astral microtubules emanating from the left spindle are illustrated by lines, while astral microtubules emerging from the right spindle are depicted with interrupted lines). (3) Defects in spindle positioning due to the longer astral microtubules ability to connect other ApsA paches at the hyphal cortex than their "own" attachment site. Consequently, spindles can become highly mobile, overpass each other and move long distances through the cytoplasm. **(B)** KipB possible role in preserving spindle shape and in establishing proper capture of chromosomes (depicted in blue). (1) KipB is probably required for efficient trapping of sister kinetochores by spindle microtubules (shown by filaments consisting of tubulin dimers - grey and white circles -) and could be implicated in generation of poleward forces during later stages of mitosis. (2) In the absence of KipB, the tension required for astral microtubules (delineated by wavy filaments) to connect and conserve the positioning of the spindle is missing (green arrows indicate the microtubule depolymerization and eliberation of free tubulin dimers from their plus ends, due to the KipB function as a microtubule destabilizer).

The effect of the *kipB* mutation on the integrity of the mitotic apparatus is also reflected by the results of the experiment using diploid strains. Heterozygous mutants displayed an increase of chromosome-loss. Interestingly, homozygous Δ*kipB* diploids showed a reduced frequency of chromosome-loss in comparison to *kipB* wild type diploids. This points to a gene dosage effect and could mean that haploidization after initial loss of one chromosome would require a certain amount of the KipB protein to reduce the chromosome number to a haploid set. In the heterozygous situation initial chromosome loss might be very frequent and then further reduction of the chromosome number would occur rapidly. Interestingly, destabilization of microtubules through increasing amounts of benomyl suppressed this effect. This suggests that disassembly of microtubules in the mitotic spindle and thus chromosome distribution are affected at different concentrations of KipB.

All the arguments presented above about KipB roles in mitosis entitle to a raising question about the reasons why we did not observe an effect on nuclear distribution in interphase cells. In *S. cerevisiae* Kip3 was shown to be involved in nuclear migration to the bud site in preparation for mitosis. Loss of Kip3 function disrupted the unidirectional movement of the nucleus toward the bud and mitotic spindle orientation, causing large oscillations in nuclear position (Fig. V.3, A). As a consequence the frequency of binucleate mother cells was increased (DeZwaan et al., 1997). The reports about Kip3 in *S. cerevisiae* provided us justification to believe in possible functions of KipB in nuclear migration in *A. nidulans*, especially because in filamentous fungi nuclei migrate long distances to follow the growing hyphal tip and the molecular motor machinery could contribute significantly to this distribution

process (Suelmann & Fischer, 2000). Thus, defects in asexual or sexual fruiting body (conidiophores or cleistothecia) formation and organization, together with reduced viability of conidiospores or ascospores were suspected in a Δ*kipB* mutant.

But, compared with wild type, *kipB* deletion strains did not exhibit alterations with regards to vegetative growth, viability of conidiospores and ascospores, content of ascospores per ascus, or sexual and asexual fruiting body formation. Also, the analysis of nuclear distribution in germlings of an *A. nidulans* Δ*kipB* mutant revealed no striking difference in the distribution pattern. All these findings suggest that besides nuclear separation through mitosis other mechanisms exist which further distribute nuclei. Indeed, that seems to be the case. First separation of the two daughter nuclei from each other occurs in mitosis. As it was presented in this study, during mitosis astral microtubules emanate from the two SPBs and are likely to make contact to the cortex. In this phase the process may resemble the situation in *S. cerevisiae*. The question is whether there are cortical proteins along the hyphae, which determine the attachment sites for astral microtubules. One candidate is the Num1 homologue ApsA in *A. nidulans*. ApsA is also a cortical protein, which is involved in nuclear positioning during conidiation, and also, to some extent, during hyphal growth (Fischer & Timberlake, 1995; Suelmann et al., 1997; Suelmann et al., 1998). Another protein, ApsB could also play a role in nuclear positioning, since deletion of the *apsB* gene results in the same phenotype as deletion of *apsA*, namely a clustering of nuclei (Clutterbuck, 1994; Suelmann et al., 1998). More interestingly, loss of *apsB* function causes nuclei to move much more rapidly, possibly by weakening the machinery required for nuclear anchorage in the hyphae (Xiang & Fischer, 2004). ApsB has recently been detected both at the SPB and at septa, it was observed to tightly bind to the lattice of the microtubule, mediating its connection with the nuclei, and thus implicated in nuclear movement by leading the nuclei along the microtubules through the hyphae (Veith et al., 2004). Exactly how ApsB affects nuclear positioning is still an open question, which has to be addressed in the future. What it could be speculated at the present is the hypothesis that in *A. nidulans* nuclear migration consists of two phases. First one might be similar with the situation in *S. cerevisiae* (therefore called yeast phase of nuclear migration), starting with nuclear separation at the exit from mitosis, where KipB could play a major role in maintaining the tension of astral microtubules, and through that in positioning of spindles at the correct sites along the hyphae, together with other cortex- and

microtubule-associated proteins (MAPs) (Fig. V.3, C-1). The second phase is likely to involve the mechanism through which SPB's guides the migration of interphase nuclei along the cytoplasmic microtubules, with help of other important proteins as dynein or MAPs (Fig. V.3, C-2). This latter phase may be specific for filamentous fungi, where nuclei have to move along the extremely long hyphae.

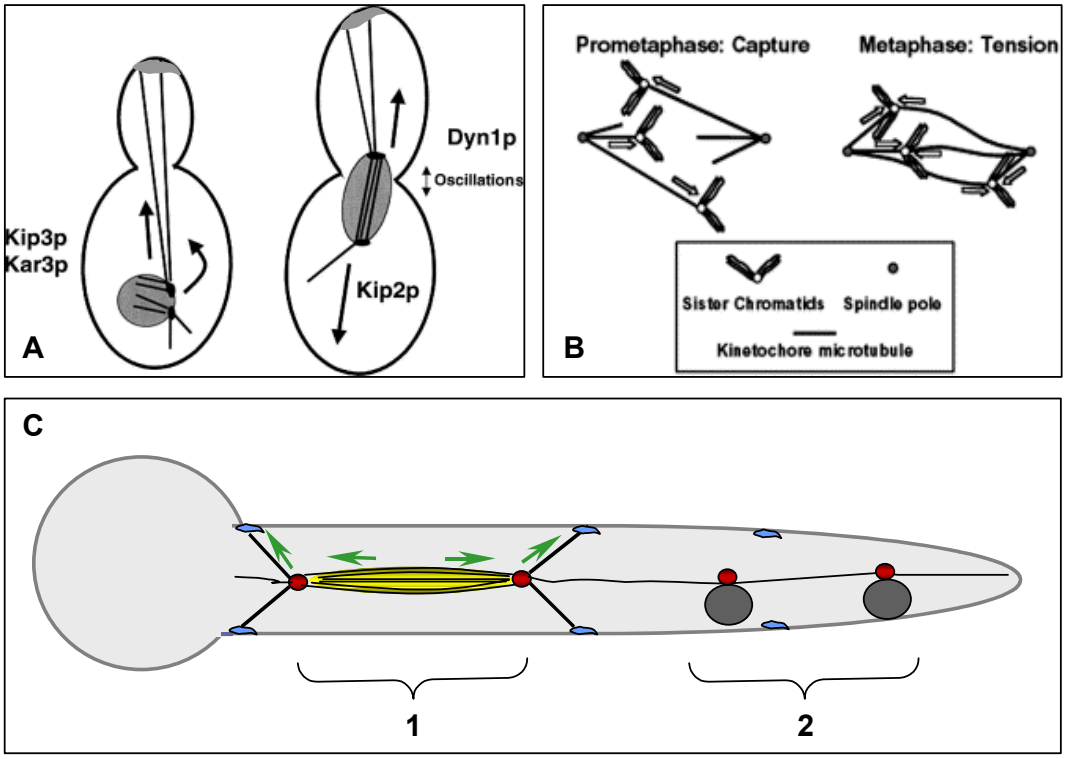

Fig. V.3. Scheme of possible roles for KipB and other Kip3 homologues in mitosis and subsequent nuclear migration in yeast (A and B) and *A. nidulans* (C). (A) Different kinesins and dynein have overlapping or counteracting functions in *S. cerevisiae*. Kip3 and Kar3 together with Dyn1 are involved in the migration of the nucleus (dark grey) toward and through the bud, Num1 (depicted as light grey patches) being at bud cortex when dynein slides microtubules along to it, whereas Kip2 antagonizes the forces of the other three motors. The oscillations observed at the budding neck are dependent on dynein (Modified after Suelmann et al., (2000)). **(B)** Klp5 and Klp6 in *S. pombe* are required for efficient capturing of sister kinetochores during prometaphase and for the generation of poleward forces during metaphase. As spindles that capture one kinetochore of sister chromatids continue to polymerize, spindles emanating from the opposite pole have difficulty capturing sister kinetochores. In the absence of Klp5/6, although both sister kinetochores are captured by spindles, tension, which should be produced between Klp5/6 and cohesin, is absent. Arrows indicate the direction of microtubule polymerisation (Taken from Garcia et al., (2002)). **(C)** Nuclear migration in *A. nidulans*. (1) Yeast-like phase of nuclear migration, where KipB could have a role in maintaining spindle (yellow) positioning and morphology, and separation of nuclei together with corresponding SPBs (red dots) by astral microtubule tension at exit from mitosis (in blue, ApsA protein at the cortex). (2) Interphase nuclear migration characteristic for filamentous fungi, with SPB-led movement of nuclei (black circles) along cytoplasmic microtubules (Adapted after Veith et al., (2004)).

4. Interactions of *kipB* with other genes

Complex interactions among kinesin subfamily members have been already described in several systems (Goldstein & Philp, 1999). In this study, the Δ*kipB* mutation was tested in combination with mutations in some kinesins, but also dynein, all of them being genes known to affect nuclear migration (*kinA, nudA1*), microtubule stability (*kinA*, *kipA, nudA1*) and/or spindle function (*bimC*) in *A. nidulans*. Of particular interest for this study was the fact that Δ*kipB* mutation showed a distinct genetic interaction with *bimC4* temperature-sensitive mutant, as the double mutant strains exhibited a stronger growth defect at intermediate temperature than the *bimC4* single mutant. Temperature-sensitive *bimC* mutants are known to exhibit failure to separate their duplicated SPBs during early stages of mitosis, which results in mitotic defects such as abnormal spindle morphology and impairment of nuclear division (Kashina et al., 1997). It could be that the combined effect of *bimC* and *kipB* mutations influenced greater the process of SPBs splitting and thus the double mutant strain displayed the additive phenotype at semi-permissive temperature. Another function reported recently for BimC bipolar kinesin is the crosslinking and sliding apart of antiparallel spindle microtubules. As fundamentally accepted, the mitotic spindle consists of two populations of microtubules, one that confers its stability and shape (interpolar microtubules), and the other, which are involved in attachment of chromosomes to the spindle and then in further chromosome segregation (kinetochore microtubules) (Mountain & Compton, 2000; Prigozhina et al., 2001). Since we had clear evidence that KipB acts as a microtubule-depolymerizing factor, perhaps KipB has also a contribution in maintaining the tension and elasticity of spindle microtubules, thus preserving spindle architecture, in concert with the other microtubule cross-linking kinesins, one of them being BimC. It might be thus likely that the cross-linking activities of BimC kinesin require the function of KipB to ensure correct microtubule plus-end dynamics and morphology during spindle assembly. This suggests that some aspects of KipB and BimC kinesins mitotic roles in spindle assembly and maintenance may be similar.

Another kinesin characterized in a parallel study in our lab, and analysed in interaction with KipB is the Kip2 homolog KipA. The KipA protein was described as required for microtubule plus-ends anchorage and maintenance of directionality of

polar growth in *A. nidulans* (Konzack et al., 2004). The Δ*kipB*/ Δ*kipA* double mutants were as viable as the parental single strains, but exhibited an obvious growth reduction at 30°C, which implicate the possibility of partially redundant functions between the two genes. However, the curved growth phenotype asserted to Δ*kipA* mutant was neither enhanced nor rescued in a Δ*kipB* background. The double mutant phenotype on benomyl displayed enhanced resistance comparable with that of a Δ*kipB* strain alone, suggesting a suppresion of the Δ*kipA* mutant sensitivity to benomyl, so a stronger function of KipB in regulation of microtubule stability then KipA. Taking into account that KipA is supposed to mediate temporal capture of microtubules at the growing tip (Konzack et al., 2004), it might be that in the double mutant the much more stable, and probable less dynamic microtubules caused by the *kipB* mutation have more difficulties in being captured at the hyphal tip than in a Δ*kipA* single mutant, therefore perhaps their cortex connection is established at sites far beyond compared with wild type conditions. This suggests that *kipA* and *kipB* may act in different pathways but still could have overlapping functions.

In contrast, the phenotype of Δ*kipB*/ Δ*kinA* double mutant did show the same benomyl resistance as the two mutans alone, suggesting the action of the two motors in independent pathways and a lack of significant functional interaction regarding the studied phenotypes among these kinesins in *A. nidulans*. The Δ*kipB/nudA1* double mutant exhibited the growth and benomyl sensitivity phenotype of dynein conditional mutant alone, showing a dominant phenotype of *nudA1* mutation onto Δ*kipB*, but no synthetic lethality. Hence, the genetic interactions between *kipB* and *kipA* and *kipB* and *nudA1* are in part, different from those described in yeast, where Kip2 and Kip3 were found to have opposite roles in nuclear migration, functioning in two different pathways, and furthermore, *kip3* was reported synthetically lethal with *dyn1*, a phenotype suspected to be caused by the cumulative effect of partial defects in sequential movements (DeZwaan et al., 1997).

5. How to get to the end?

In this study three different GFP constructs were studied, an N-terminal fusion with the full-length KipB protein, an N-terminal fusion with a truncated version of KipB, which only consisted of the first 408 amino acids from the N-terminus and a C-terminal GFP fusion, which deleted about 300 amino acids from KipB. Whereas the

truncated versions stained the entire length of the filaments, the full-length protein predominantly displayed a discontinuous distribution along microtubules and the GFP spots moved along the filaments. This could suggest that the C-terminal part is required for KipB movement, as long as the truncated version does not display the same localization pattern. But the question that rises is how KipB moves along microtubules.

Since Klp5 and Klp6 in *S. cerevisiae* were described as fission yeast KinI homologues in two recent studies (Garcia et al., 2002; Garcia et al., 2002), we considered that KipB could reach the plus ends by one-dimensional diffusion, as it was proposed for KinI kinesins (Hunter et al., 2003; Moores et al., 2003), and once there might be activated to depolymerize the microtubules. Addition of benomyl to the GFP-KipB tagged strain stopped or caused the complete disappearance of the spots, supporting partially the diffusion model, but loss of intrinsic dynamics or depolymerization of the microtubules due to the benomyl action could only be the proof of GFP-KipB association with microtubule's lattice and not implying simultaneously protein diffusion. Also, at the hyphal tip, where microtubules extend just their plus ends (Konzack et al., 2004; Zhang et al., 2003), GFP-KipB signals were accumulating in the same fashion, all directed exclusively toward the hyphal apex, which could stand for a plus-end biased movement of the protein. In the middle and the rear of the hyphal tip area, where microtubule polarity is mixed (Konzack et al., 2004), GFP-KipB spots moved into both directions (see also movie 16). Moreover, we have eliminated the possibility that GFP-KipB spots are transported passively with the plus-ends of the microtubules, since comparison between the speeds of microtubule growth and GFP-KipB movement showed no pronounced peak and a greater range of speeds for GFP-KipB spots than microtubule plus end dynamics. But those arguments would contradict the premise of GFP-KipB movement in a KinI-like pattern, because this should involve diffusion of the protein to the both ends of microtubules, as diffusion is not a directional motion in comparison with conventional motility (Walczak, 2003), and we have highlighted the dynamic localization of KipB in particular to the plus ends of microtubules, so a directed movement. Of course one cannot exclude the possibility that KipB could display processivity and intrinsic motility along the microtubules.

One accepted model for conventional kinesin movement is the hand-over-hand model, which requires dimerization of the protein. In KipB, as in Klp5, Klp6 and Kip3,

only short regions for a potential coiled-coil formation were found. Nevertheless, they might be sufficient for the mediation of an interaction. Indeed for Klp5 and Klp6 heterodimerization has been shown (Garcia et al., 2002). Therefore, KipB may form homodimers (since we only found one kinesin of this family in the *A. nidulans* genome) and move along microtubules in the conventional sense rather than by diffusion. However, we observed GFP-KipB forming a discontinuous distribution pattern along microtubules. Since the fluorescence signal from single GFP-KipB molecules would be below the detection level, it is likely that we observed aggregates of GFP-KipB or vesicles, which contain or which were decorated with GFP-KipB. Those vesicle-like structures could be the unit with which KipB could be transported towards the microtubule plus ends where it would act as depolymerase. This mechanism would be different from the one described for the transportation of dynein towards the plus end of microtubules in *A. nidulans*. In this case, conventional kinesin appears to be the main driving force, but spots along the microtubules were not visible. Thus it is more likely that individual dynein motor proteins are the cargo for kinesin (Zhang et al., 2003). It might be so that one of the other kinesins in *A. nidulans* genome is able to transport or target the KipB protein to the microtubule plus-ends, good candidates for this function being conventional kinesin or the two Unc-104 representatives, all of them kinesin motors which are known as involved in transport of organelles such as nuclei (Requena et al., 2001), mitochondria (Nangaku et al., 1994) or Golgi intermediates (Dorner et al., 1998), and also shown to be involved in binding endosomes, moving them in concert with dynein (Wedlich-Soldner et al., 2002).

For the Kip3 family of kinesins the idea was already advanced that they are capable of both motile and depolymerizing activities, as is for example another kinesin, Kar3. However, the weak structural and sequence correspondence between KinI and Kip3 kinesin families suggests that the mechanism of microtubule destabilization by Kip3 kinesins may be different from that of KinIs (Ovechkina & Wordeman, 2003). The challenge for future experiments will be to identify motor proteins, which may be involved in the transportation of KipB or to prove if fungal Kip3 kinesins itself can processively move along microtubule filaments.

6. Conclusions and future directions

Fifteen years ago, only a few molecular motors were known. In contrast, complete inventories of molecular motors are now available in a number of diverse organisms. While these remarkable accomplishments have answered many questions, the genomic inventories also have exposed many areas of ignorance. The unusual collections of motors in *Arabidopsis*, *Giardia*, and *Malaria* certainly highlight how little we know about intracellular transport in plants and parasites compared with animal cells. Understanding motors in such organisms is likely to provide general insights into how transport processes are used in biology (Vale, 2003).

Some of the most important processes in the cell, which require molecular motors as kinesins, are mitosis and microtubule dynamics. Kinesins participate in various aspects of spindle assembly and function including spindle bipolarity, spindle pole architecture, chromosome attachment and movement, regulation of microtubule dynamics, and cytokinesis.

The present work has highlighted some new but also partially conserved cellular functions of KipB, a Kip3-like kinesin in *A. nidulans*. KipB localizes to interphase cytoplasmic microtubules and mitotic astral and spindle microtubules. This localization pattern, in particular to the plus ends, suggests that KipB regulates microtubule dynamics in general during both interphase and mitosis, as KinI homologues. It plays an important role for proper mitotic progression, because in the absence of this molecule cells spend a longer time in anaphase, and is involved in establishment of spindle architecture and positioning.

Revealing of KipB function in spindle and probably chromosome motility represents an important step forward in understanding the basis of cell division in *A. nidulans*. Still to be identified are the cellular roles of many other mitotic spindle proteins and their mechanism of function, the interactions of the proteins with one another and with components of the mitotic apparatus, also the regulation of the motors in the cell cycle. Nowadays, with the completion of the *A. nidulans* genome sequencing project this work should be much easier and surely much faster.

Elucidating the precise role that each motor plays in spindle assembly will shed light not only on the basic process of chromosome segregation in mitosis and meiosis, but may lead to insights into clinically relevant conditions that arise from errors in chromosome segregation. For example, chromosome non-disjunction in

meiosis causes Down, Klinefelter, and Turner syndromes, severe developmental disorders resulting from conceptuses with aneuploidy (improper chromosome number). In somatic tissues, chromosome non-disjunction during mitosis is an important factor contributing to aneuploidy, which is critical for tumor cell progression. In addition to the consequences on chromosome segregation if the spindle does not function properly, an understanding of motor function could unveil new avenues of intervention into cancer cell growth. Thus, the study of microtubule motor function during mitosis and meiosis is an important area of research with potential impacts in understanding some common birth defects, as well as the etiology and treatment of cancer (Mountain & Compton, 2000).

How Kip3 kinesins influence dynamics of the microtubules and whether they have intrinsic properties of processive movement is also an interesting challenge for future study. In vitro and/or gliding assays regarding Kip3 kinesins movement onto microtubules could unravel new mechanisms for their motility. It seems reasonable to propose that the association of kinesin-related proteins with the depolymerizing ends of microtubules would have significant effects on the stability of microtubules, with variable and distinct effects depending on the properties of the specific protein. This is why deciphering the similar and opposite mechanisms throught which Kip3 and KinI-like kinesins influence microtubule dynamics may bring new answers for understanding motor-cytoskeleton interactions within the cell.

VI. Literature

Aist, J. R. & Morris, N. R. (1999). Mitosis in filamentous fungi: how we got where we are. *Fungal Genet. Biol.* **27**, 1-25.

Allen, R. D., Metuzals, J., Tasaki, I., Brady, S. T. & Gilbert, S. P. (1982). Fast axonal transport in squid giant axon. *Science* **218**, 1127-9.

Aramayo, R., Adams, T. H. & Timberlake, W. E. (1989). A large cluster of highly expressed genes is dispensable for growth and development in *Aspergillus nidulans*. *Genetics* **122**, 65-71.

Asbury, C. L., Fehr, A. N. & Block, S. M. (2003). Kinesin moves by an asymmetric hand-over-hand mechanism. *Science* **302**, 2130-4.

Ausubel, F., Brent, R., Kingston, R. E., Moore, D. D., Seidman, J. G., Smith, J. A. & Struhl, K. (1995). *Short protocols in molecular biology*: John Wiley & Sons, Inc.

Badoual, M., Julicher, F. & Prost, J. (2002). Bidirectional cooperative motion of molecular motors. *Proc. Natl. Acad. Sci. U S A* **99**, 6696-701.

Behrens, R. & Nurse, P. (2002). Roles of fission yeast Tea1p in the localization of polarity factors and in organizing the microtubular cytoskeleton. *J. Cell Biol.* **157**, 783-93.

Bradford, M. M. (1976). A rapid and sensitive method for the quantitation of microgram quantities of protein utilizing the principle of protein dye binding. *Anal. Biochem.* **72**, 248-254.

Bray, D. (1992). *Cell Movements*. New York, USA: Garland Publishing, Inc.

Case, R. B., Pierce, D. W., Hom-Booher, N., Hart, C. L. & Vale, R. D. (1997). The directional preference of kinesin motors is specified by an element outside of the motor catalytic domain. *Cell* **90**, 959-66.

Chandra, H. S. (1996). *Journal of Genetics.* Bangalore, India:Indian Academy of Science.

Clutterbuck, A. J. (1969). A mutational analysis of conidial development in *Aspergillus nidulans*. *Genetics* **63**, 317-327.

Clutterbuck, A. J. (1994). Mutants of *Aspergillus nidulans* deficient in nuclear migration during hyphal growth and conidiation. *Microbiology* **140 (Pt 5)**, 1169-74.

Cottingham, F. R., Gheber, L., Miller, D. L. & Hoyt, M. A. (1999). Novel roles for *Saccharomyces cerevisiae* mitotic spindle motors. *J. Cell Biol.* **147**, 335-50.

Cottingham, F. R. & Hoyt, M. A. (1997). Mitotic spindle positioning in *Saccharomyces cerevisiae* is accomplished by antagonistically acting microtubule motor proteins. *J. Cell Biol.* **138**, 1041-53.

Dagenbach, E. M. & Endow, S. A. (2004). A new kinesin tree. *J Cell Sci* **117**, 3-7.

Desai, A. & Mitchison, T. J. (1997). Microtubule polymerization dynamics. *Annu. Rev. Cell Dev. Biol.* **13**, 83-117.

Desai, A., Verma, S., Mitchison, T. J. & Walczak, C. E. (1999). Kin I kinesins are microtubule-destabilizing enzymes. *Cell* **96**, 69-78.

DeZwaan, T. M., Ellingson, E., Pellman, D. & Roof, D. M. (1997). Kinesin-related KIP3 of *Saccharomyces cerevisiae* is required for a distinct step in nuclear migration. *J. Cell Biol.* **138**, 1023-40.

Dorner, C., Ciossek, T., Muller, S., Moller, P. H., Ullrich, A. & Lammers, R. (1998). Characterization of KIF1C, a new kinesin-like protein involved in vesicle

transport from the Golgi apparatus to the endoplasmic reticulum. *J. Biol. Chem.* **273**, 20267-75.

Endow, S. A. (2003). Kinesin motors as molecular machines. *Bioessays* **25**, 1212-9.

Endow, S. A. & Barker, D. S. (2003). Processive and nonprocessive models of kinesin movement. *Annu. Rev. Physiol.* **65**, 161-75.

Endow, S. A. & Higuchi, H. (2000). A mutant of the motor protein kinesin that moves in both directions on microtubules. *Nature* **406**, 913-6.

Endow, S. A. & Waligora, K. W. (1998). Determinants of kinesin motor polarity. *Science* **281**, 1200-2.

Enos, A. P. & Morris, N. R. (1990). Mutation of a gene that encodes a kinesin-like protein blocks nuclear division in *A. nidulans*. *Cell* **60**, 1019-27.

Etienne-Manneville, S. & Hall, A. (2002). Rho GTPases in cell biology. *Nature* **420**, 629-35.

Farkasovsky, M. & Kuntzel, H. (2001). Cortical Num1p interacts with the dynein intermediate chain Pac11p and cytoplasmic microtubules in budding yeast. *J. Cell Biol.* **152**, 251-62.

Fischer, R. & Timberlake, W. E. (1995). *Aspergillus nidulans apsA* (anucleate primary sterigmata) encodes a coiled-coil protein required for nuclear positioning and completion of asexual development. *J. Cell Biol.* **128**, 485-98.

Gandhi, R., Bonaccorsi, S., Wentworth, D., Doxsey, S., Gatti, M. & Pereira, A. (2004). The *Drosophila* kinesin-like protein KLP67A is essential for mitotic and male meiotic spindle assembly. *Mol. Biol. Cell* **15**, 121-31.

Garcia, M. A., Koonrugsa, N. & Toda, T. (2002). Spindle-kinetochore attachment requires the combined action of Kin I-like Klp5/6 and Alp14/Dis1-MAPs in fission yeast. *EMBO J.* **21**, 6015-24.

Garcia, M. A., Koonrugsa, N. & Toda, T. (2002). Two kinesin-like Kin I family proteins in fission yeast regulate the establishment of metaphase and the onset of anaphase A. *Curr. Biol*. **12**, 610-21.

Garcia, M. A., Vardy, L., Koonrugsa, N. & Toda, T. (2001). Fission yeast ch-TOG/XMAP215 homologue Alp14 connects mitotic spindles with the kinetochore and is a component of the Mad2-dependent spindle checkpoint. *EMBO J.* **20**, 3389-401.

Goldstein, L. S. & Philp, A. V. (1999). The road less traveled: emerging principles of kinesin motor utilization. *Annu. Rev. Cell Dev. Biol.* **15**, 141-83.

Goodson, H. V., Kang, S. J. & Endow, S. A. (1994). Molecular phylogeny of the kinesin family of microtubule motor proteins. *J. Cell Sci.* **107 (Pt 7)**, 1875-84.

Gundersen, G. G. & Bretscher, A. (2003). Microtubule asymmetry. *Science* **300**, 2040-1.

Han, G., Liu, B., Zhang, J., Zuo, W., Morris, N. R. & Xiang, X. (2001). The *Aspergillus* cytoplasmic dynein heavy chain and NUDF localize to microtubule ends and affect microtubule dynamics. *Curr. Biol.* **11**, 19-24.

Heil-Chapdelaine, R. A., Oberle, R. J. & Cooper, A. J. (2000). The Cortical Protein Num1p Is Essential for Dynein-dependent Interactions of Microtubules with the Cortex. *J. Cell Biol.* **151**, 1337-1343

Hirokawa, N. (1998). Kinesin and dynein superfamily proteins and the mechanism of organelle transport. *Science* **279**, 519-526.

Howard, J. & Hyman, A. A. (2003). Dynamics and mechanics of the microtubule plus end. *Nature* **422**, 753-8.

Hua, W., Chung, J. & Gelles, J. (2002). Distinguishing inchworm and hand-over-hand processive kinesin movement by neck rotation measurements. *Science* **295**, 844-8.

Hunter, A. W., Caplow, M., Coy, D. L., Hancock, W. O., Diez, S., Wordeman, L. & Howard, J. (2003). The kinesin-related protein MCAK is a microtubule depolymerase that forms an ATP-hydrolyzing complex at microtubule ends. *Mol. Cell.* **11**, 445-57.

Itoh, R., Fujiwara, M. & Yoshida, S. (2001). Kinesin-related proteins with a mitochondrial targeting signal. *Plant. Physiol.* **127**, 724-6.

Iwabe, N. & Miyata, T. (2002). Kinesin-related genes from diplomonad, sponge, amphioxus, and cyclostomes: divergence pattern of kinesin family and evolution of giardial membrane-bounded organella. *Mol. Biol. Evol.* **19**, 1524-33.

Jung, M. K., May, G. S. & Oakley, B. R. (1998). Mitosis in wild-type and β-tubulin mutant strains of *Aspergillus nidulans*. *Fungal Genet. Biol.* **24**, 146-160.

Käfer, E. (1977). Meiotic and mitotic recombination in *Aspergillus* and its chromosomal aberrations. *Adv. Genet.* **19**, 33-131.

Kallipolitou, A., Deluca, D., Majdic, U., Lakamper, S., Cross, R., Meyhofer, E., Moroder, L., Schliwa, M. & Woehlke, G. (2001). Unusual properties of the fungal conventional kinesin neck domain from *Neurospora crassa*. *EMBO J.* **20**, 6226-35.

Kamal, A., Stokin, G. B., Yang, Z., Xia, C. H. & Goldstein, L. S. (2000). Axonal transport of amyloid precursor protein is mediated by direct binding to the kinesin light chain subunit of kinesin-I. *Neuron* **28**, 449-59.

Karcher, R. L., Deacon, S. W. & Gelfand, V. I. (2002). Motor-cargo interactions: the key to transport specificity. *Trends Cell. Biol.* **12**, 21-7.

Karos, M. & Fischer, R. (1999). Molecular characterization of HymA, an evolutionarily highly conserved and highly expressed protein of *Aspergillus nidulans*. *Mol. Genet.Genom.* **260**, 510-521.

Karp, J. (1996). *Cell and Molecular Biology, 2nd Edition*. Palatino, USA: John Wiley & Sons, Inc.

Kashina, A. S., Rogers, G. C. & Scholey, J. M. (1997). The bimC family of kinesins: essential bipolar mitotic motors driving centrosome separation. *Biochim. Biophys. Acta* **1357**, 257-71.

Kim, A. J. & Endow, S. A. (2000). A kinesin family tree. *J. Cell Sci.* **113 Pt 21**, 3681-2.

Kirchner, J., Woehlke, G. & Schliwa, M. (1999). Universal and unique features of kinesin motors: insights from a comparison of fungal and animal conventional kinesins. *Biol. Chem.* **380**, 915-21.

Konzack, S., Rischitor, E. P. & Fischer, R. (2004). The kinesin motor KipA is required for microtubule anchorage and maintenance of directionality of polar growth in *Aspergillus nidulans* (submitted).

Kozminski, K. G., Johnson, K. A., Forscher, P. & Rosenbaum, J. L. (1993). A motility in the eukaryotic flagellum unrelated to flagellar beating. *Proc. Natl. Acad. Sci. U S A* **90**, 5519-23.

Kreis, T. & Vale, R. (1999). *Guidebook to the Cytoskeletal and Motor Proteins*. Oxford: Sambrook and Tooze Publication at Oxford University Press.

Lakamper, S., Kallipolitou, A., Woehlke, G., Schliwa, M. & Meyhofer, E. (2003). Single fungal kinesin motor molecules move processively along microtubules. *Biophys. J.* **84**, 1833-43.

Lawrence, C. J., Malmberg, R. L., Muszynski, M. G. & Dawe, R. K. (2002). Maximum likelihood methods reveal conservation of function among closely related kinesin families. *J. Mol. Evol.* **54**, 42-53.

Levesque, A. A. & Compton, D. A. (2001). The chromokinesin Kid is necessary for chromosome arm orientation and oscillation, but not congression, on mitotic spindles. *J. Cell. Biol.* **154**, 1135-46.

Li, Y. & Chang, E. C. (2003). *Schizosaccharomyces pombe* Ras1 effector, Scd1, interacts with Klp5 and Klp6 kinesins to mediate cytokinesis. *Genetics* **165**, 477-88.

Lupas, A. N., Lupas, J. M. & Stock, J. B. (1992). Do G protein subunits associate via a three-stranded coiled coil? *FEBS Lett.* **314**, 105-108.

Maekawa, H., Usui, T., Knop, M. & Schiebel, E. (2003). Yeast Cdk1 translocates to the plus end of cytoplasmic microtubules to regulate bud cortex interactions. *EMBO J.* **22**, 438-49.

Maney, T., Hunter, A. W., Wagenbach, M. & Wordeman, L. (1998). Mitotic centromere-associated kinesin is important for anaphase chromosome segregation. *J. Cell Biol.* **142**, 787-801.

Martinelli, S. D. & Kinghorn, J. R. (1997). *Aspergillus: 50 years on*. Amsterdam, The Netherlands: Elsevier Science B. V.

Meluh, P. B. & Rose, M. D. (1990). KAR3, a kinesin-related gene required for yeast nuclear fusion. *Cell* **60**, 1029-41.

Miki, H., Setou, M., Kaneshiro, K. & Hirokawa, N. (2001). All kinesin superfamily protein, KIF, genes in mouse and human. *Proc. Natl. Acad. Sci. U S A* **98**, 7004-11.

Miller, R. K., Heller, K. K., Frisen, L., Wallack, D. L., Loayza, D., Gammie, A. E. & Rose, M. D. (1998). The kinesin-related proteins, Kip2p and Kip3p, function differently in nuclear migration in yeast. *Mol. Biol. Cell* **9**, 2051-68.

Moores, C. A., Hekmat-Nejad, M., Sakowicz, R. & Milligan, R. A. (2003). Regulation of KinI kinesin ATPase activity by binding to the microtubule lattice. *J. Cell Biol.* **163**, 963-71.

Moores, C. A., Yu, M., Guo, J., Beraud, C., Sakowicz, R. & Milligan, R. A. (2002). A mechanism for microtubule depolymerization by KinI kinesins. *Mol. Cell* **9**, 903-9.

Morris, N. R. (1976). Mitotic mutants of *Aspergillus nidulans*. *Genet. Res.* **26**, 237-254.

Mountain, V. & Compton, D. A. (2000). Dissecting the role of molecular motors in the mitotic spindle. *Anat. Rec.* **261**, 14-24.

Nakagawa, T., Setou, M., Seog, D., Ogasawara, K., Dohmae, N., Takio, K. & Hirokawa, N. (2000). A novel motor, KIF13A, transports mannose-6-phosphate receptor to plasma membrane through direct interaction with AP-1 complex. *Cell* **103**, 569-81.

Nangaku, M., Sato-Yoshitake, R., Okada, Y., Noda, Y., Takemura, R., Yamazaki, H. & Hirokawa, N. (1994). KIF1B, a novel microtubule plus end-directed monomeric motor protein for transport of mitochondria. *Cell* **79**, 1209-20.

Nogales, E., Whittaker, M., Milligan, R. A. & Downing, K. H. (1999). High-resolution model of the microtubule. *Cell* **96**, 79-88.

Oakley, B. R. (2004). Tubulins in *Aspergillus nidulans*. *Fungal Genet. Biol.* **in press**.

O'Connell, M. J., Meluh, P. B., Rose, M. D. & Morris, N. R. (1993). Suppression of the *bimC4* mitotic spindle defect by deletion of *klpA*, a gene encoding a KAR3-related kinesin-like protein in *Aspergillus nidulans*. *J. Cell Biol.* **120**, 153-62.

Ovechkina, Y., Maddox, P., Oakley, C. E., Xiang, X., Osmani, S. A., Salmon, E. D. & Oakley, B. R. (2003). Spindle formation in *Aspergillus* is coupled to tubulin movement into the nucleus. *Mol. Biol. Cell* **14**, 2192-200.

Ovechkina, Y. & Wordeman, L. (2003). Unconventional motoring: an overview of the Kin C and Kin I kinesins. *Traffic* **4**, 367-75.

Page, B. D., Satterwhite, L. L., Rose, M. D. & Snyder, M. (1994). Localization of the Kar3 kinesin heavy chain-related protein requires the Cik1 interacting protein. *J. Cell Biol.* **124**, 507-19.

Papadaki, P., Pizon, V., Onken, B. & Chang, E. C. (2002). Two ras pathways in fission yeast are differentially regulated by two ras guanine nucleotide exchange factors. *Mol. Cell Biol.* **22**, 4598-606.

Pereira, A. J., Dalby, B., Stewart, R. J., Doxsey, S. J. & Goldstein, L. S. (1997). Mitochondrial association of a plus end-directed microtubule motor expressed during mitosis in *Drosophila*. *J. Cell Biol.* **136**, 1081-90.

Pontecorvo, G., Roper, J. A., Hemmons, L. M., MacDonald, K. D. & Bufton, A. W. J. (1953). The genetics of *Aspergillus nidulans*. *Adv. Genet.* **5**, 141-238.

Prigozhina, N. L., Walker, R. A., Oakley, C. E. & Oakley, B. R. (2001). Gamma-tubulin and the C-terminal motor domain kinesin-like protein, KLPA, function in the establishment of spindle bipolarity in *Aspergillus nidulans*. *Mol. Biol. Cell* **12**, 3161-74.

Requena, N., Alberti-Segui, C., Winzenburg, E., Horn, C., Schliwa, M., Philippsen, P., Liese, R. & Fischer, R. (2001). Genetic evidence for a microtubule-destabilizing effect of conventional kinesin and analysis of its consequences for the control of nuclear distribution in *Aspergillus nidulans*. *Mol. Microbiol.* **42**, 121-32.

Sambrook, J., Fritsch, E. F. & Maniatis, T. (1989). *Molecular Cloning: A laboratory manual*. Cold Spring Harbor, New York: Cold Spring Harbor Laboratory Press.

Savage, C., Hamelin, M., Culotti, J. G., Coulson, A., Albertson, D. G. & Chalfie, M. (1989). *mec-7* is a beta-tubulin gene required for the production of 15-protofilament microtubules in *Caenorhabditis elegans*. *Genes Dev.* **3**, 870-81.

Schliwa, M. (2003). *Molecular motors*. Weinheim: Wiley-VCH Verlag GmbH and Co. KGaA.

Schnapp, B. J. (2003). Trafficking of signaling modules by kinesin motors. *J. Cell Sci.* **116**, 2125-35.

Schoch, C. L., Aist, J. R., Yoder, O. C. & Gillian Turgeon, B. (2003). A complete inventory of fungal kinesins in representative filamentous ascomycetes. *Fungal Genet. Biol.* **39**, 1-15.

Severin, F., Habermann, B., Huffaker, T. & Hyman, T. (2001). Stu2 promotes mitotic spindle elongation in anaphase. *J. Cell Biol.* **153**, 435-42.

Song, Y. H., Marx, A., Muller, J., Woehlke, G., Schliwa, M., Krebs, A., Hoenger, A. & Mandelkow, E. (2001). Structure of a fast kinesin: implications for ATPase mechanism and interactions with microtubules. *EMBO J* **20**, 6213-25.

Steinberg, G. (2000). The cellular roles of molecular motors in fungi. *Trends Microbiol.* **8**, 162-168.

Stringer, M. A., Dean, R. A., Sewall, T. C. & Timberlake, W. E. (1991). *Rodletless*, a new *Aspergillus* developmental mutant induced by directed gene inactivation. *Genes Dev.* **5**, 1161-1171.

Suelmann, R. & Fischer, R. (2000). Mitochondrial movement and morphology depend on an intact actin cytoskeleton in *Aspergillus nidulans*. *Cell. Mot. Cytoskel.* **45(1)**, 42-50.

Suelmann, R. & Fischer, R. (2000). Nuclear migration in fungi - Different motors at work. *Res. Microbiol.* **151**, 247-254.

Suelmann, R., Sievers, N. & Fischer, R. (1997). Nuclear traffic in fungal hyphae: in vivo study of nuclear migration and positioning in *Aspergillus nidulans*. *Mol. Microbiol.* **25**, 757-69.

Suelmann, R., Sievers, N., Galetzka, D., Robertson, L., Timberlake, W. E. & Fischer, R. (1998). Increased nuclear traffic chaos in hyphae of *Aspergillus nidulans*: molecular characterization of *apsB* and in vivo observation of nuclear behaviour. *Mol. Microbiol.* **30**, 831-42.

Svoboda, K., Schmidt, C. F., Schnapp, B. J. & Block, S. M. (1993). Direct observation of kinesin stepping by optical trapping interferometry. *Nature* **365**, 721-7.

Vale, R. D. (2003). The molecular motor toolbox for intracellular transport. *Cell* **112**, 467-80.

Vale, R. D. & Fletterick, R. J. (1997). The design plan of kinesin motors. *Annu. Rev. Cell Dev. Biol.* **13**, 745-77.

Vale, R. D. & Milligan, R. A. (2000). The way things move: looking under the hood of molecular motor proteins. *Science* **288**, 88-95.

Vale, R. D., Reese, T. S. & Sheetz, M. P. (1985). Identification of a novel force-generating protein, kinesin, involved in microtubule-based motility. *Cell* **42**, 39-50.

Veith, D., Efimov, V. P. & Fischer, R. (2004). The microtubule minus-end directed motor dynein transports nuclei along microtubules. *submitted*.

Verhey, K. J., Meyer, D., Deehan, R., Blenis, J., Schnapp, B. J., Rapoport, T. A. & Margolis, B. (2001). Cargo of kinesin identified as JIP scaffolding proteins and associated signaling molecules. *J. Cell Biol.* **152**, 959-70.

Wade, R. H., Meurer-Grob, P., Metoz, F. & Arnal, I. (1998). Organisation and structure of microtubules and microtubule-motor protein complexes. *Eur. Biophys. J.* **27**, 446-54.

Walczak, C. E. (2003). The Kin I kinesins are microtubule end-stimulated ATPases. *Mol. Cell* **11**, 286-8.

Walczak, C. E., Verma, S. & Mitchison, T. J. (1997). XCTK2: a kinesin-related protein that promotes mitotic spindle assembly in *Xenopus laevis* egg extracts. *J. Cell Biol.* **136**, 859-70.

Waring, R. B., May, G. S. & Morris, N. R. (1989). Characterization of an inducible expression system in *Aspergillus nidulans* using *alcA* and tubulin coding genes. *Gene* **79**, 119-130.

Wedlich-Soldner, R., Straube, A., Friedrich, M. W. & Steinberg, G. (2002). A balance of KIF1A-like kinesin and dynein organizes early endosomes in the fungus *Ustilago maydis*. *EMBO J.* **21**, 2946-57.

Wei, H., Scherer, M., Singh, A., Liese, R. & Fischer, R. (2001). *Aspergillus nidulans* α-1,3 glucanase (mutanase), *mutA,* is expressed during sexual development and mobilizes mutan. *Fungal Genet. Biol.* **(34)** 3, 217-227.

West, R. R., Malmstrom, T. & McIntosh, J. R. (2002). Kinesins klp5(+) and klp6(+) are required for normal chromosome movement in mitosis. *J. Cell Sci.* **115**, 931-40.

West, R. R., Malmstrom, T., Troxell, C. L. & McIntosh, J. R. (2001). Two related kinesins, klp5+ and klp6+, foster microtubule disassembly and are required for meiosis in fission yeast. *Mol. Biol. Cell* **12**, 3919-32.

Wood, K. W., Sakowicz, R., Goldstein, L. S. & Cleveland, D. W. (1997). CENP-E is a plus end-directed kinetochore motor required for metaphase chromosome alignment. *Cell* **91**, 357-66.

Xiang, X., Beckwith, S. M. & Morris, N. R. (1994). Cytoplasmic dynein is involved in nuclear migration in *Aspergillus nidulans*. *Proc. Natl. Acad. Sci. U S A* **91**, 2100-4.

Xiang, X. & Fischer, R. (2004). Nuclear migration and positioning in filamentous fungi. *Fungal Genet. Biol.* **in press**.

Xiang, X. & Plamann, M. (2003). Cytoskeleton and motor proteins in filamentous fungi. *Curr. Opin. Microbiol.* **6**, 628-33.

Yelton, M. M., Hamer, J. E. & Timberlake, W. E. (1984). Transformation of *Aspergillus nidulans* by using a *trpC* plasmid. *Proc. Natl. Acad. Sci. U S A* **81**, 1470-1474.

Zhang, J., Li, S., Fischer, R. & Xiang, X. (2003). The accumulation of cytoplasmic dynein and dynactin at microtubule plus-ends is kinesin dependent in *Aspergillus nidulans*. *Mol. Biol. Cell* **14**, 1479-1488.

EUKARYOTIC CELL, 2004

Copyright © 2004, American Society for Microbiology. All Rights Reserved.

The Kip3-like kinesin KipB Moves along Microtubules and Determines Spindle Position during Synchronized Mitoses in Hyphae of *Aspergillus nidulans*

Patricia E. Rischitor, Sven Konzack and Reinhard Fischer

Kinesins are motor proteins, which are classified into eleven different families. We identified eleven kinesin-like proteins in the genome of the filamentous fungus *Aspergillus nidulans*. Relatedness analyses based on the motor domains grouped them into nine families. In this paper we characterized KipB as a member of the Kip3 family of microtubule depolymerases. The closest homologues of KipB are *Saccharomyces cerevisiae* Kip3 and *Schizosacchromyces pombe* Klp5 and Klp6 but sequence similarities outside the motor domain are very low. Disruption of *kipB* demonstrated that it is not essential for vegetative growth. Δ*kipB* mutant strains were resistant to high concentrations of the microtubule-destabilizing drug benomyl suggesting that KipB destabilizes microtubules. *kipB* mutation caused a failure of spindle positioning in the cell, a delay in mitotic progression, an increased number of bent mitotic spindles, and a decrease of depolymerization of cytoplasmic microtubules during interphase and mitosis. Meiosis and ascospore formation were not affected. Disruption of the *kipB* gene was synthetically lethal with the temperature-sensitive mitotic kinesin motor mutation *bimC4* suggesting an important but redundant role of KipB in mitosis. KipB localized to cytoplasmic, astral and mitotic microtubules in a discontinuous pattern and spots of GFP moved along microtubules towards the plus ends.

in press.

The Kinesin Motor KipA is Required for Microtubule Anchorage and Maintenance of Directionality of Polar Growth in *Aspergillus nidulans*

Sven Konzack, Patricia E. Rischitor and Reinhard Fischer

Polarized growth in filamentous fungi requires the integrity of the microtubule cytoskeleton. We found that growing microtubules in *Aspergillus nidulans* merge at the center of fast growing tips and discovered that a kinesin motor protein, KipA, related to Tea2 of *Schizosaccharomyces pombe,* is required for their temporal anchorage. In a *ΔkipA* strain microtubule plus ends reach the tip but fail to anchor and show continuous lateral movement. Hyphae loose directionality and grow in curves due to mislocalization of a vesicle supply center in the tip. GFP-KipA localizes to microtubule plus ends and jams behind them, suggesting that KipA is a moving motor. Using KipA as a microtubule plus end marker we found bi-directional organization of microtubules and determined the location of MTOCs at nuclei, in the cytoplasm and at septa. We also analyzed a Kelch-protein, TeaA, as a putative cargo of KipA. *teaA* deletion causes a different polarized growth defect than *ΔkipA* mutation, suggesting additional functions for KipA.

submitted.

Curr Genet (2004)

Establishment of mRFP1 as fluorescent marker in *Aspergillus nidulans* and construction of expression vectors for high-throughput protein tagging using recombination *in vitro* (GATEWAY)

W. M. Toews, J. Warmbold, S. Konzack, P. E. Rischitor, D. Veith, K. Vienken, C. Vinuesa, H. Wei and R. Fischer

Abstract. The advent of fluorescent proteins as vital dyes had a major impact in many research fields. Different GFP variants have been established in pro- and eukaryotic organisms within the past ten years as well as other fluorescent proteins discovered and applied. We expressed the red fluorescent protein, DsRed (T4), the improved version mRFP1 (monomeric red fluorescent protein) and the blue fluorescent protein, BFP, in the filamentous fungus *Aspergillus nidulans*. Whereas DsRed requires tetramer formation for fluorescence, mRFP1 functions as monomer. We have used sGFP, DsRed (T4), mRFP1 and BFP for nuclear and/or mitochondrial labelling. To facilitate gene tagging, we established a number of cloning vectors for efficient, simultaneous fusion of any protein with mRFP1, BFP (blue fluorescent protein) and sGFP (green fluorescent protein) or the hemagglutinin epitope 3xHA. A PCR-amplified gene of interest can be inserted into the expression vectors without cloning but using homologous recombination *in vitro* (GATEWAY). The vectors contain the *argB* gene as selection marker for *A. nidulans*, and the inducible *alcA* promoter for control of expression. The system allows labelling of a protein with several tags in one recombination reaction. The nutritional marker gene as well as the promoter, are frequently used in other fungi, suggesting that this set of expression vectors will be very useful tools for gene analyses in a genome-wide scale.

in press.

Curriculum vitae

Name:	Patricia Elena Rischitor
Birth date:	25. 03. 1971
Birth place:	Iaşi, România
Family status:	Married, no children

Education

08/2000-Present	PhD student, Laboratory of Microbiology, Faculty of Biology, the Philipps University and Max-Planck Institute for Terrestrial Microbiology, Marburg, Germany
10-11/1999	Individual research project in collaboration with Centre de Recherches sur la Conservation des Documents Graphiques, Muséum national d'histoire naturelle, Paris, France
10/1996-07/1997	MS, Biology, Al.I. Cuza University, Iaşi, România
09-10/1993	Awarded competitive biology scholarship, Université Paris VII, "Denis Diderot", Paris, France
10/1990-07/1995	BS, Ecology, Al.I. Cuza University, Iaşi, România
06/1989	General Qualification for University Entrance ("Baccalaureate"), "M. Eminescu" High school, Iaşi, România

Positions held

02/1997-08/2000	Biologist, specialist in biological investigations of patrimony objects, Regional Laboratory of Conservation-Restoration within "MOLDOVA" National Complex of Museums, Iaşi, România
08/1995-02/1997	Biologist, Research Assistant in Aquatic Microbiology, Research Department of Fishery Research Station „ACVARES", Iaşi, România

Marburg, Germany, February 2004

Aknowledgments

First and foremost I would like to deeply thank to HD Dr. Reinhard Fischer for trusting me and offering me the opportunity to work in his team as a PhD student at an interesting and captivating topic, and for his tireless support through suggestions and discussions concerning the scientific research. Also my entire gratitude for his patience and prompt help every time I needed outside the lab walls.

Cordial thanks I address to Prof. Dr. R.K. Thauer for offering me outstanding working conditions in the Department of Biochemistry at the Max-Planck Institute for Terrestrial Microbiology, in Marburg, Germany. I would like to thank Prof. Dr. M. Bölker for sharing with me his opinions and fruitful ideas in connection with my project within the framework of our “Friday seminar” with his group. Here I wish to express my gratitude to Prof. Dr. Unai Ugalde, visitor professor from San Sebastian University, Spain, for the permanent encouragements and stimulative scientific debate during all his sabbatical year in our lab.

My special thanks to Prof. Dr. Michel Petitjean, Paris VII University, France, for supporting me constantly ever since we met, and for his enthousiastic confidence in all my actions.

To all my colleagues, formerly (N. Schier, M. Scherer, H. Wei) and presently (S. Konzack, K. Vienken, D. Veith) in the group I would like to say a sincere “Danke schön”, for the nice and friendly atmosphere given to the lab and to everyday work. Special thanks for the girls in our group, K. Koch, N. Scherr, C. Enke, C. Vinuesa and A. Blumenstein for being always beside me with small tips and jokes, which made the life in the lab more easy. To U. Grünwald my thanks for his kindness and the friendly time spent together, both with writing our PhD’s.

I am also grateful to R. Liese, J. Scheld and D. Stöhr for their technical support and I would like to thank R. Böcher and Dr. M. Irmler for their patience with my “huge” personal folder and for real support with the computer in general.

All my deep gratitude belongs to my family, to my parents who always guided me towards discovering new beginnings and to my husband who is sharing with me the life around and outside the “biological” world.